ผลของมวลโมเลกุลของไดออลต่อสมบัติของเบนซอกซาซีน-ยูรีเทนพอลิเมอร์อัลลอย
สำหรับประยุกต์ใช้ในงานด้านเกราะกันกระสุน

นางสาวผกาวัลย์ กมลชัยวานิช

วิทยานิพนธ์นี้เป็นส่วนหนึ่งของการศึกษาตามหลักสูตรปริญญาวิศวกรรมศาสตรมหาบัณฑิต
สาขาวิชาวิศวกรรมเคมี   ภาควิชาวิศวกรรมเคมี
คณะวิศวกรรมศาสตร์   จุฬาลงกรณ์มหาวิทยาลัย
ปีการศึกษา 2549

EFFECTS OF DIOL MOLECULAR WEIGHT ON PROPERTIES OF BENZOXAZINE-
URETHANE POLYMER ALLOYS FOR BALLISTIC ARMOR APPLICATIONS

Miss Pakawan Kamonchaivanich

A Thesis Submitted in Partial Fulfillment of the Requirements

for the Degree of Master of Engineering Program in Chemical Engineering

Department of Chemical Engineering
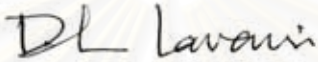
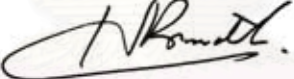Faculty of Engineering

Chulalongkorn University

Academic Year 2006

Thesis Title	EFFECTS OF DIOL MOLECULAR WEIGHT ON PROPERTIES OF BENZOXAZINE-URETHANE POLYMER ALLOYS FOR BALLISTIC ARMOR APPLICATIONS
By	Miss Pakawan Kamonchaivanich
Field of Study	Chemical Engineering
Thesis Advisor	Assistant Professor Sarawut Rimdusit, Ph.D.
Thesis Co-advisor	Associate Professor Tharathon Mongkhonsi, Ph.D.

Accepted by the Faculty of Engineering, Chulalongkorn University in Partial Fulfillment of the Requirements for the Master's Degree

.... Dean of the Faculty of Engineering

(Professor Direk Lavansiri, Ph.D.)

THESIS COMMITTEE

.... Chairman

(Associate Professor Chirakarn Muangnapoh, Dr. Ing.)

.... Thesis Advisor

(Assistant Professor Sarawut Rimdusit, Ph.D.)

.... Thesis Co-advisor

(Associate Professor Tharathon Mongkhonsi, Ph.D.)

.... Member

(Associate Professor Siriporn Damrongsakkul, Ph.D.)

.... Member

(Kuljira Sujirote, Ph.D.)

ผกาวัลย์ กมลชัยวานิช : ผลของมวลโมเลกุลของไดออลต่อสมบัติของเบนซอกซาซีน-ยูรีเทนพอลิเมอร์อัลลอยสำหรับประยุกต์ใช้ในงานด้านเกราะกันกระสุน (EFFECTS OF DIOL MOLECULAR WEIGHT ON PROPERTIES OF BENZOXAZINE-URETHANE POLYMER ALLOYS FOR BALLISTIC ARMOR APPLICATIONS) อ. ที่ปรึกษา: ผศ. ดร. ศราวุธ ริมดุสิต, อ. ที่ปรึกษาร่วม: รศ. ดร. ธราธร มงคลศรี, 118 หน้า.

จุดมุ่งหมายของงานวิจัยนี้เพื่อพัฒนาเกราะกันกระสุนน้ำหนักเบาจากเส้นใยเคฟลา และเบนซอกซาซีน-ยูรีเทนพอลิเมอร์อัลลอยเมตริกเรซิน โดยพอลิเบนซอกซาซีน (BA-a) เป็นพอลิเมอร์ในตระกูลฟีนอลิกที่มีคุณสมบัติเด่นหลายประการ ได้แก่ สังเคราะห์ได้ง่าย ความหนืดต่ำ ไม่มีผลพลอยได้จากการบ่ม ค่าการหดตัวจากการขึ้นรูปใกล้ศูนย์ เสถียรภาพทางความร้อนและสมบัติทางกลสูง นอกจากนี้สามารถทำอัลลอยร่วมกับเรซินอื่นได้หลายชนิดเนื่องจากมีหมู่ฟังก์ชันที่หลากหลาย งานวิจัยนี้ใช้ยูรีเทนอิลาสโตเมอร์ (PU) ที่สังเคราะห์ด้วยไดออลมวลโมเลกุลต่างกัน 4 ค่า เพื่อเพิ่มความยืดหยุ่นของพอลิเบนซอกซาซีนอัลลอย โดยศึกษาผลของมวลโลกุลของไดออลต่อสมบัติต่างๆ เช่น สมบัติทางความร้อน สมบัติทางกล เป็นต้น และศึกษาผลกระทบของความเป็นเกราะกันกระสุนของเมตริกลูกผสมที่มวลโมเลกุลต่างๆ จากผลการทดลองพบว่าอุณหภูมิ ณ จุดสูงสุดของปฏิกิริยาการบ่มของลูกผสมที่มวลโมเลกุลต่างๆกันจะมีค่าเท่ากันที่อัตราส่วน BA:PU ค่าเดียวกัน ค่าอุณหภูมิการเปลี่ยนสถานะคล้ายแก้วจะสูงขึ้นจาก 165°C ในพอลิเบนซอกซาซีน เป็น 240-245°C และอุณหภูมิการสลายตัวทางความร้อนเพิ่มขึ้นจาก 330°C เป็น 344°C ใน 70:30 BA:PU พอลิเมอร์อัลลอยของทุกๆมวลโมเลกุล โดยปริมาณเถ้าจะเพิ่มขึ้นเมื่อมวลโมเลกุลขอลไดออลมีค่าสูงขึ้น ในส่วนของสมบัติทางกล จากการทดสอบสมบัติด้านการดัดโค้งของพอลิเมอร์อัลลอย พบว่า ค่ามอดูลัสพอลิเบนซอกซาซีนลดลงจาก 6.2 GPa เป็น 2.2-2.8 GPa ใน 70:30 BA:PU พอลิเมอร์อัลลอยของทุกๆมวลโมเลกุล นอกจากนี้จากการทดสอบค่าความแข็งแรง จากการทดสอบยิงเบื้องต้นด้วยปืนขนาด 9 มม. พบว่ามวลโมเลกุลไดออลในเมตริกอัลลอยที่เหมาะสมที่สุด คือ 3000 โดยใช้ปริมาณยูรีเทนที่ 20 เปอร์เซ็นต์โดยน้ำหนัก

ภาควิชา....วิศวกรรมเคมี........................	ลายมือชื่อนิสิต..ผกาวัลย์ กมลชัยวานิช..
สาขาวิชา....วิศวกรรมเคมี......................	ลายมือชื่ออาจารย์ที่ปรึกษา....................
ปีการศึกษา....2549.............................	ลายมือชื่ออาจารย์ทีปรึกษาร่วม...............

4870388921 : MAJOR CHEMICAL ENGINEERING

KEY WORD: POLYBENZOXAZINE / DIOL MOLECULAR WEIGHT / KEVLAR™-REINFORCED COMPOSITE / BALLISTIC ARMOR

PAKAWAN KAMONCHAIVANICH: EFFECTS OF DIOL MOLECULAR WEIGHT ON PROPERTIES OF BENZOXAZINE-URETHANE POLYMER ALLOYS FOR BALLISTIC ARMOR APPLICATIONS. THESIS ADVISOR: ASST. PROF. SARAWUT RIMDUSIT, Ph.D., THESIS COADVISOR: ASSOC. PROF. THARATHON MONGKHONSI, Ph.D., 118 pp.

This study aims to develop a light weight ballistic armor from Kevlar™-reinforcing fiber having polybenzoxazine alloys as a matrix. Polybenzoxazine (BA-a), a novel class of phenolic resin, possesses several outstanding properties, for example, ease of synthesis, low viscosity, near-zero shrinkage, lack of by-product upon curing, high thermal stability and high mechanical property. Moreover, the benzoxazine resins can be alloyed with various types of resins because of the various function groups in its structure. In this work, urethane elastomer (PU) at various polyol molecular weights is used to enhance toughness of the polybenzoxazine and its effects on properties of BA:PU polymer alloys and also the ballistic characteristics of their Kevlar™-reinforced composite are investigated. The experiment reveals that the similar curing peaks of the matrices at various polyol molecular weights, with the same urethane mass fraction, in the resin mixtures were obtained. The glass transition temperature increased from 165°C of polybenzoxazine to 240-245°C in the 70:30 BA:PU system and the degradation temperature also increased from 330°C to 344°C in the same alloy for all molecular weights of the polyol. In addition, the char yield increased when the higher molecular weight of polyol was added. The flexural modulus of polybenzoxazine also decreased from 6.2 GPa to be in range of 2.0-3.0 GPa with 30wt% of PU at every molecular weight of the polyol. Furthermore, the synergism with ultimate flexural strength in 90:10 BA:PU was obtained at all molecular weights used. The firing test suggested that the TDI-polyol (MW 3000) based urethane prepolymer had the suitable chain length for alloying with the benzoxazine resin particularly at the mass ratio of 80:20 BA:PU to yield a composite of best ballistic performance.

Department....Chemical Engineering.... Student's Signature. พากวัลย์ กมลไชยวานิช

Field of Study...Chemical Engineering... Advisor's Signature.

Academic Year.........2006............... Co-advisor's Signature.

ACKNOWLEDGEMENTS

CONTENTS

CHAPTER

LIST OF FIGURES

LIST OF TABLES

CHAPTER I

INTRODUCTION

1.1 Introduction

1.1.1 Armor History

The first known use of armor was by the Egyptians. The primitive armors were a cloth, shirtlike garment overlapped with bronze scales or plates sewn to it. The armor was very heavy, causing this style of protection to be short-lived. After that there is Greek technology refined armor by fashioning bronze plates to fit over distinct parts of the body. Their armor was the bronze breastplate and backplate, termed the cuirass, greaves, which protected the shins, and brass helmets (http://www.nps.gov). The armor was developed continuously until now. For soft armor, the aramid fabric body armor was used by U.S. army in 1973-1975. Moreover, During the Vietnam War, soft armors were prepared from fabrics of fiberglass and nylon and used for ballistic protection (Yang, 1993).

1.1.2 High performance fibers

The selection of the type, amount, and orientation of fibers is very important:
1. Specific gravity
2. Tensile strength and modulus
3. Compressive strength and modulus
4. Fatigue strength and fatigue failure mechanisms
5. Electric and thermal conductivities
6. Cost

High performance fibers have important characteristics such as light weight, high strength, high toughness, and high modulus so these pure fibers were used as soft armor many years ago.

Table 1.1: Comparison of selected high performance fibers (www.toyobo.co.jp).

Fiber types	Tenacity (GPa)	Modulus (GPa)	Elongation (%)	Density (g/cm^3)	Moisture Regain (%)	LOI	Heat Resistance (^{o}C)
p-Aramid	2.8	109	2.4	1.45	4.5	29	550
m-Aramid	0.65	17	22	1.38	4.5	29	400
Steel Fiber	2.8	200	1.4	7.8	0	-	-
HS-PE	3.5	110	3.5	0.97	0	16.5	150
PBI	0.4	5.6	30	1.4	15	41	550
Polyester	1.1	15	25	1.38	0.4	17	260
S-Glass	4.8	85	5.3	2.48	0.1	100	300

Note: HS-PE is high strength polyethylene, PBI is polybenzimidazole.

Kevlar^{TM} aramid fiber is an outstanding high performance fiber because of its high strength and high modulus. Its tenacity (strength per linear density unit) is greater than all conventional fibers. The continuous-use temperature of aramid fibers ranges from 160 to 200°C, and other advantageous properties are excellent fatigue and wear resistance, good electrical properties, high toughness, and good chemical resistance. There is a range of fiber types. In the case of DuPont, the Kevlar^{TM} range covers a spectrum of strength and modulus values, from low modulus Kevlar^{TM} 29, through high modulus Kevlar^{TM} 49, to very high modulus Kevlar^{TM} 149 and very high strength Kevlar^{TM} 129. (Schwartz, 1996) A variety of woven fabrics is also used in aircraft and helicopter parts, electrical wiring boards, coated fabrics, and also soft ballistic body armor. Woven fabrics of Kevlar^{TM} fiber are widely used in composites, armor, aircraft cargo liners, and marine applications. Besides the high strength and high modulus, Kevlar^{TM} has other properties that useful for ballistic application. These useful properties are its excellent thermal properties, highly crystalline and

highly oriented fine structure as well as high tensile properties. However, fibers alone can only exhibit tensile properties along the fiber's length. Composite structure was used to improve the properties of soft armors.

1.1.3 Polymer matrix for ballistic composite

Polymeric resins have been the most widely used matrix materials for composites reinforced by synthetic fiber. The resin matrix spreads the load applied to the composite between each of the individual fibers and also protects the fibers from damage caused by abrasion and impact. High strengths and stiffnesses, ease of moulding complex shapes, high environmental resistance all coupled with low densities, make the resultant composite superior to metals for many applications. The major advantages of composite materials are their high strength and stiffness, lightweight, corrosion resistance, crack and fatigue resistance, and design flexible as compared to metals and natural materials. Thermoset and thermoplastic resins are used as matrices for Kevlar^{TM}-reinforced composites. Thermoset composites are generally stiffer, more thermally stable, and more brittle than thermoplastic composites. Using of thermoset resin in a composite must be preformed by impregnating the fibers with a resin precursor, gelling, and curing to the solid state. The matrix material has the primary influence on mechanical properties if interlaminar shear strength, and compression and flexural strength, especially at high temperatures and also dictates the processibility of the composite and its environmental resistance.

A novel class of thermoset resin is called benzoxazine resin which has various outstanding properties such as high thermal stability, easy processibility because of its low viscosity, low water absorption, near zero shrinkage after processing with excellent mechanical properties, and ability to alloy with various types of resins.

Alloying benzoxazine resin with urethane prepolymer can improve the flexibility of the more rigid polybenzoxazine. Moreover, the synergism in glass transition temperature (T_g) has been observed and that the T_gs of the alloys are significantly greater than those of the parent polymers (Rimdusit et al., 2005). Because of the interesting properties of this polymer alloys, they are applied in the

ballistic armor applications. The ballistic composite that used Kevlar[TM] and benzoxazine-urethane alloys as reinforcing fiber and matrix, respectively was developed and under patent pending (Rimdusit et al., 2005). It was reported that the thickness of Kevlar[TM]-reinforced 80/20 BA/PU composite panel was 30 plies and 50 plies in order to resist the penetration from the ballistic impact of levels II-A and III-A, respectively. In this work, the molecular weight of polyol used for the synthesis of the urethane prepolymer was fixed at 2000. Varying the molecular weight of polyol is an interesting aspect. Studying about the effect of soft segment length on properties of polyurethanes suggested that the phase separation was enhanced with increasing soft segment length. It can also and can help decrease hydrogen bond distance and promote bond strength of fluorinated polyurethanes (Wang et al., 2005). The chain distance between junction points would affect the movement of the network, the number of crosslinked density, long heterogeneous network behavior, and ability to absorb the impact energy from projectile impact on ballistic armor, etc. All of those reasons are strongly support the use this polymer alloys with varied polyol molecular weight as the matrix resin in ballistic armor composite. In this work we will investigate the resistant of the armor composite penetration using benzoxazine-urethane alloys as matrix with various the molecular weight of polyol which used in urethane prepolymer synthesis. The effect on other mechanical and thermal properties of the matrices and their Kevlar[TM]-reinforced composites will also be studied.

1.2 Objectives

1. To study the effects of diol molecular weight on mechanical and thermal properties of benzoxazine-urethane polymer alloys for use as ballistic armor composite materials.
2. To study the suitable composition ratios of the polymeric alloys between benzoxazine and urethane resins to produce ballistic composites with the protection of level IIA or higher.

1.3 Scope of the Study

1. Determining of molecular weight of polyols using gel permeation chromatography (GPC).
2. Synthesizing of BA-a type benzoxazine resin and flexible urethane resin based on TDI-polypropylene glycol at various molecular weights of polypropylene glycol i.e. 1000, 2000, 3000 and 5000.
3. Mixing of the benzoxazine-urethane resins with composition ratios of 100:0, 90:10, 80:20, and 70:30 at 150 ^{o}C for at least 15 minutes or until the homogeneous mixture is obtained.
4. Investigating of the effect of polyol molecular weights on curing reaction or crosslinking process of the alloys at the above compositions.
5. Fabricating the Kevlar^{TM}-reinforced composites using the suitable matrices in (2) at a resin content of about 20 wt %
6. Fire test with 9 mm hand gun with full metal jacket, 124 grain projectile, (8.0g) (level IIA).
7. Evaluating of the relevant mechanical and thermal properties of the composite armor.

CHAPTER II

THEORY

2.1 Kevlar^{TM} Aramid Fiber

The discovery of Kevlar^{TM} aramid fiber began in 1965 when a Du Pont research scientist synthesized a series of *para*-oriented symmetrical super-rigid molecular chain and fiber of ultra-high modulus (Yang, 1993). In general, Kevlar^{TM} aramid fiber has a high breaking tenacity which is several times that of wire, industrial nylon, and polyester yarns. It also has a much higher tensile modulus than steel wire, fiberglass, nylon, and polyester fibers. Kevlar^{TM} has a low elongation at break, which is comparable to that of steel. It has a low density than steel and glass, which makes most Kevlar^{TM}-reinforced structures of a lighter weight for a given strength and stiffness. As an aramid, Kevlar^{TM} fiber is inherently stable at relatively high temperatures. It has a very small shrinkage at elevated temperatures, low creep, and a rather high glass transition temperature. In addition, it is corrosion resistant, non-conductive, and resistant to most chemicals except strong acids and bases. These outstanding properties make Kevlar^{TM} fiber products useful for many industrial and civilian applications. At present, it is offered in continuous filament yarns, staple, short fibers, colored yarns, pulp, and elastomeric masterbatch for a wide range of applications. It is used as a reinforcing fiber for composites, thermoplastics, tires, and mechanical rubber goods. Woven fabrics of Kevlar^{TM} aramid are used in protective apparel, parachute, ballistic body armor, and hard armor. It is also used in ropes and cables, friction products, gaskets, thixotropic sealants, and adhesives.

Kevlar^{TM} fiber offers excellent thermal stability which is inherent of aromatic polyamides. It will undergo severe degradation at temperatures above 500°C. Between 500°C and 540°C, the pyrolysis produced *p*-phenylenediamine, benzonitrile, aniline, benzanilide, and *N*-(4-aminophenly benzamide), which indicated the initiation of polymer degradation by the homolytic cleavage of the CO-NH and aromatic –NH

bonds and subsequent decarboxylation of carbonyl end groups. Many other pyrolysis by-products were observed at higher temperatures.

2.1.1 Typical properties of Kevlar[TM] aramid yarns

Table 2.1: Properties of various grades of Kevlar[TM] fiber (Yang, 1993)

Yarn properties	Kevlar[TM] 29	Kevlar[TM] 49	Kevlar[TM] 68	Kevlar[TM] 119	Kevlar[TM] 129	Kevlar[TM] 149
Tensile strength (GPa)	2.90	2.90	2.90	3.03	3.34	2.34
Initial modulus (GPa)	71.02	119.97	99.28	55.16	96.53	144.79
Elongation (%)	3.6	2.8	3.0	4.4	3.3	1.5
Density (g/cm^3)	1.44	1.45	1.44	1.44	1.45	1.47
Moisture regain (%)	6	4.3	4.3	-	-	1.5

Note: Yarn properties determined on 10 in twisted yarns (ASTM D-885)

Many wholly aromatic polyamides have been synthesized and shown to give excellent fiber properties. Kevlar[TM], Twaron (a registered trademark of Akzo BV, The Netherlands) and Technora (a registered trademark of Teijin Ltd, Japan) aramid fibers are those in commercial production at the present time.

2.2 Benzoxazine Resin

As the solubility of the majority of the bisphenols in the typical solvent used for benzoxazine synthesis is limited, a novel solventless synthesis procedure was a convenient method for preparation of benzoxazine monomer series as shown in Figure 2.1 (Ishida, 1996). Stoichiometric amounts of solid bisphenol, para-formal-

dehyde and liquid 3-aminophenylacetylene were mixed together at 110°C. The synthesis of monofunctional benzoxazines based on phenol is shown in Figure 2.2.

The molecular structure of polybenzoxazine often superb design flexibility that allows the properties of the cured materials to be controlled for the specific requirements of a wide variety of individual applications. This is because polybenzoxazine can be synthesized from a wide selection of raw materials consisting of phenolic derivatives and primary amines. Figure 2.1 shows two major types of polybenzoxazines.
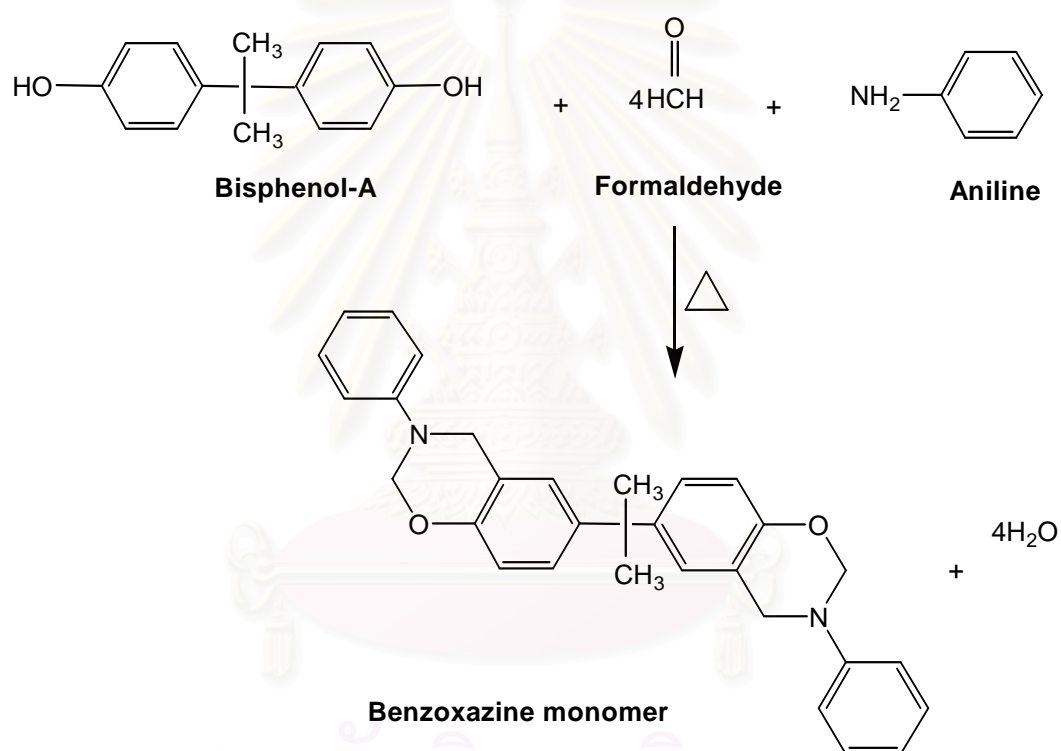
Figure 2.1: Synthesis of BA-a benzoxazine a bifunctional monomer.

Benzoxazine resins can be polymerized by heating and do not need a catalyst or curing agent. These two kinds of polybenzoxazines are different in reactants. The benzoxazine bifunctional monomers use bi-phenol and the benzoxazine monofunctional monomers use phenol to synthesize. Their properties are also different. The benzoxazine bifunctional monomer can be polymerized to yield network structure and the later can be polymerized to yield linear structure.
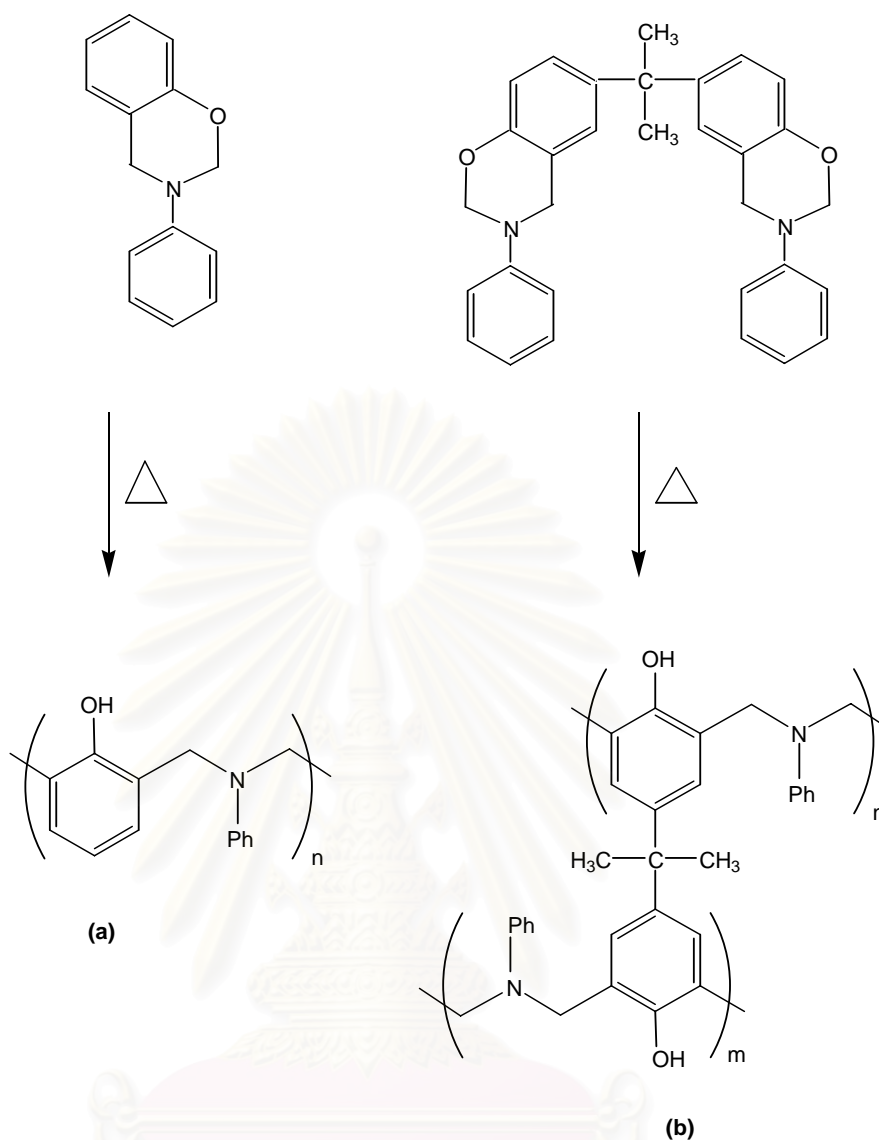
Figure 2.2: Structures of monofunctional and bifunctional.

2.3 Urethane Elastomer

Polyurethanes are a family of polymers that have widely different properties. They can be molded into pliable or rigid parts, formed into soft and resilient or hard and rigid foams, and applied as durable coatings. Polyurethanes can be either thermoplastics or thermosets.

A polyol (which means multiple alcohols or multiple OH groups) can have from two to many OH groups. Just as with a stepwise polymerization reaction, the polyol monomer must have at least two reactive groups in order to polymerize. If three or more reactive groups are present, crosslinks can form. The other monomer in the

reaction to form a urethane bond is an isocyanate which is the NCO combination of atoms. The type of chemical compounds that have two isocyanate groups are called diisocyanates. When a polyol reacts with an isocyanate, a molecular rearrangement occurs that creates a more stable molecular structure. The hydrogen bond is formed from the hydrogen on the polyol with the carbon in the isocyanate. Some previous bonds in the polyol and in the isocyanate break to allow these new bonds to form.

A urethane elastomer can be regarded as a linear block copolymer of the type as shown in Figure 2.3. This segmented polymer structure can affect its properties over a very wide range of strength and stiffness by modification of its three basic building blocks: the polyol, diisocynate, and chain extender. Essentially, the hardness range covered is that of soft jelly-like structures to hard rigid plastics. Properties are related to segmented flexibility, chain entanglement, interchain forces, and crosslinking.
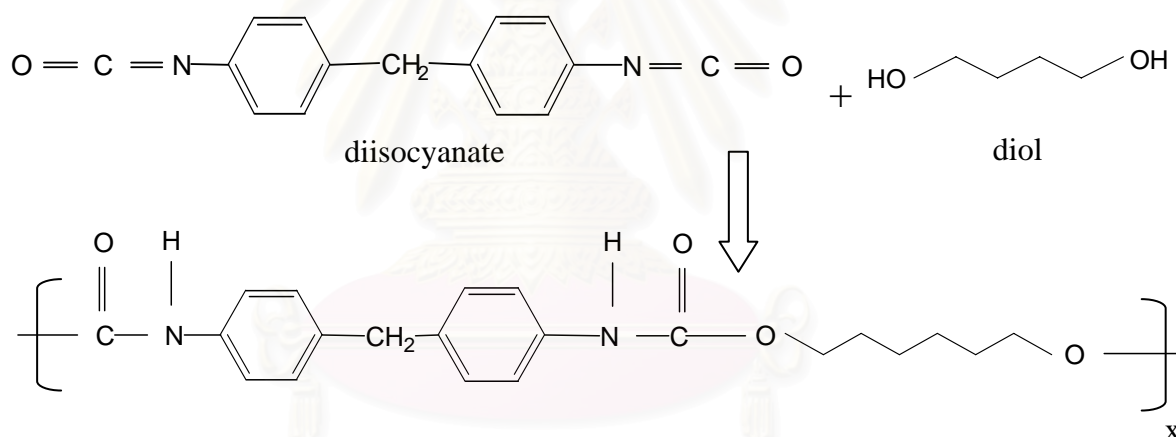
Figure 2.3: The basic unit in a urethane block copolymer.

2.3.1 Network between Benzoxazine Resin and Urethane Prepolymer

From previous work, Takeichi studied about synthesis and characterization of poly(urethane-benzoxazine) flims. The poly(urethane-benzoxazine) films as novel polyurethane (PU)/phenolic resin composites were prepared by blending a benzoxazine monomer (BA) and TDI-polyethylene adipate polyol (MW 1000) based PU prepolymer. FT-IR spectroscopic technique was used to investigate the reaction between benzoxazine resin and urethane prepolymer. From the experiment, the

mechanism of benzoxazine-urethane alloys was reported as the figure 2.4. (Takeichi et al, 2000)
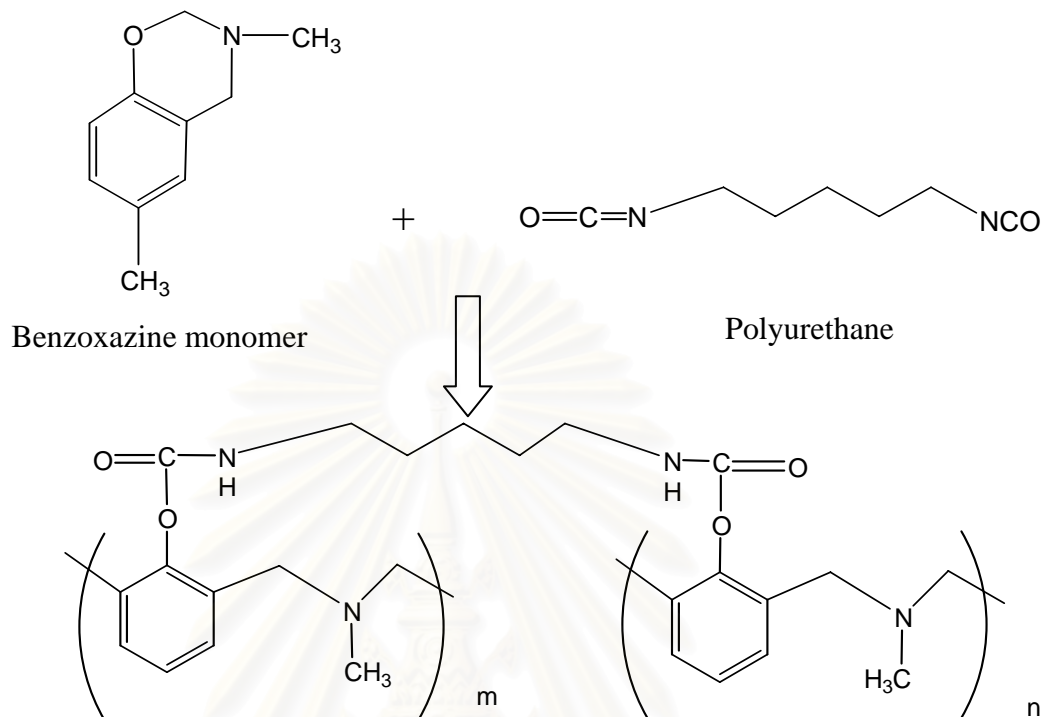
Figure 2.4: Benzoxazine-Urethane crosslinked

2.4 Armor Systems

2.4.1 Fibrous armor systems

2.4.1.1 Soft armor system

There are two types of armor that are prepared from woven fabrics. They are the soft body armor and the soft armor structure. Soft body armor is used as the protective garment for military and law enforcement personnel against ballistic injuries. There are presently two types of ballistic threats: the penetration of handgun bullets and the piercing of fragmented shells. The soft body armor is prepared in the form of a vest to protect the torso of a human body as shown in Figure 2.5.

Figure 2.5: A Soft Body Armor

2.4.1.2 Composite armor system

Non-structural composite armor is often regarded as a parasitic armor element because it is added to an existing structure to provide ballistic protection. The existing structure may be a car, truck, ship, engine case, or shelter.

Structural armors are load-bearing while providing ballistic resistance. They are used on armored vehicles, military vessels and vehicles, shelters, shields, etc. They are prepared from multiple layers of fabrics combined with a resin binder. The resin content is carefully controlled to achieve a balance of structural and ballistic properties.

2.4.1.3 Ballistic resistance of p-aramid fibers

Ballistic performance is determined by more than simple fiber toughness or area under the stress-strain curves. In Figure 2.6 shows that a fiber is struck transversely by a high speed projectile, a longitudinal stress wave propagates outward at the speed of sound in the fiber. Figure 2.6, it is evident that there must be some transverse deflection to load the fiber effectively in tension; otherwise the fiber will be sheared and ballistic resistance considerably reduced. Woven fabrics were found to be a practical product form for ballistic resistant articles because of their extensive interactions among yarns due to crossovers.

Transverse deflection causes loading of crossover yarns so that up to 50% of the total energy absorption may occur in these secondary yarns. There are negative aspects to crossover, however, and fabrics must be carefully constructed to balance these effects.
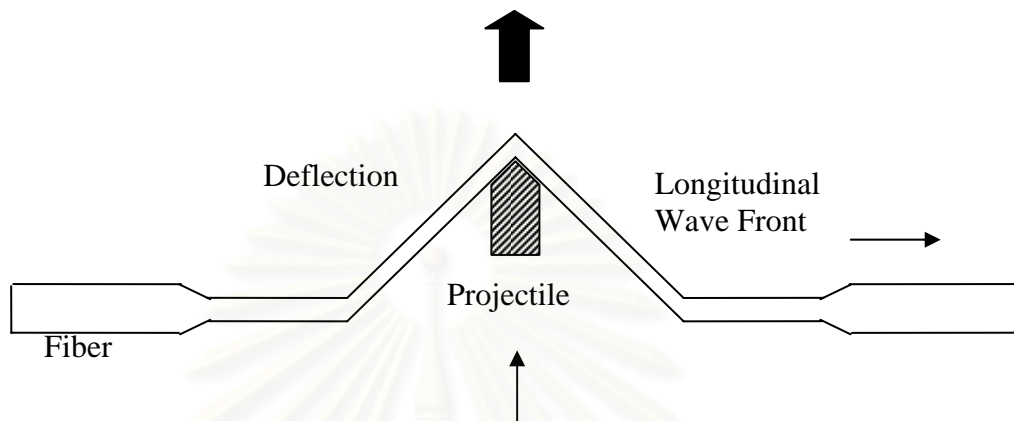
Figure 2.6: A fiber being hit by a projectile. (Lewin et al, 1989)

2.4.2 Ballistic standard of body armor.
(www.justnet.org/txtfiles/BodyArmorStd/NIJSTD010103.html)

2.4.2.1 NIJ Standard for the Ballistic Resistance of Police Body Armor

Police body armors covered by this standard are classified into seven types, by level of ballistic protection performance. The classification of an armor panel that provides two or more levels of ballistic protection at different locations on the ballistic panel shall be that of the minimum ballistic protection provided at any location on the panel.

2.5 Guideline for Ballistic Resistant Test

Firstly, the test specimen should be conditioned at a temperature of 20 to 28°C (68 to 82°F) for at least 24 hours prior to test. Then the triggering devices are placed 2 and 3 m (6.6 and 9.8 ft.), respectively from the muzzle of the test weapon as shown in Figure 2.7, and arranged them so that they define planes perpendicular to the line of flight of the bullet. The distance between the devices should be measured with an

accuracy of 1.0 mm. (0.04 in.) using the time of flight and distance measurements to calculate the velocity of each test round. After the specified test weapon has been supported, leveled, and positioned, fire one or more pretest rounds (as needed) through a witness plate to determine the point of impact. Place the test specimen in the support fixture and position it 5 m. (16 ft.) from the muzzle of the test weapon. Then position an imperforated witness plate 15 cm. (6 in.) beyond the test specimen. Fire a test round and record the velocity of the bullet as measured by the chronograph. Examine the witness plate to determine penetration, and examine the specimen to see if the bullet made a fair hit. If no penetration occurred, reposition the test specimen and repeat the procedure with additional test rounds until the test is completed. Space the hits as evenly as possible so that every portion of the test specimen is subject to test.
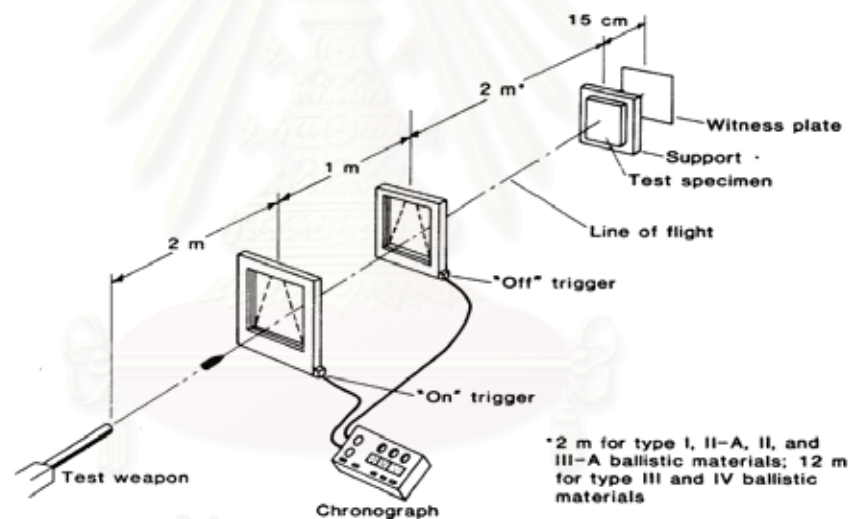
Figure 2.7: Ballistic test setup

Table 2.2: Test summary.

Bullet	Armor Type	Test Ammunition	Nominal Bullet Mass	Suggested Barrel Length	Required Bullet Velocity
	I	.22 LRHV Lead	2.6 g 40 gr	15 to 16.5 cm 6 to 6.5 in	320 ± 12 m/s 1050 ± 40 ft/s
		38 Special RN Lead	10.2 g 158 gr	15 to 16.5 cm 6 to 6.5 in	259 ± 15 m/s 850 ± 50 ft/s
	II-A	.357 Magnum JSP	10.2 g 158 gr	10 to 12 cm 4 to 4.75 in	381 ± 15 m/s 1250 ± 50 ft/s
		9 mm FMJ	8.0 g 124 gr	10 to 12 cm 4 to 4.75 in	332 ± 12 m/s 1090 ± 40 ft/s
	II	.357 Magnum JSP	10.2 g 158 gr	15 to 16.5 cm 6 to 6.5 in	425 ± 15 m/s 1395 ± 50 ft/s
		9 mm FMJ	8.0 g 124 gr	10 to 12 cm 4 to 4.75 in	358 ± 12 m/s 1175 ± 40 ft/s
	III-A	.44 Magnum Lead SWC Gas Checked	15.55 g 240 gr	14 to 16 cm 5.5 to 6.25 in	426 ± 15 m/s 1400 ± 50 ft/s
		9 mm FMJ	8.0 g 124 gr	24 to 26 cm 9.5 to 10.25 in	426 ± 15 m/s 1400 ± 50 ft/s
	III	7.62 mm 308 Winchester FMJ	9.7 g 150 gr	56 cm 22 in	838 ± 15 m/s 2750 ± 50 ft/s
	IV	30.06 AP	10.8 g 166 gr	56 cm 22 in	868 ± 15 m/s 2850 ± 50 ft/s

Abbreviations: AP - Armor Piercing   LRHV - Long Rifle High Velocity

FMJ - Full Metal Jacket   RN - Round Nose

JSP - Jacketed Soft Point   SWC - Semi-Wad cutter

2.5.1 Theories on ballistic impact (Yang, 1993)

According to classical ballistic theories, the ballistic resistance of a textile fabric to a projectile is generally attributed to its absorption of kinetic energy upon ballistic impact. This is analyzed by a way of simple ballistic impact in the longitudinal (axial) and transverse directions of a fiber. When a longitudinal impact is applied to a fiber at velocity V, a longitudinal wave will be generated along the fiber at a velocity c. The fiber material behind the wave is subjected to a strain e of

$$e = V/c \qquad\qquad (2.1)$$

$$c = \sqrt{E/\rho} \qquad\qquad (2.2)$$

where c is the velocity of the longitudinal, E is fiber modulus and ρ is fiber density. Thus, the velocity of wave propagation increases with the square root of fiber modulus and inversely with the square root of fiber density. The higher the fiber modulus, the higher the wave velocity and the greater the volume of fiber capable of interacting with the projectile.

If E is expressed in grams per denier and c in m/s, the above equation can be written as

$$c = \sqrt{kE} \qquad\qquad (2.3)$$

where $k = 88260$. The stress associated with the strain e is given by

$$\rho = Ee = V\sqrt{E/k} \qquad\qquad (2.4)$$

The ballistic dynamics is considerably more complicated when a fiber is impacted transversely than longitudinally.

In general, there are three major modes of failure: matrix cracking in the lamina, fiber breakage, and delamination. Among all these modes of impact damage, delamination has a major effect on impact energy absorption. Therefore, the impact

energy of the composites is related to change of delamination area. Park and Jang observed the effect of laminate thickness on impact behaviour of aramid fiber/vinylester composites. Flexibility of the composite was decreases with increasing of the laminate thickness. The increase of brittleness changes the failure mode of thick laminates. The impact property of thick laminates is primarily dominated by local stress rather than plate bending stress. The impact damage initiates on the impacted surface by the large local stress generated close to the point of impact as shown in Figure 2.8(b). Each aramid layer cannot undergo full deformation because adjacent aramid layers restrict its deformation. This leads to a gradual increase in total impact energy of thick laminates in spite of a large increment of initiation energy (Park and Jang, 2003). From the report suggested the delamination is a key parameter on the energy absorption.
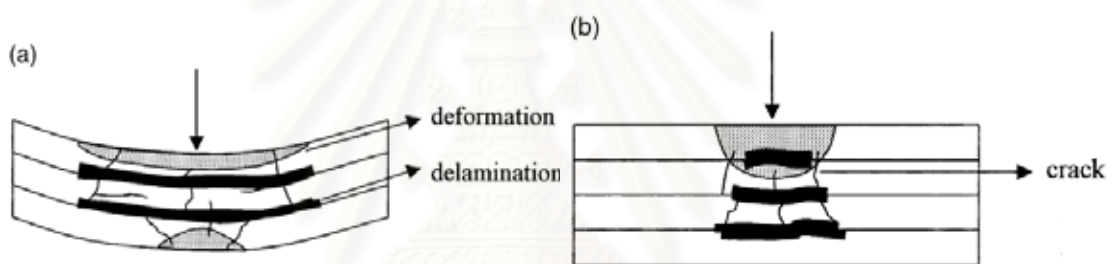
Figure 2.8: The impact damage of thin and thick laminates: (a) thin laminate
(b) thick laminate

CHAPTER III

LITERATURE REVIEWS

As long as man has been around, there has been fighting, and as long as there has been fighting, one individual has sought an advantage over his enemy. Governments have always funded research in order to better understand the world around them, and part of this understanding has been to develop better weapons. Modern armor was born during World War II and the Korean War became the testing ground for more capable and light weight body armor. Technical advances in our ability to composite materials for ballistic protection have changed rapidly in the last 30 years. Most important aspects in ballistic protection are the mechanisms of energy absorption at ballistic speeds. The tenacity and elongation to break determine the amount of energy that can be absorbed by an amount of fibers. The specific modulus determines the sonic velocity in the fiber and that indicates the area of the fabric that is involved in stopping the projectile. Figure 3.1 shows the specific energy absorption and the sonic velocity of fibers: the primary factors that determine the weight needed to stop a projectile.
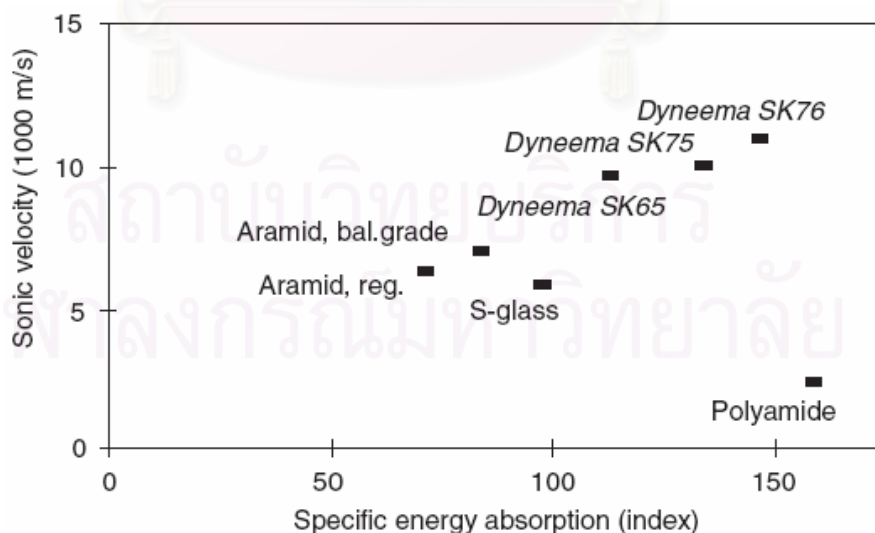
Figure 3.1: Energy absorption and sonic velocity in ballistic fibers
(Mukhopadhyay and Joyce, 1993)

Kevlar[TM] fiber was used in lightweight soft body-armor which the plies have a collective areal density of no greater than 6.36 kg/m^2, and a V50 ballistic limit no less than 587 m/s using a .22 caliber, 17 grain FSP at 0 degrees obliquity (Park, 2003). The improvement of ballistic armor by composite technology was reported. Bhatnagar and coworkers disclosed a system of a fabric woven from a high strength, high modulus yarn, a surface coating of a low modulus elastomer and a plastic film bonded to its elastomer-coated surface. The woven fabric laminates was reported to possess superior resistance to penetration by ballistic projectiles (Bhatnagar et al., 2003). A fibrous layer comprising a network of high strength filaments having a tenacity of at least about 0.88 GPa, a tensile modulus of at least about 20 GPa and energy-to-break of at least about 8 J/g in a rigid matrix material was evaluated by Li et al. The matrix of the composite can be both of thermoplastic and thermosetting polymers (Li et al., 1994). Therefore, an advantage of ballistic composite armor was widely use with various polymer matrix. A composite fabric having an areal density of less than about 4.64 kg/m^2 and being able to pass the NIJ IIIA specification in response to a 0.44 magnum projectile incoming at a velocity of about 427- 442 m/s was reported. The composite woven fabric made up of at least two plies of individual woven fabric bonded together by a layer of flexible bonding resin disposed on the juxtaposed surfaced of the individual woven fabrics. An anti-ballistic composite fabric is made up of at least these bonded woven fabrics sub-composites, preferably in combination with conventional non-woven fabric layers. This composite attributed to reduce the truma conventionally caused by the impact of a ballistic projectile. (Coppage et al., 2000) Modern armor was born during World War II and the Korean War became the testing ground for more capable and light weight body armor. Prior to the Korean War, the materials used as armor protection were relatively simple in form and basic in composition. Technical advances in our ability to fabricate composite materials for ballistic protection have changed rapidly in the last 30 years. Characteristic of matrix resin was known to play a key role in the performance of each ballistic composite. Some important parameters for suitable matrix resins needed to be considered include its rigidity, processing ability, its viscosity, curing temperature, and shelf-life. Table 3.1 reveals some of the United States patents of polymer composite ballistic armor.

Table 3.1: Review on United States patents of polymer composite ballistic armor

Fiber	Matrix	Matrix Properties	Reference
1. Spectra™	Thermosetting - epoxy	- elastomer - modulus 500,000 psi - strength 3,000 psi at high temp. below the melting point of fiber	Patent No. 4,748,064 Date: May 31, 1988 Patent No. 4,403,102 Date: Sep 6, 1983
	Matrix	**Matrix Properties**	**Reference**
	Thermoplastic elastomer - thermoplastic elastomer - urethanes - styrene-isoprene-styrene (SIS) dissolved in methylene chloride	- areal density 4.5 oz/yd. - T_g = -70 to 0°C - low modulus - below the melting point of fiber - T_g = -55°C - melt index = 9 g/min using - modulus 100 psi at 300% elongation	Patent No. 5,724,670 Date: Mar 10, 1998 Patent No. 5,534,343 Date: Jul 9, 1996 Patent No. 4,403,102 Date: Sep 6, 1983 Patent No. 5,480,706 Date: Jan 2, 1996 Patent No. 5,093,158 Date: Mar 3, 1992 Patent No. 4,748,064 Date: May 31, 1988
2. Kevlar™	Thermosetting - phenolic resin - polyester - epoxy	- impact strength 17 J/m, 32 mm thick - T_g = 170°C - elastomer - modulus 500,000 psi strength 3,000 psi at high temp	Patent No. 5,190,802 Date: Mar 2, 1993 Patent No. 4,748,064 Date: May 31, 1988 Patent No. 4,639,387 Date: Jan 27, 1987 Patent No. 4,550,044 Date: Oct 29, 1985 Patent No. 5,102,723 Date: Apr 7, 1992 Patent No. 3,956,447 Date: May 11, 1976
	Thermoplastic - urethanes - styrene-isoprene-styrene (SIS)	- T_g = -70 to 0°C - low modulus - T_g = -55°C - melt index = 9 g/min using - modulus 100 psi at 300% elongation	Patent No. 4,639,387 Date: Jan 27, 1987 Patent No. 5,480,706 Date: Jan 2, 1996

Fiber	Matrix	Matrix Properties	Reference
3. Glass Fiber	Thermosetting - phenolic - polyester	- moldable - MW. Range 800 to 5,000 or more	Patent No. 5,215,813 Date: Jan 1, 1993 Patent No. 4,639,387 Date: Jan 27, 1987 Patent No. 4,550,044 Date: Oct 29, 1985
	Thermoplastic - urethane - styrene-isoprene-styrene (SIS)	- flexibility - resistance to degradtion - T_g = -55°C - melt index = 9 g/min using - modulus 100 psi at 300% elongation	Patent No. 4,639,387 Date: Jan 27, 1987 Patent No. 4,822,439 Date: Apr 18, 1989
4.Polybenzoxazole and Polybenzothiazoe	- are not limited to thermoplastic or thermosetting		Patent No. 6,268,301 B1 Date: Jul 31, 2001
	Thermoplastics - polybenzoxazole or polybenzothiazoe	- low flammability - low smoke - high temperature stability - high chemical and solvent resistance - high strength and modulus	Patent No. 5,196,259 Date: Mar 23, 1993
5. Mixed Fibers - aramid andcarbon - aramid and glass - carbon and glass - carbon, glass and spectra	- ethylene-acrylate, methacrylate copolymer, vinyl ester phenilic polyimide, polycarbonate or the like	- high modulus - higher in impact resistance	Patent No. 4,732,803 Date: Mar 22, 1988

Table 3.1 suggests that several types of fibers can be used with thermoplastics and also thermosets which have relatively broad range of properties depending on the intended applications. The matrix resins which are thermoplastic resins can be heated and softened, cooled, and hardened for limitless times without undergoing a basic alteration. On the other hand the thermosetting resins do not tolerate thermal cycling and cannot be reworked after molding. The outstanding characteristic of

thermosetting resins is their inherent structural integrity, high thermal stability whereas common-typed thermoplastic polymers are more flexible and less thermally stable. (Li et al., 1994)

Benzoxazine resins have various outstanding properties such as high thermal stability, easy processibility, low water absorption, near zero shrinkage after processing with excellent mechanical properties. The monomer of this resin is synthesis by solventless method and has no by-product during polymerization. Other advantage of this new resin is an ability to alloy with several kinds of resins. Alloying of benzoxazine resins with other resins was reported by many researchers. For example, the addition of epoxy to the polybenzoxazine network greatly increases the crosslink density of the thermosetting matrix and strongly influences its mechanical properties (Ishida et al., 1996). A ternary system of benzoxazine, epoxy, and phenolic resins was also developed as a new class of electronic packaging materials. In this system, a glass transition temperature as high as 170 ^{o}C and considerable thermal stability at 5% weight loss up to 370 ^{o}C can be obtained (Rimdusit et al., 2000).

In 2005, Rimdusit et al. reported the comparison of benzoxazine alloying with IPDI-based urethane prepolymers and with flexible epoxy. Interestingly, the positive deviation on the glass transition temperature (T_g) of the benzoxazine-urethane alloys was clearly observed, i.e. T_g of the benzoxazine-urethane alloys were significantly greater (T_g beyond 200 ^{o}C) than those of the parent polymers (Tg of the polybenzoxazine is equal to 165 ^{o}C and that for urethane is equal to -71 ^{o}C). Furthermore, the glass transition temperature of the benzoxazine-urethane alloy was increased with an increase of the polybenzoxazine content. The poly(benzoxazine-urethane) films also showed excellent resistance to solvents such as tetrahydrofuran and the thermal stability of polyurethane was greatly enhanced even with the incorporation of a small amount of the polybenzoxazine (Takeichi et al., 2000). The alloying of benzoxazine resin and urethane resin is highly suitable for use as a matrix resin in ballistic armor composite because the benzoxazine resin possesses high rigidity while polyurethane is highly flexible. The benzoxazine-urethane alloy can be tailored its properties to be not too rigid like the neat polybenzoxazine. Pathomsap reported that the thickness of Kevlar^{TM}-reinforced 80/20 BA/PU composite panel was

30 plies and 50 plies in order to resist the penetration from the ballistic impact of levels II-A and III-A, respectively. The molecular weight of polyol used for the synthesis of the urethane prepolymer was fixed at 2000 (Pathomsap, 2005). There are some investigations about the effect of molecular weight of soft segment (polyol) in polyurethane. Those studies suggested that phase separation increased as the soft-segment molecular weight increased also, T_g decreased when the soft-segment molecular weight increased. The lower molecular weight of polyols presented more miscibility between the hard and soft segment (Jimenez et al., 2000). Phase separation is enhanced with increasing soft segment length and decrease hydrogen bond distance and promotes bond strength (Wang et al., 2005). The mechanical properties of polyurethane based on poly(ε-caprolactone) and 1,4-butane diisocyanate by varying molecular weights of polyol with uniform hard segment was reported as shown in figure 3.2 and table 3.2. The lower molecular weight of polyol yields a higher rubber plateau but the modulus will decrease (Heijkants et al, 2005).
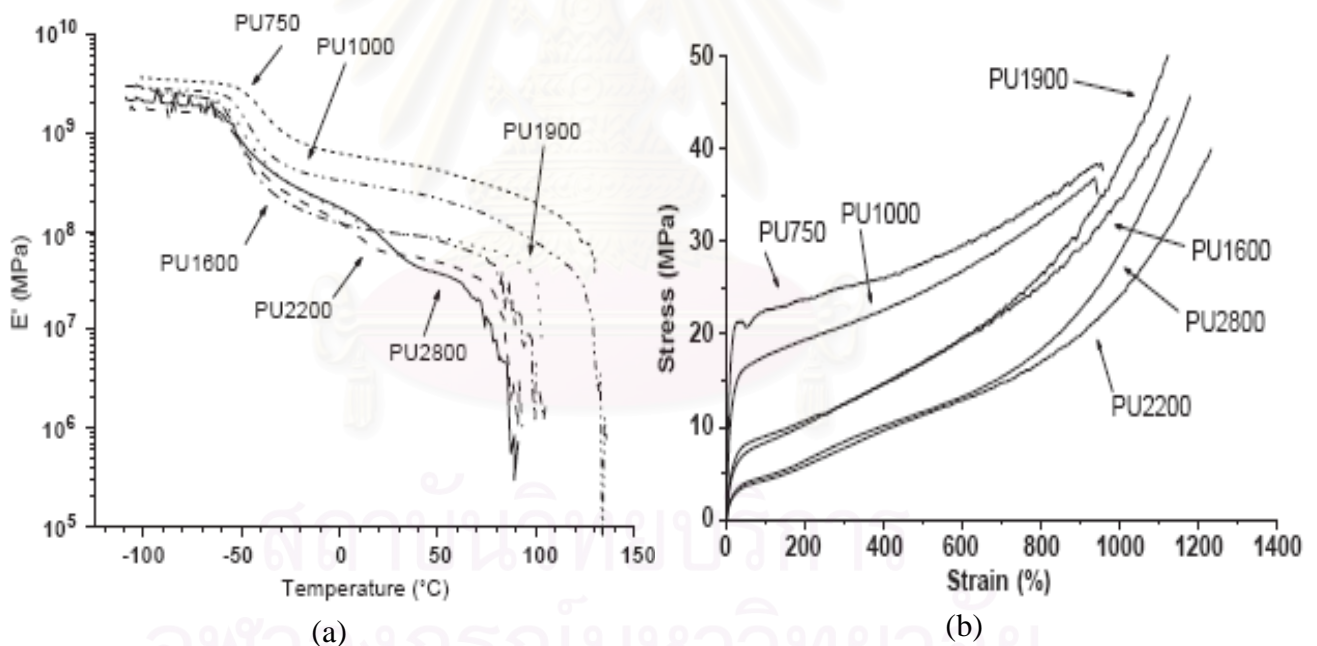
Figure 3.2: a) Storage modulus versus temperature for PU_x polyurethanes

b) Stress strain curves of PU_x copolymers at room temperature

Table 3.2: Mechanical properties of PU_x polymers

Polymer code	Young's modulus (MPa)	Strain at break (%)	Tensile strength (MPa)	Yield stress (MPa)	Toughness (MPa)
PU 750	263.9	870	38.7	16.2	251.3
PU1000	149.0	994	37.8	10.3	245.3
PU1600	64.6	1081	43.6	6.4	229.2
PU1900	54.6	1173	55.0	5.5	215.9
PU2200	30.1	1150	38.4	4.8	169.8
PU2800	33.8	1196	47.8	4.7	201.8

The alloying of these two types of resins by various the molecular weights of polyol that use in polyurethane prepolymer synthesis and use it's as ballistic matrix composite strongly optimize the molecular weight of polyol that suitable for the ballistic application included the energy absorption and also used for life protection.

CHAPTER IV

EXPERIMENT

4.1 Materials

The materials used in this research are benzoxazine resin, urethane resin and Kevlar™ fiber. The fiber was purchased from Thai Polyadd Limited Partnership. Benzoxazine resin is based on bisphenol, aniline and paraformaldehyde. The bisphenol A (polycarbonate grade) was supplied by Thaipolycarbonate Co., Ltd (TPCC). Para-formaldehyde and aniline were purchased from Merck Company and Panreac Quimica SA Company, respectively. Urethane prepolymer was prepared using toluene diisocyanate and polyether polyol. The toluene diisocyanate was obtained from South City Group and the poly(propylene glycol) with the molecular weights of 1000, 2000, 3000. and 5000 were supported by TPI Polyol CO., LTD.

4.2 Preparation of Resins

4.2.1 Benzoxazine resin preparation

Bisphenol A, aniline, and paraformaldehyde at a 1:2:4 molar ratio were used for the synthesis of benzoxazine monomer (Ishida, 1996). These three reactants were continuously mixed at about 110°C for approximately 2 hours. The benzoxazine monomer was obtained as clear-yellowish solid at room temperature. The product was then ground into fine powder and can be kept in a refrigerator for future-use.

4.2.2 Urethane resin preparation

The urethane prepolymer was prepared from toluene diisocyanate and poly(propylene glycol) at a stoichiometric molar ratio using various molecular weights of the poly(propylene glycol) i.e. 1000, 2000, 3000 and 5000. The two reactants were directly mixed in a four-necked round bottomed flask and the mixture

was continuously stirred under a nitrogen stream at about 60°C for 2 hours to yield a light yellow prepolymer. Then, the urethane prepolymer was cooled to room temperature and was kept in a refrigerator for future-use. The urethane prepolymers were labeled as PU1K, PU2K, PU3K, and PU5K according to the molecular weights of the poly(propylene glycol) of 1000, 2000, 3000, and 5000 respectively.

4.3   Benzoxazine:Urethane Binary Mixture Preparation

The benzoxazine monomer was mixed with PU1K, PU2K, PU3K, and PU5K at a desirable mass fraction. The mixtures were heated at 150°C in an aluminum pan and were mixed mechanically for about 15 minutes to obtain a homogeneous mixture. The weight ratios of the benzoxazine (BA) and urethane (PU) binary mixtures at BA:PU = 100:0, BA:PU = 90:10, BA:PU = 80:20, and BA:PU = 70:30 were evaluated as potential matrices for Kelar[TM]-reinforced composites for ballistic armor application.

4.4   Kevlar[TM] Reinforce Composites Preparation

The Kevlar[TM] fabric was pre-impregnated with the binary mixture resins using the hand-lay up procedure at 80°C. The weight fraction of the fiber was maintained at approximately 70-80% by weight which is the optimal fiber content reported by Park, 2003. The compound was compression-molded at 160°C and at a hydraulic pressure of 13.7 MPa for 120 minutes. The samples were then removed from the compression molder to an air-circulated oven for post step-curing at 170°C, 180°C, and 200°C for 120 minutes at each temperature. The specimens were finally left to cool down to room temperature and were ready for the characterizations.

4.5   Characterization Methods

4.5.1   Gel permeation chromatography (GPC)

The molecular weights of the polyol for the urethane prepolymer preparation were measured by gel permeation chromatography. The analysis was performed at 40°C on a Waters 600 using three Waters Styragel® HT columns (Styragel® HT 0.5, Styragel® HT 1, and Styragel® HT 4). The detector is Waters 2414 refractive index measurement (RID). Molecular weights are relative to monodisperse polystyrene standards. GPC measurements were performed with THF. Sample solutions were prepared at a concentration of 0.25% (w/v) by dissolving the polyol (polypropylene glycol) in tetrahydrofuran (THF) mobile phase at room temperature.

4.5.2　Differential scanning calorimetry (DSC)

A differential scanning calorimeter (DSC) model 2910 from TA Instruments was used to study the curing behaviors of the benzoxazine resin:urethane prepolymer mixtures and their prepregs. All samples were placed in a non-hermetic aluminum pan with aluminum lid. The mass of the sample is in range of 3-5 mg. The experiment was performed at a heating rate of 10°C/min under nitrogen purging. The glass transition of the alloys and their composites can also be obtained using a DSC scan in the range of 30-300°C at a heating rate of 10°C/min under N$_2$ purging.

4.5.3　Fourier transform infrared spectroscopy (FT-IR)

FT-IR spectra of all samples under various curing methods were acquired by using a Spectrum GX FT-IR spectrometer from Perkin Elmer. The apparatus is equipped with a KBr beam splitter and a deuterated triglycine sulfate (DTGS) detector. All spectra were taken with 32 scans at a resolution of 4 cm^{-1} and a spectral range of 4000-400 cm^{-1}. For urethane prepolymer samples, a tiny amount of a viscous liquid sample, about 0.5-1.0 mg., was swept on a potassium bromide (KBr) window.

4.5.4　Thermal degradation evaluation

Thermal stability and thermal decomposition of the cured polymer alloys were studied using a Simultaneous DSC-TGA Q600 SDT from TA Instruments. The

experiment was done using a heating rate of 20°C/min under nitrogen atmosphere. The temperature was ramped from 30°C to 900°C using a sample mass of about 10 mg. The degradation temperature at 5% weight loss and the char yield at 900°C were recorded for each specimen.

4.5.5 Density measurement

The density of the polymer alloys were measured by a water displacement method according to ASTM D792-91 (Method A). All specimens were prepared in a rectangular shape of 50 mm$\times$25 mm$\times$1 mm and weighted both in air and in water. The density was calculated using the following equation:

$$\rho = \left(\frac{A}{A-B} \right) \rho_o \qquad (4.1)$$

where ρ = Density of the specimen (g/cm^3)

A = Weight of the specimen in air (g)

B = Weight of the specimen in water (g)

ρ_o = Density of the liquid at the given temperature (g/cm^3)

4.5.6 Solvent extraction

The polymer alloy and composite specimens at a mass of approximately 1 g. were immersed in 20 ml of chloroform for crosslinking network investigation. The mass of the residual solid and pictures of the specimen were measured up to 30 days.

4.5.7 Flexural property measurement

The flexural properties of the BA:PU alloys and their composite specimens were determined using a universal testing machine (model 5567) from Instron Co., Ltd. The test method was a three-point bending mode with a support span of 32 mm using a constant crosshead speed of 0.85 mm. /min. The sample dimension is 25 mm.

in width, 50 mm. in length, and 2 mm. in thickness. The flexural properties were determined following ASTM D 790M-93 according to the equations:

$$E_B = \frac{L^3 m}{4bd^3} \tag{4.2}$$

$$S = \frac{3PL}{2bd^2} \tag{4.3}$$

where
E_B = Flexural modulus (MPa)

S = Flexural strength (MPa)

P = Load at a given point on the load-deflection curve (N)

L = Support span (mm)

b = Width of beam tested (mm)

d = Depth of beam tested (mm)

m = Slope of the tangent to the initial straight-line portion of the load-deflection curve (N/mm)

4.5.8 Dynamic mechanical analysis

A dynamic mechanical analyzer (DMA) model DMA242 from NETZSCH was used to investigate specimens' dynamic mechanical properties. The dimension of each specimen was 50 mm×10 mm×2 mm. The strain was applied sinusoidally with a frequency of 1 Hz and the specimen was heated at a rate of 2°C/min from room temperature to 300°C. The storage modulus (G'), loss modulus (G''), and loss tangent (tan δ) were then obtained. The glass transition temperature was taken as the maximum point on the loss modulus curve in the temperature sweep test.

4.5.9 Ballistic impact test

The tested composite panel was approximately 12.5 cm×12.5 cm with varied thicknesses depending on the number of layers of Kevlar[TM] cloth used. Only one impact per specimen was chosen in the fire test. The Kevlar[TM]–reinforced

polybenzoxazine alloy plates were approximate 2.0 mm thick corresponding to 4-plies of the laminated composite. The laminates were tested using a 9 mm handgun as shown in Figure 4.1 and were impacted by a standard grain (124 grains) of a round lead projectile with copper outer coating. The obtained velocity of the projectile was measured to be about 358 m/s. The first test was to evaluate the most suitable composition of the benzoxazine-urethane matric alloys for ballistic protection. The laminates with a combined thickness of 2 pieces of Kevlar^{TM}-reinforced composite having 4 plies per piece were used in the test. The second test was to evaluate the most suitable molecular weights of the polyol that used for the preparation of the urethane prepolymers in benzoxazine-urethane matric alloys. A pair of laminates of Kevlar^{TM}-reinforced composite plates similar to the first test was used in the test.

Figure 4.1 The 9 mm handgun for the fire test
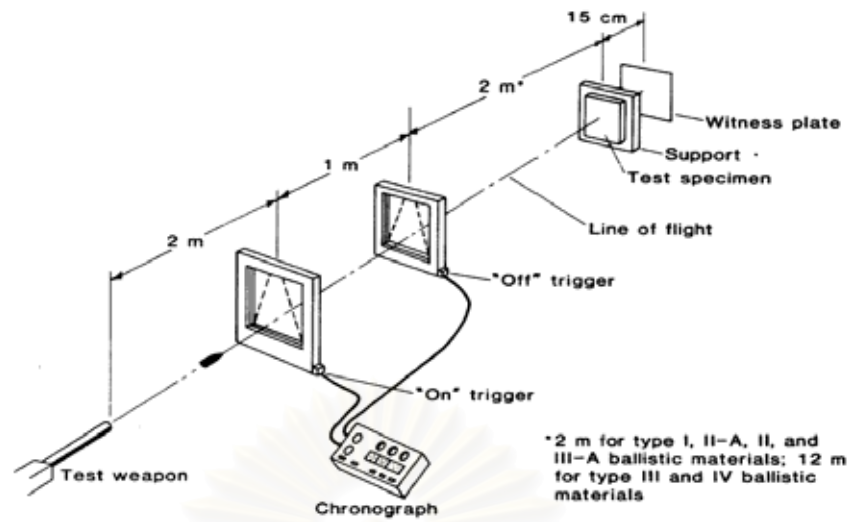
Figure 4.2 Testing scheme used for the NIJ standard ballistic test

CHAPTER V

RESULTS AND DISCUSSION

5.1 Determination of Polyol Molecular Weight

Table 5.1 shows the molecular weight of polyols utilized in this work. It was evaluated and compared with the molecular weights given by the supplier (TPI Polyol CO., Ltd.). The results showed that the molecular weight of polyols measured by Gel Permeation Calorimeter (GPC) was in relatively good agreement with the molecular weight derived from the monomer/initiator ratio obtained from the supplier. The polydispersity index (PDI) of the polyols was relatively narrow and quite constant with different molecular weights. Moreover, the PDI values of all types of polyol were close to unity. This behaviour indicated that most of chain lengths of the all types of polyols molecule were equal.

5.2 Determination of Density

In this study, the density measurements of all specimens were applied to evaluate the presence of void in polymeric alloys specimens. Figure 5.1 shows the density of all specimens with various molecular weights comparing with their theoretical density. Adding the urethane prepolymer, which is a more viscous resin into benxozaxine resin, slightly affects the density of polymeric alloys. This figure indicated that the densities gradually decreased with increasing the PU mass fraction. In addition, the density also tended to decrease with increasing the molecular weight of polyol. Because of the high viscosity of urethane prepolymer, adding more urethane prepolymer directly affected on the mixing behaviour. Their densities were deviated from theoretical density to a lower value possiblly because of the presence of void in the specimens as a result of mixing difficulty of the urethane fraction.

5.3 Fourier Transform Infrared Spectroscopic Investigation

The chemical structures of neat resins and their formation reactions were studied by FT-IR spectroscopic technique. The urethane prepolymer using in this work was synthesized by a reaction between toluene diisocyanate (TDI) and polyether polyol with various molecular weights e.g. 1000, 2000, 3000, and 5000. The important functional groups of the PU prepolymer are N=C=O, C=O, CH_2 and CH_3 which were used to characterize the presence of the prepolymer in the polymerization reaction. Figure 5.2 shows the spectra of the urethane prepolymer at various molecular weights. In general, the absorbance of urethane carbonyl linkage (C=O) is located at 1740-1710 cm^{-1}. The band at 2280-2240 cm^{-1} is assigned to the N=C=O stretching absorption peak which is an unreacted-isocyanate group. In our spectrum the peak observed at 1729 cm^{-1} was designated to the urethane carbonyl group and the N=C=O stretching absorption peak was assigned at 2274 cm^{-1}. In these spectra, we observed that an increase in the molecular weight of polyol tended to decrease the peak height at 1729 wavenumber. It is also confirmed that the urethane carbonyl linkage were decreased with increasing the molecular weight compared at the same mass of the resins. Moreover, the spectrum of the reactant mixture before synthesis showed only one peak at 2274 cm^{-1} of an unreacted-isocyanate group. From the figure, all spectra of the prepolymer indicated that the C=O absorption peak at 1715 cm^{-1} and the N=C=O peak at 2270 cm^{-1} significantly decreased with the progress of the reaction to form the urethane prepolymer. The reaction was confirmed to be completed at $60^{o}C$ for 120 minutes under N_2 purging.

5.4 Thermal Properties of BA:PU Alloys

5.4.1 Differential scanning calorimetry for curing condition observation

The investigation of the curing condition of the BA:PU alloys at various compositions i.e. 100:0, 90:10, 80:20, 70:30 mass ratios was performed in DSC experiment. Figure 5.3 shows the DSC thremogram of curing exothermic peaks of the neat benzoxazine resin and the binary mixtures between benzoxazine and urethane prepolymer using a heating rate of 10 ^{o}C/ min. at temperature range of 30 – 300 ^{o}C.

From this graph, the exothermic peak of the neat benzoxazine resin was located at 232°C. Adding the urethane prepolymer into the benzoxazine resin, exotermic peak was shifted to higher temperature. In this figure, the temperature at the exothermic peak of BA:PU at 90:10, 80:20, 70:30, and 60:40 were 232, 236, 240,and 242°C, respectively. The curing retardation was attributed to the dilution effect of the urethane prepolymer. In principle, the reactions between BA and PU were expected to comprise of at least two reactions; the first reaction is the exothermic curing peak among the benzoxazine monomers while the second one is likely to be the reaction between the isocyanate group on the urethane monomer with the phenolic hydroxyl group on the polybenzoxazine. The phenolic hydroxyl group from the ring opening of the benzoxazine monomer was produced after that the reaction between phenolic hydroxyl group on the polybenzoxazine with the isocyante group was expected to proceed (Takeichi et al, 2000). Moreover, as the urethane prepolymer could not react to form a homopolymer by itself, its presence with an increasing amount might cause a dilution effect on the resulting BA:PU mixtures. The thermogram also showed the decrease of the area under the curing peak of the binary mixtures when the amount of the urethane resin increased. This behaviour is ascribed to the change from the BA:BA interaction to a more BA:PU interaction with increasing the PU fraction in the binary mixture. The systematic decrease of the exotherms with the PU implied that the BA:PU interaction possessed a lower heat of reaction per mole of the reactant compared to that of the BA:BA interaction. Excessive amount of the PU in the binary mixtures might also lead to the presence of the unreacted PU in the fully cured alloys.

Figure 5.4 exhibits the DSC thermograms of the mixtures of the benzoxazine resins and urethane prepolymer (MW 2000) at a mass ratio of 70:30 at various curing conditions. For determining the fully cured condition of every composition used in this work, the specific mixture i.e. BA:PU at 70:30 was selected based on the ratio that required the most thermal energy for curing. The heat of reaction determined from the area under the exothermic peak is 273.6 J/g for the uncured 70:30 BA:PU mixture. It was reduced to 125.2 J/g after curing at 160°C for 2 hrs and decreased to10.8 J/g after further curing at 170°C, 180°C for 2 hrs. each, and post curing 200°C for 1 hr. Furthermore, after post-curing at 200°C for 2 hrs, the exothermic peak was

disappeared, corresponding to 100% conversion of the mixture. The degree of conversion of the sample was determined according to the following relationship:

$$\% \text{ conversion} = (1 - \frac{H_{rxn}}{H_o}) \times 100 \qquad (5.1)$$

where; H_{rxn} is the heat of reaction of the partially cured specimens

            H_o is the heat of reaction of the uncured resin.

DSC experiments were performed to determine both quantities above. The obtained curing conversion indicated that the curing reaction of the BA:PU polymer alloys could rapidly occur at higher temperature. Figure 5.5 showed that the exothermic peaks of BA:PU at 80:20 alloys at various molecular weights were located at the same temperature of about 240°C. Figure 5.6 to Figure 5.9 indicate the condition for complete curing of BA:PU alloys was 160°C, 170°C, 180°C, and 200°C for 2 hrs at each temperature. Figure 5.6 showed the glass transition temperatures of the fully cured BA:PU alloys using polyol molecular weight of 1000 to be 170°C in 90:10 BA:PU, 205°C in 80:20 BA:PU ,and 240°C in 70:30 BA:PU. The glass transition temperature of the binary mixture was increased with increasing of the urethane mass ratio. The similar trend in the glass transition temperature enhancement from other polyol molecular weights i.e. 2000, 3000 and, 5000, was also observed. Figure 5.7 to Figure 5.9 indicated the glass transition temperature of the fully cured BA:PU alloys using the polyol molecular weight of 2000 to be 175°C in 90:10 BA:PU, 200°C in 80:20 BA:PU, and 245°C in 70:30 BA:PU and also with the polyol molecular weights of 3000 and 5000 to be 170°C and 168°C in 90:10 BA:PU, 195°C and 190°C in 80:20 BA:PU, and 250°C and 245°C in 70:30 BA:PU, respectively. Figure 5.10 illustrates the corresponding glass transition temperatures obtained from the thermograms of the fully cured BA:PU matrix alloys at various molecular weight. In this graph, the glass transition temperature seemed to be unaffected by the molecular weights of the urethane polyol comparing at the same BA:PU mass ratio.

The effect of the urethane mass fraction on the glass transition temperature of the BA:PU polymer alloys was previously reported by Rimdusit, et al., 2005 using DMA. In their case, T_g of the polymer alloys at each composition was defined using

the maximum of the loss modulus. In these alloy systems, their glass transition temperatures showed a synergistic behavior as T_gs were found to increase to the higher value than the T_gs of both parent polymers with the mass fraction of the PU. The T_gs of the BA:PU alloys in this case were also increased with the mass fraction of the PU confirming the previous report (Rimdusit et al., 2005). The glass transition temperatures of the IPDI-based polyurethane elastomer and the BA-a based polybenzoxazine were reported to be about -70°C and 165°C, respectively. Whereas the BA:PU = 70:30 exhibited the T_g of 220°C. The observed increase in the cross-linked density of the binary systems with PU is one possible reason for the enhancement in the T_g of the resulting alloys though PU is a softer molecular species having much lower T_g and was expected to lower the T_g of the binary alloys. The ability of the urethane prepolymer to enhance the cross-linked density of the polybenzoxazine is thus attributed to the observed phenomenon. The crosslinking was reported to be caused by the reaction between an isocyanate group on a urethane monomer with a hydroxyl group on polybenzoxazine after the phenolic hydroxyl group from the ring opening of benzoxazine monomer was produced. This crosslinking mechanism had already been explained by Takeichi at al. (Takeichi et al., 2000)

5.4.2 Thermal Degradation and Thermal Stability Investigation

The TGA thermogram of the polybenzoxazine and BA:PU2K alloys at various compositions was shown in Figure 5.11. The degradation temperature (T_d) e.g. at 5% weight loss, is one of the key parameters needed to be examined for temperature stability of polymers. From the figure, the degradation temperatures of the polymer alloys were found to be slightly higher than that of the neat polybenzoxazine. The TGA curves of the binary mixture at various mass ratio of urethane prepolymer e.g. 10%, 20%, and 30%, suggested that an addition of the 30 wt% of urethane resin into the benzoxazine resin gradually enhanced the thermal degradation temperature of the obtained alloys. The degradation temperature of the polybenzoxazine homopolymer at 5 wt% loss was determined to be 330°C which was consistent with the value reported previously by Rimdusit and co workers, 2005. The degradation temperatures of BA:PU alloys at the urethane mass ratio of 10 wt%, 20 wt% and 30 wt% were

determined to be 336°C, 334°C, and 344°C, respectively. Therefore, one advantage of mixing the urethane resin into the benzoxazine network was to improve the thermal stability of the polybenzoxazine. This result was attributed to the crosslinking density enhancement as explained earlier. On the other hand, the char yield i.e. the residual weight at 800°C, of the polymer alloys was found to decrease with increasing the PU fraction in the binary system. The char yield at 800°C of the polybenzoxazine was determined to be 25 wt% which is consistent with the value reported by Rimdusit and co workers, 2005. The TDI-poly(ethylene adipate) based polyurethane possessed a smaller value of char yield of only 8 wt% at 800°C (Takeichi et al., 2000). As a result, the increase of the PU fractions reduced the char yield of the alloys as shown in Figure 5.11. The char yields of BA:PU alloys at 10%, 20%, and 30% mass fractions of urethane were determined to be 23.6 wt%, 20.6 wt%, and 18.2 wt%, respectively. This can be explained as the chemical structure of the polyurethane composed of a less thermally stable aliphatic structure of the polyol compared to the benzene rings in the structure of polybenzoxazine. Therefore, the addition of the urethane resulted in the lowering of the char yield in the polymer alloys.

Furthermore, the observation of the thermal degradation of the BA:PU alloys (at a fixed mass ratio of 80:20) at various molecular weights of the polyol was illustrated in Figure 5.12. Increasing the molecular weights of the polyol resulted in only marginal enhancement of the T_d at 5% weight loss of the fully cured specimens, i.e., 332°C in average. From a previous work, Ubaghs and coworkers studied the effects of the molecular weight of amino alcohol which used for encapped a poly(urea urethane)s. They reported that the degradation temperature did not increase with increasing the molecular weights of the encapping moieties as well (Ubaghs et al., 2005). Moreover, the char yield of this system was observed to increase with the molecular weights of the polyol. Figure 5.12 shows the char yield of the binary mixture using PU1K, PU2K, PU3K, and PU5K that were determined to be 18.3 wt%, 20.6 wt%, 22.6 wt%, and 22.9 wt%, respectively. Low and Ishida proposed that the char yield was increased as a possible result of carbonyl functional groups formation. Upon thermal decomposition, the carbonyl functional groups formed a higher concentration of carbondioxide gaseous was be proposed to cause the reduction of flammability of polybenzoxazines (Low and Ishida, 2006). In our system, the increase

in char yield at a greater molecular weight of the polyol tended to reduce the flammability of binary systems.

5.5 Mechanical Properties of BA:PU Alloys

5.5.1 Flexural Property Characterization

Figures 5.13 and 5.14 show flexural properties of the poly-benzoxazine alloys specimens. Figure 5.13 shows flexural modulus of the binary system specimens at various urethane mass fractions as well as at different molecular weights of polyols. The maximum modulus value of 6.2 GPa belongs to the neat polybenzoxazine specimens. At a fixed molecular weight of the polyol, the alloy with 30 wt% of the PU showed the flexural moduli to be in range of 2.2 – 2.8 GPa. The modulus of the binary systems tended to decrease in a linear manner with the composition of the PU in the alloys following the rule of mixture. The storage modulus of 1.8 GPa for poly(ether polyol)-based polyurethane was reported by Pattanayak and Jana, 2005. The phenomenon was due to the basic principle that the addition of the rubbery urethane polymer into the adamantine polybenzoxazine was able to lower the stiffness of the resulting polybenzoxazine alloys as clearly seen in Figures 5.13. On the other hand, the effects of the molecular weights of the polyol on the flexural moduli of the alloys were not significant. Flexural strength of the BA:PU alloys was also evaluated. The strength of the binary systems did not show a linear relationship with the compositions of the alloys but exhibited the synergistic behaviour with the maximum at BA:PU = 90:10 for all molecular weights of the polyol. The behaviour was consistent with that reported by Rimdusit and co workers, 2005. The flexural strength of neat polymenzoxazine was determined to be 145.9 MPa. The BA:PU1K provided the ultimate flexural strength of 163.9 MPa at 90:10 of BA:PU alloys. Adding 20 wt% and 30 wt% mass ratios of PU1K systematically lowered the flexural strength to 140.2 MPa and 89.7 MPa, respectively. The optimum values of the flexural strengths of BA:PU1K, BA:PU2K, BA:PU3K, and BA:PU5K were determined to be 163.9 MPa, 162.2 MPa, 150.5 MPa, and 149.4 MPa, respectively. The enhancement of the crosslink density of the alloys with the addition of the PU was likely to be responsible to the synergistic behaviour in their flexural strengths above.

5.5.2 Dynamics Mechanical Analysis

Dynamic mechanical properties of the BA:PU1K, BA:PU2K, BA:PU3K, and BA:PU5K polymeric alloys at various compositions are shown in Figures 5.15 -5.26. All specimens were fully cured to form highly cross-linked structures. From the DMA thermograms, the storage moduli of a solid sample, in glassy state, tended to decrease with increasing the mass fraction of the urethane prepolymer as shown in Figure 5.15. The toughening enhancement from the presence of the more flexible PU was the reason of the above behaviour. In case of BA:PU1K polymeric alloys, the storage moduli at room temperature were systematically reduced from 6.5 GPa to 3.0 GPa with the addition of the PU from 0 to 30 wt%. The values showed similar trend to our previous work (Rimdusit et al., 2005). Furthermore, the greater mass fraction of the PU was found to enhance the rubbery plateau modulus and glass transition temperature of the resulting alloys. Figure 5.16, Figure 5.17, and Figure 5.18 show the storage moduli of BA:PU2K, BA:PU3K, and BA:PU5K, respectively. In the similar compositional range of 0 to 30 wt% of the urethane resin, the storage moduli in glassy state and rubbery plateau modulus displayed a similar trend. For example, the storage moduli of BA:PU2K binary system decreased from 6.5 GPa to 2.6 GPa. The reduction of storage moduli to 2.1 GPa and 1.8 GPa at 30 wt% of the PU was observed for the BA:PU3K and BA:PU5K binary systems, respectively.

In addition, the glass transition temperature (T_g) of each BA:PU alloys specimen was detected in the dynamic mechanical thermograms using the maximum of the loss modulus, E", peak. Increasing the amount of the PU mass ratio was found to increase the T_g values of the BA:PU at each molecular weight of the polyol in the polymer alloys. The result is consistent with the observation in the DSC experiments. Figure 5.15 to Figure 5.18 show the higher crosslink density of the matrix alloys observed from the higher plateau modulus with increasing the amount of the PU of the binary systems. The Fox and Loshaek equation was used to explain the effect of a crosslink density on T_g of the polymer network as follow: (Mark, 1996)

$$T_g = T_g\left(\infty\right) - \frac{k}{M_n} + k_x\rho \tag{5.2}$$

where $T_g(\infty)$ is the T_g of infinite molecular weight linear polymer, k and k_x are the numerical constants, M_n is the number averaged molecular weight which equals infinity in the crosslinked system; therefore, this term can be neglected, and ρ is the crosslink density. According to the equation, the higher molecular weight (Mw) and cross-linked density (ρ) are the key parameters of increasing T_g of polymer networks, which is supporting to our experiment results. Figure 5.19 to Figure 5.22 indicate the shift of glass transition temperature at maximum of the loss modulus peak to a higher value when more urethane prepolymer at various molecular weight of the binary system was added.

The α-relaxation peaks of the loss factor or tan δ is a ratio of a viscous to an elastic component of dynamic moduli of a specimen. Figure 5.23 to Figure 5.26 illustrate the similar magnitude of tan δ which was investigated to decrease with the increasing PU fraction in the BA:PU alloys. As the results, all of various molecular weight of polyol in the polymeric alloys, the maximum of the tan δ was decreased in the urethane-rich samples can be imply to the more elastic characteristics of the alloys as the earlier explanation. In addition, the greater broading peak of tan δ when adding a higher amount of PU was investigated. This may be described the broader distribution network structure

The comparison of the effect of molecular weights of the polyol on the alloy's dynamic mechanical thermograms are shown in Figure 5.27 to Figure 5.29. The storage moduli and loss moduli of those alloys at different polyol molecular weights were found to show a similar trend. The glass transition temperatures at different polyol molecular weights were in good agreement with the DSC investigation. From the height of tan δ, the alloys of BA:PU5K exhibited the most viscous characteristic of all the alloy systems whereas the alloys of BA:PU1K, BA:PU2K, and BA:PU3K showed similar viscoelastic characteristic of the alloys. In addition, the rather broad tan δ peak of those BA:PU alloys comparing with that of the neat polybenzoxazine suggested the broad distribution of polymer network structure in the BA:PU alloys.

5.6 Properties of Kevlar^{TM}-reinforced Composites

5.6.1 Determination of Polymer Matrix Content in the Composites

Thermogravimetric analyzer was used for the determination of the polymer matrix content in the composite. The optimal range of polymer matrix content in ballistic armor composites was reported to be about 20-25 % (Park, 2003). In this study, the percent content of the polymer alloys in their composites was calculated using Figure 5.11 and Figure 5.31, effect of compositions, and in Figure 5.12 and Figure 5.32, effect of polyol molecular weights. The sample mass used was about 15-20 mg. The percent of matrix content of 22% in BA:PU2K = 100:0, 24% in BA:PU2K = 80:20, and 22% in BA:PU2K = 70:30 were obtained. At different molecular weights of the polyol using fixed BA:PU = 80:20, the percent of matrix content of 26% at MW 1000, 24% at MW 2000, 25% at MW 3000, and 25% at MW 5000 were obtained. As a result, the fiber content was thus about the same for all composites using the same hot-pressing condition. The polymer matrix content was also in the suggested range for producing composite armors reported by Park, 2003. This composition of the Kevlar^{TM} fiber was fixed for all composites produced in this work.

5.6.2 Thermal Degradation and Thermal Stability Investigation

In Figure 5.31 and Figure 5.32, the degradation temperatures at 5 wt% loss of Kevlar^{TM}-reinforced benzoxazine alloy composites were found to increase with the PU in the matrix alloys. The degradation temperatures at 5% weight loss of the Kevlar^{TM}-reinforced benzoxazine alloys with the PU compositions of 0%, 10%, 20%, and 30 % by weight were 389°C, 385°C, 375°C, and 383°C, respectively. Those of the Kevlar^{TM}-reinforced benzoxazine alloys with the polyol having MW 1000, MW 2000, MW 3000, and MW 5000 were also found to be 354°C, 375°C, 384°C, and 374°C, respectively. Moreover, the weight residue at 800°C of the Kevlar^{TM}-reinforced benzoxazine alloys was found to systematically reduce from 35.9% to 34.2% with an additional of the PU from 0 to 30% by weight. In addition, the char yield was

systematically reduced from 34.1 % to 33.1% with the decreasing of the molecular weight of the polyol from 5000 to 1000.

5.7 Mechanical Properties of BA:PU Alloys

5.7.1 Flexural Properties of the BA:PU Composite Armor

The universal testing machine was used for the characterization of flexural properties of the Kevlar[TM]-reinforced polybenzoxazine alloys and the results were shown in Figures 5.33 and 5.34. Figure 5.33 shows flexural modulus of the Kevlar[TM]-reinforced poly-benzoxazine alloys at various urethane mass fractions as well as at different molecular weights of the polyol. The flexural modulus of 17.3 GPa was obtained in Kevlar[TM]-reinforced polybenzoxazine specimens. As different molecular weights of the polyol but at fixed urethane resin of 30 wt% the flexural moduli slightly increased from 20 – 24 GPa. Additionally, the flexural strengths of the Kevlar[TM]-reinforced polybenzoxazine alloys at various urethane mass fractions as well as at different molecular weights of the polyol were depicted in Figure 5.34. The flexural strength of the Kevlar[TM]-reinforced polybenzoxazine was determined to be 160.6 MPa. The flexural strength of the Kevlar[TM]-reinforced BA:PU2K alloys slightly increased to be 169.0 MPa with increasing the PU mass fraction in the polymer matrix alloys. On the contrary, the flexural strength of the other three polyol molecular weights i.e. MW 1000, MW 3000, and MW 5000, were dramatically reduced when the PU was less than 20% by weight. On the other hand, those flexural strengths were rapidly increased when 30 wt% of the PU was added. Figure 5.33 and Figure 5.34 indicated that damages of ballistic composite may be not only from the result of fiber or polymer matrix failure but also from delamination between the fiber and the polymer matrix in the composite. Therefore, the flexural properties of the composite were different from their unfilled polymer alloys. For the Kevlar[TM]-reinforced BA:PU2K alloys, the high flexural strength obtained was attributed to the optimal adhesion between Kevlar[TM] fiber and BA:PU2K alloys.

5.8 Solvent Extraction of BA:PU Alloys

Solvent extraction of the BA:PU binary systems was studied using chloroform as a solvent. This experiment investigated the ability of network formation of the BA:PU alloys at different composition and at various molecular weights of the polyol. Figure 5.35 and Figure 5.36 are the pictures of BA:PU2K alloy specimens at different compositions before and after being immersed in chloroform up to 30 days. The BA:PU2K = 70:30 specimen was found to be changed from its original state. Figures 5.39 to Figure 5.41 clearly explained the change due to extraction for 14 days. The BA:PU2K = 70:30 rendered the color change of the chloroform from colorless to clear yellow and deeper yellow after immersing for 30 days. Whereas the solvent of the other three compositions were still to be colorless throughout the whole evaluation period. As a result, the network of the binary system at 30 wt% of PU tended to be the weakest network; therefore, dissolved in the solvent i.e. 20.4% extraction. The percents of solvent extraction of other specimens were determined to be 0.5% and 0.6% for BA:PU2K = 100:0 and BA:PU2K = 90:10, respectively. The opposite behaviour of the BA:P2K = 80:20 was displayed. The mass of the BA:PU2K specimen after immersed in solvent was slightly increased even after drying for 48 hours at $105^{o}C$. The BA:PU2K alloys may trap the solvent inside their infinite networks thus no weight loss was observed but the weight gain from the solvent.

The pictures of BA:PU (80:20) alloy specimens at various molecular weights of the polyol before and after being immersed in chloroform for 30 days are shown in Figure 5.37 and Figure 5.38. The BA:PU5K sample was slightly swelled as seen in Figure 5.36(d). The swelling of the edges of this specimen corresponded to the highest percent swell specimen of 11.3% of BA:PU5K. The percent swell was reduced from 11.3% to 3.8% when the molecular weights of the polyol were decreased from 5000 to 2000. The network of the binary systems tended to have large space between networks junction points when adding the higher molecular weight of the polyol. On the other hand, the percent extraction of 0.6% in the BA:PU1K was observed to be due to the rather short chain length of the polyol. This may result in a rather tight network structure for solvent penetration. No color change of chloroform

was observed in the specimens having different diol molecular weight i.e. fixed BA:PU = 80:20.

5.9 Ballistic Impact Tests of the BA:PU Composite Armors

5.9.1 Low Level Ballistic Impact Test

5.9.1.1 Specimen Characterization

At low level ballistic impact evaluation, a series of ballistic tests were performed on the composite laminates which were made of Kevlar[TM] fabric impregnated with BA:PU resins and cured using the curing condition as suggested in the previous section. The Kevlar[TM] fabric used has the areal density of about 0.049 g/cm^2. The dimension of the laminated specimens was 130 mm×130 mm×2.0 mm, corresponding to four plies of the Kevlar[TM] cloth impregnated with about 20 % by weight of the resin mixtures as determined in section 5.6.1.

5.9.1.2 Ballistic Impact Test for Optimum Composition of the Alloys

In this test, a 9 mm handgun with standard lead projectiles having lead outer-coating was impacted on the composite laminates fabricated with a thickness of 8 plies of the Kevlar[TM]-reinforced composite at various BA:PU2K alloy compositions from 100:0 to 70:30. The 8 piles of Kevlar[TM]-reinforced panels with 4/4 panel arrangement were selected for the tests. Each panel of 4 piles was selected with the areal density of 0.23 g/cm^3 as evaluated previously by Pathomsap, 2005. In addition, the bisphenol A-based flexible epoxy, hard epoxy, and the blend of these two resins were also evaluated as polymer matrices in Kevlar[TM]-reinforced composites (i.e. cured by amine hardener) at the same fiber content of 20% by weight. Their ballistic impact performance was compared with our BA:PU2K matrix alloys. In addition, the 8-ply of Kevlar[TM], equivalent to 2 panels of Kevlar[TM] composite, was also used in the ballistic impact test for comparison with the other Kevlar[TM]-reinforced composites.

The ballistic test results of the 8-ply Kevlar[TM]-reinforced BA:PU2K as well as epoxy composites are listed in Table 5.2. From the results, the ballistic performance of all types of bisphenol-A based epoxy composites with the 4/4 configuration of the composite panels and 8-ply of Kevlar[TM] cloth could not resist the projectiles in this test as illustrated in Figure 5.45. Moreover, the 8-ply of Kevlar[TM] cloth cannot resist the penetration of this level of ballistic impact and the plies were disoriented after the test. From Figure 5.45, the more flexible epoxy used as a polymer matrix exhibited a higher delamination area and larger cone deformation. This investigation greater indicated that the more flexible polymer matrix in the composite provided greater possibility to resist the ballistic penetration. In addition, the polybenzoxazine alloy composites panel exhibited an obvious improvement in the energy absorption characteristics having the penetration resistance with greater delaminated area. The area was significantly larger than that of the epoxy composites as shown in Figure 5.46. The firing results indicated that all of the PU mass fractions of the BA:PU2K matrices used in this study i.e. 0%, 10%, 20%, and 30%, exhibited ballistic penetration resistance better than the epoxy matrices. Although, the first panel of the system based on 70:30 BA:PU2K matrix cannot resist the ballistic penetration but both of the panel of this system can. However, the composite from the 80:20 of BA:PU2K matrix alloys exhibited the best penetration resistant properties as evidently seen in Figure 5.46(c). As shown in Table 5.3, the cone dimension of the back panel of the Kevlar[TM]-reinforced with 80:20 BA:PU matrix was determined to be 18 mm. in depth and 58 mm. in diameter. The hole depth of this system was determined to be 25 mm. with the hole diameter of 55 mm. and the damage volume was measured to be 35 ml. From the above results, the composite using 80:20 of BA:PU2K was selected for the BA:PU alloy system for our ballistic resistant composite.

5.9.1.3 Ballistic Impact Test for Determining Optimum Molecular Weight of the Polyol in the BA:PU Alloys

In this test, we used similar firing condition to the test in the previous section. The effect of varied polyol molecular weights on the composite ballistic performance was observed in this experiment. Table 5.4 shows the ballistic performance of the Kevlar[TM]-reinforced with 80:20 BA:PU matrix with 4/4

configuration of the composite panels. The composite systems were able to resist the projectiles in this test. The penetration resistant behaviour using both BA:PU2K and BA:PU3K as polymer matrices were nearly the same. Figure 5.47(b) and Figure 5.47 (c) showed the back plates of both composite systems. The corresponding penetration resistant properties, such as damage volume, were shown in Table 5.5. The damage volume of 80:20 BA:PU3K matrix composite was measured to be 23 ml which the minimum value of all this tested composite. As a result, it could be concluded that the TDI-polyol (MW 3000) based urethane prepolymer had the suitable chain length for alloying with benxozazine resin in 80:20 BA:PU binary system to yield a composite of best ballistic performance.

5.9.2 High Level of Ballistic Impact Test

5.9.1.1 Specimen Characterization

At high level ballistic impact test, NIJ level III and ss109 ammunition ballistic impact, a series of tests were performed on the composites which were assembled from ceramics, metal, and Kevlar^{TM} fabric. Alumina hexagons with a nominal area of 800 mm^2 with 10 mm in thickness were assembled on metal mesh placed on top of an aramid fiber in approximately 300 x 300 mm^2 in dimension. Stainless of 300 $\times$ 300 $\times$ 1 mm^3. was used as a metal layer. Kevlar^{TM} fabric was also impregnated with BA:PU resins and cured using the same condition as the samples tested at low level ballistic impact. The dimension of the polymeric laminated specimens was 300 mm.$\times$ 300 mm. $\times$ 11 mm. corresponding to 25 plies of Kevlar^{TM} cloth impregnated with about 20 % by weight of the BA:PU resin mixtures as determined in section 5.6.1. The alumina, stainless, and Kevlar^{TM} composite was assembled to form a hard armor composite. The total weight of the hard armor composite was about 6.4 kg. which composes of 4 kg. of the alumina, 0.7 kg. of the stainless, and 1.3 kg. of the Kevlar^{TM} composite. The remaining weight was those of Kevlar^{TM} fabric which used for alumina assembly. The areal density of 7.1 g/cm^2 was obtained from the composite.

5.9.2.2 Ballistic Impact Test

In this test a 7.62 mm full metal jacket and ss109 ammunition with 3 ammunition in each type were impacted on the same composite specimen. Figure 5.49 illustrates the ability of the hard armor composite to clearly resist the penetration of those ammunitions. Figure 5.49(a) shows the damaged and delaminated area of the composite. The deformation due to the 7.62 mm ammunition was greater than that of the ss109 ammunition. A penetration depth up to the stainless layer was observed using the 7.62 mm ammunition one of them was penetrated and the other two damages were also ruptured by the 7.62 mm ammunitions with of about 20 mm. of their cone depth. Their cone diameters were about 62 mm. On the other hand, layer of the stainless plate was not penetrated by an ss109 ammunition. The cone depths of only about 6 mm. and the cone diameters of about 43 mm. were measured. The investigation of Kevlar^{TM}-reinforced composite set as a back plate of hard armor composite can resist all the ballistic penetration in this study. The cone depths of 15 mm. and 12 mm. on Kevlar^{TM}-reinforce composite were measured at the penetrated and ruptured position, respectively. Another of cone depth of Kevlar^{TM}-reinforce composite was delaminated to be 9 mm. All cone diameters were the same with the value of about approximately 54 mm. Finally, the deformation produced by ss109 ammunition was not significant on both cone depth and cone diameter.

The above results suggested that the performance of the hard armor composite based on NIJ standard level III could resist the penetration of 7.62 ammunition which had approximately 840 m/s in bullet velocity. The Kevlar^{TM}-reinforce composite plays a key role in the penetration resistance of the armor and is the layer that absorbed the rest of the impacting energy of the ammunition. Finally, the penetration resistance up to NIJ level III was not possible if only the alumina and the stainless layers were used as shown in Figure 5.49 and Figure 5.50. The pictures confirm the necessity of using highly tough material of the polymeric armor layer of the Kevlar^{TM}-reinforced BA:PU composite to stop the penetration of the fragments of the ammunition at this relatively impact level.

Table 5.1: Molecular weights of the polyols determined via GPC

Types of Polyol	Mn (M/I ratio) (g/mol)	GPC		PDI
		Mn (g/mol)	Mw (g/mol)	
Polyol 1010	1000	1028	1098	1.07
Polyol 1020	2000	2022	2137	1.06
Polyol 3003	3000	2887	3061	1.06
Polyol 3009	5000	4396	5564	1.27

(M/I ratio: monomer/initiator ratio).

Table 5.2: Effect of BA:PU2K alloy compositions on ballistic impact resistance using standard lead projectiles with lead outer coating typically used in 9 mm handgun

Composite Number	Types of Matrix	Number of Plies 1st plate/2nd plate	Penetration Resistance	
			1st plate	2nd plate
1	Epoxy 200	4/4	No	No
2	Epoxy 400	4/4	No	No
3	Epoxy 200 + Epoxy 400	4/4	No	No
4	Pure Kevlar	4/4	No	No
5	BA:PU 100:0	4/4	Yes	Yes
6	BA:PU 90:10	4/4	Yes	Yes
7	BA:PU 80:20	4/4	Yes	Yes
8	BA:PU 70:30	4/4	No	Yes

Table 5.3: The damage properties of Kevlar^{TM}-reinforced composite using BA:PU2K as polymer matrix fired test using standard lead projectiles with lead outer coating typically used in 9 mm handgun

Mass Ratio of Urethane (%)	Cone Properties		Hole Properties		Damage Volume (ml)
	Depth (mm)	Diameter (mm)	Depth (mm)	Diameter (mm)	
0	19	60	26	64	37
10	23	61	26	65	40
20	18	58	25	55	35
30	23	65	26	66	40

Table 5.4: Effect of polyol molecular weight of BA:PU=80:20 on ballistic impact resistance using standard lead projectiles with lead outer coating typically used in 9 mm handgun

Composite Number	Types of Matrix	Number of Plies 1st plate/2nd plate	Penetration Resistance	
			1st plate	2nd plate
1	MW 1000	4/4	Yes	Yes
2	MW 2000	4/4	Yes	Yes
3	MW 3000	4/4	Yes	Yes
4	MW 5000	4/4	Yes	Yes

Table 5.5: The damage properties of Kevlar^{TM}-reinforced composite using BA:PU=80:20 as polymer matrix fired test using standard lead projectiles with lead outer coating typically used in 9 mm handgun

Molecular Weight Of polyol	Cone Properties		Hole Properties		Damage Volume (ml)
	Depth (mm)	Diameter (mm)	Depth (mm)	Diameter (mm)	
1000	23	66	30	74	42
2000	18	58	25	55	35
3000	19	63	20	64	23
5000	26	71	30	81	63

Table 5.6: The solvent extraction data at various mass fractions of PU

Composition (BA:PU2K)	Mass of specimen (mg)		Percent Extraction (%)	Percent Swell (%)
	Initial	After Immersed for 30 days		
100:0	1364	1357	0.5	-
90:10	1114	1108	0.6	-
80:20	1146	1192	-	3.8
70:30	1088	865	20.4	-

Table 5.7: The solvent extraction data at various molecular weights of polyol

Molecular Weight of Polyol (BA:PU=80:20)	Mass of specimen (mg)		Percent Extraction (%)	Percent Swell (%)
	Initial	After Immersed for 30 days		
1000	1122	1115	0.6	-
2000	1146	1192	-	3.8
3000	1196	1247	-	4.1
5000	1209	1363	-	11.3
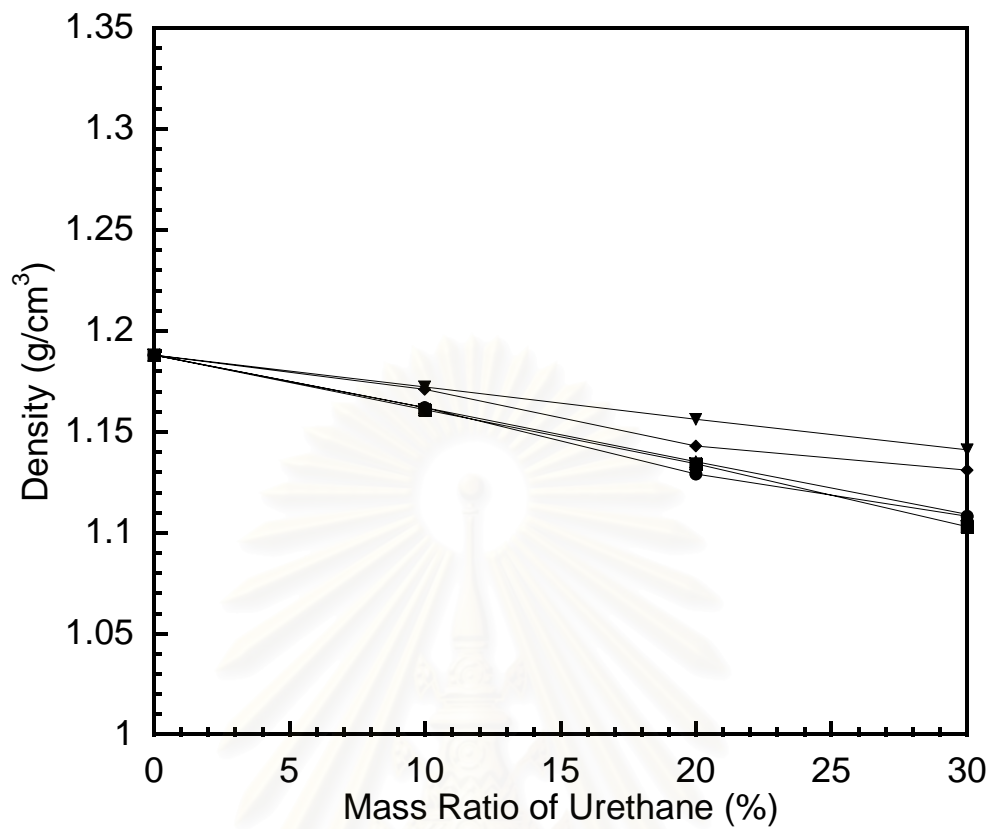
Figure 5.1: Density of BA: PU alloys specimens: (▼) Theoretical density, (◆) actual density of the BA:PU1K, (■) actual density of the BA:PU2K, (▲) actual density of the BA:PU3K, (●) actual density of the BA:PU5K
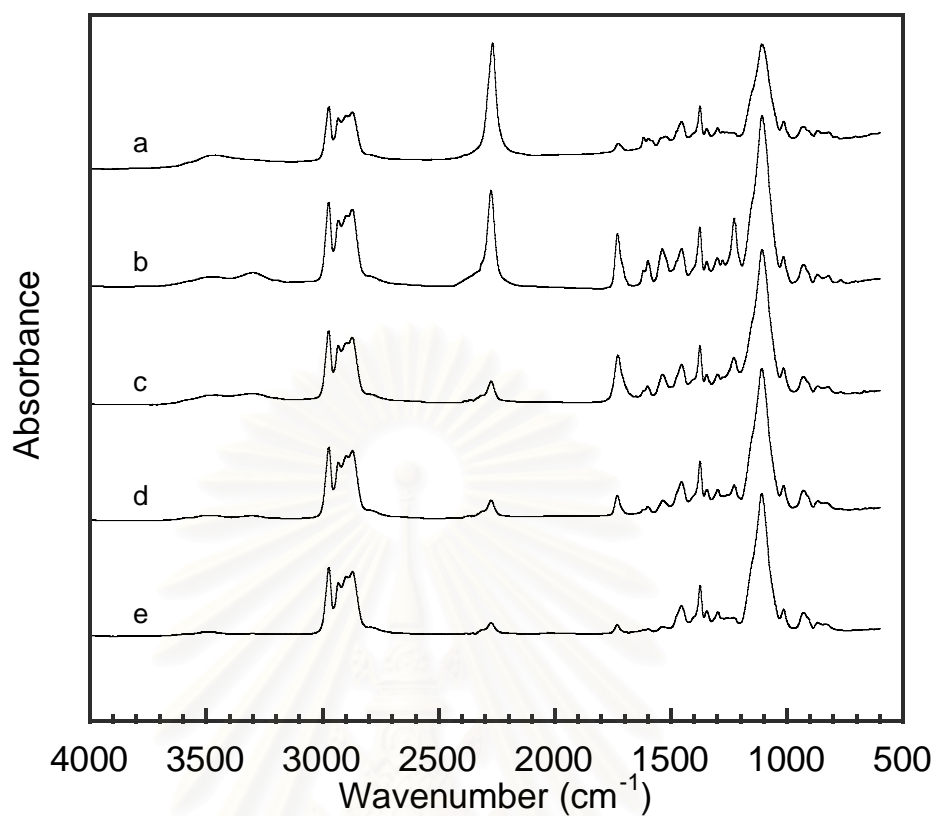
Figure 5.2: FT-IR Spectra of urethane prepolymer:

(a) TDI+Polyol mixture before synthesis

(b) TDI+Polyol (MW 1000) prepolymer

(c) TDI+Polyol (MW 2000) prepolymer

(d) TDI+Polyol (MW 3000) prepolymer

(e) TDI+Polyol (MW 5000) prepolymer
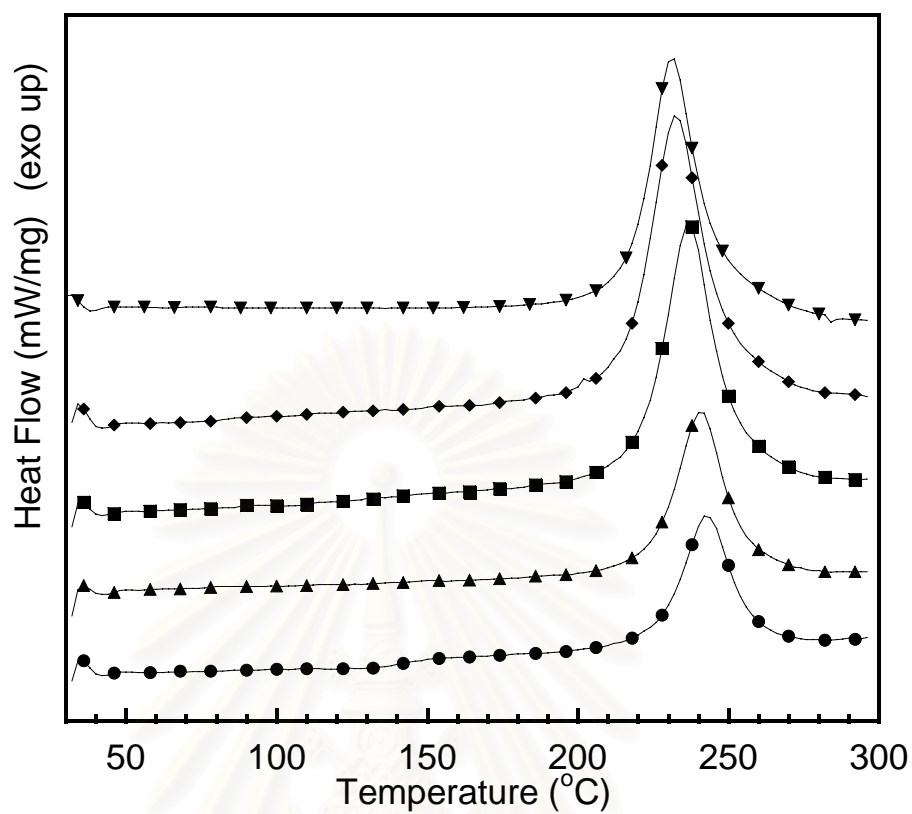
Figure 5.3: DSC thermogram of BA:PU2K alloys at various compositions: (▼) 100:0, (◆) 90:10, (■) 80:20, (▲) 70:30, (●) 60:40
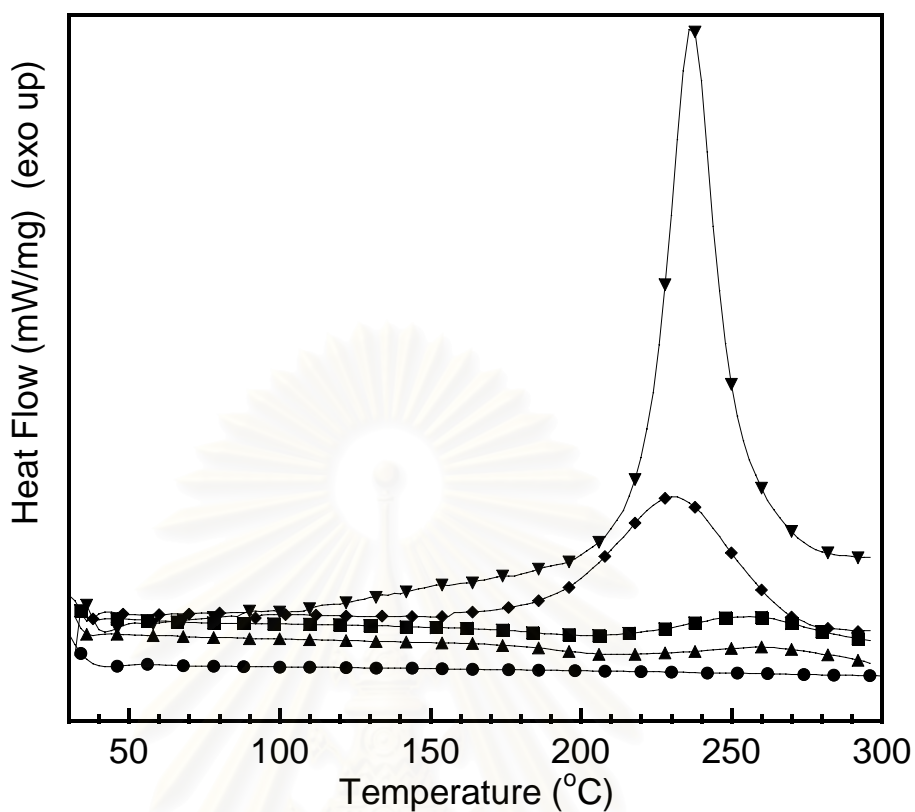
Figure 5.4: DSC thermogram of BA:PU5K alloys at the mass ratio of 70:30 various curing conditions : (▼) uncured, (◆) 160°C/2hrs., (■) 160°C/2hrs., 170°C /2hrs., and 180°C/2hrs., (▲) 160°C/2hrs., 170°C/ 2hrs., 180°C/2hrs., and 200°C/1hr, (●) 160°C /2hrs., 170°C/2hrs., 180°C /2hrs., and 200°C/2hrs.
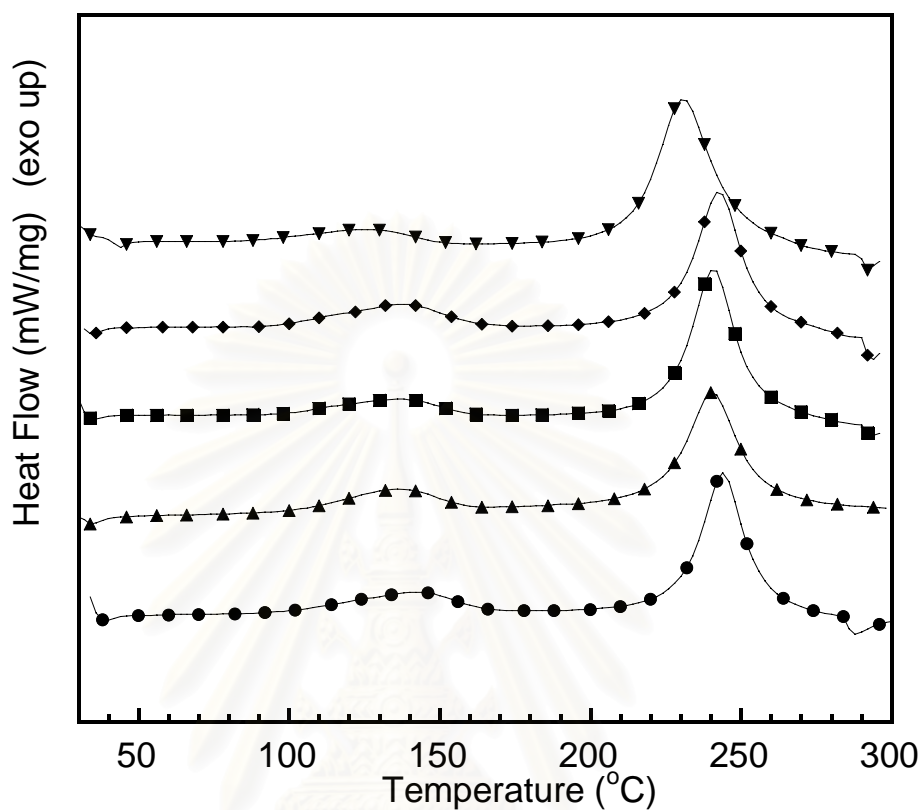
Figure 5.5: DSC thermogram of BA:PU (80:20) alloys at various molecular weights : (▼) Pure BA, (◆) MW 1000, (■) MW 2000, (▲) MW 3000, (●) MW 5000
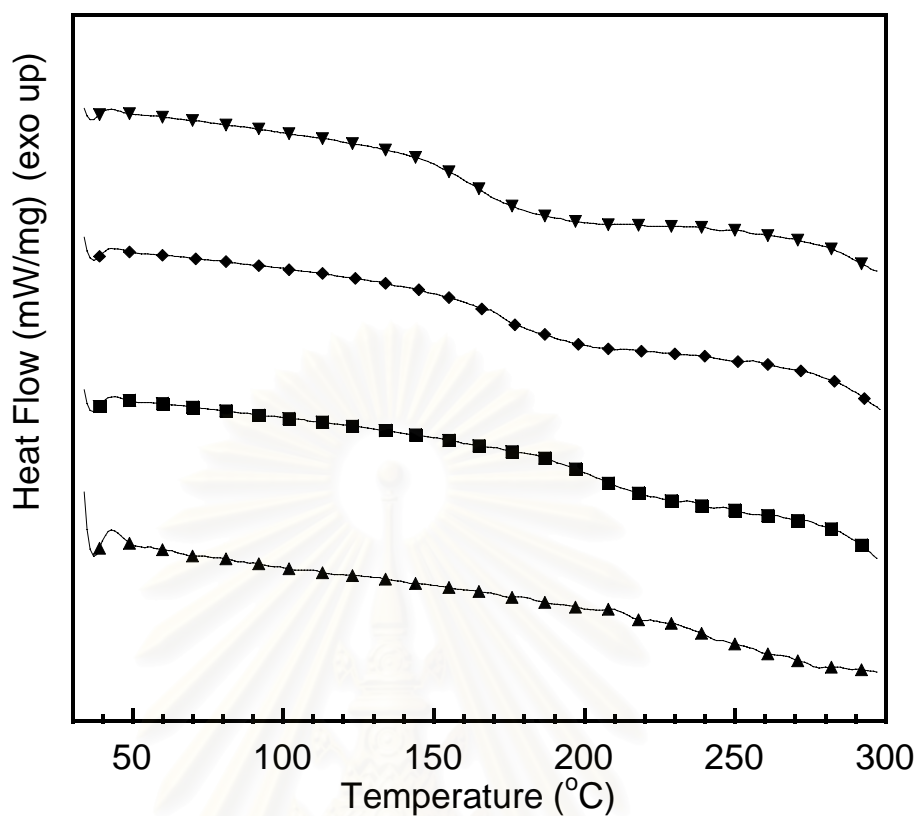
Figure 5.6: DSC thermograms of the fully cured BA:PU1K polymer alloys at various compositions: (▼) 100:0, (◆) 90:10, (■) 80:20, (▲) 70:30
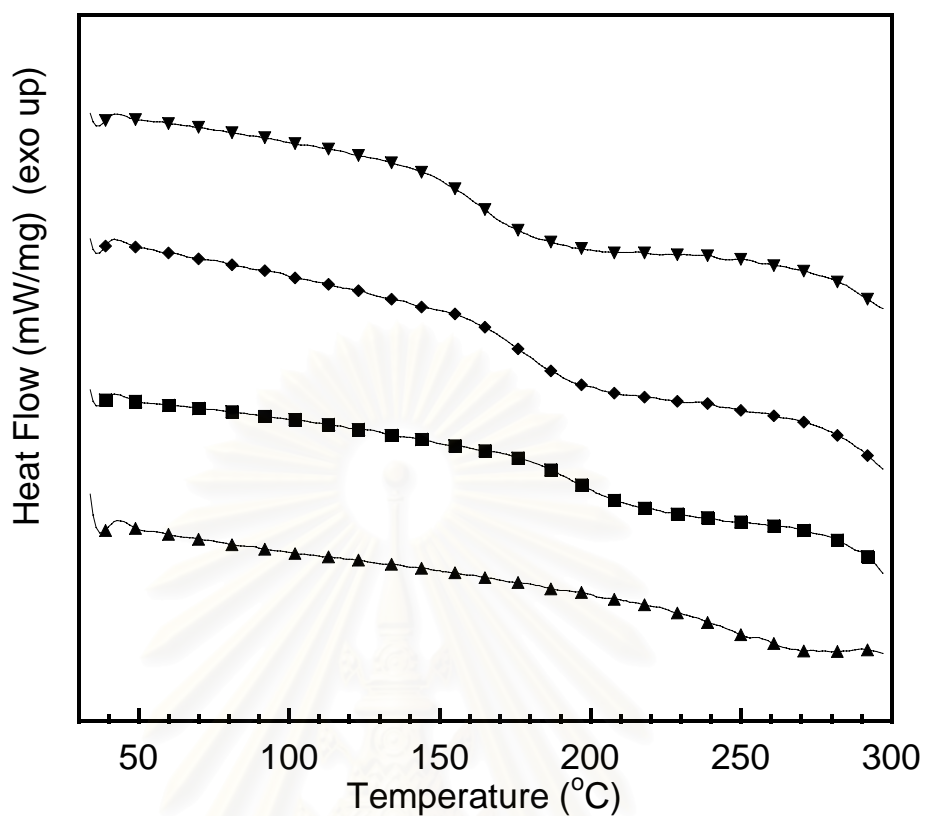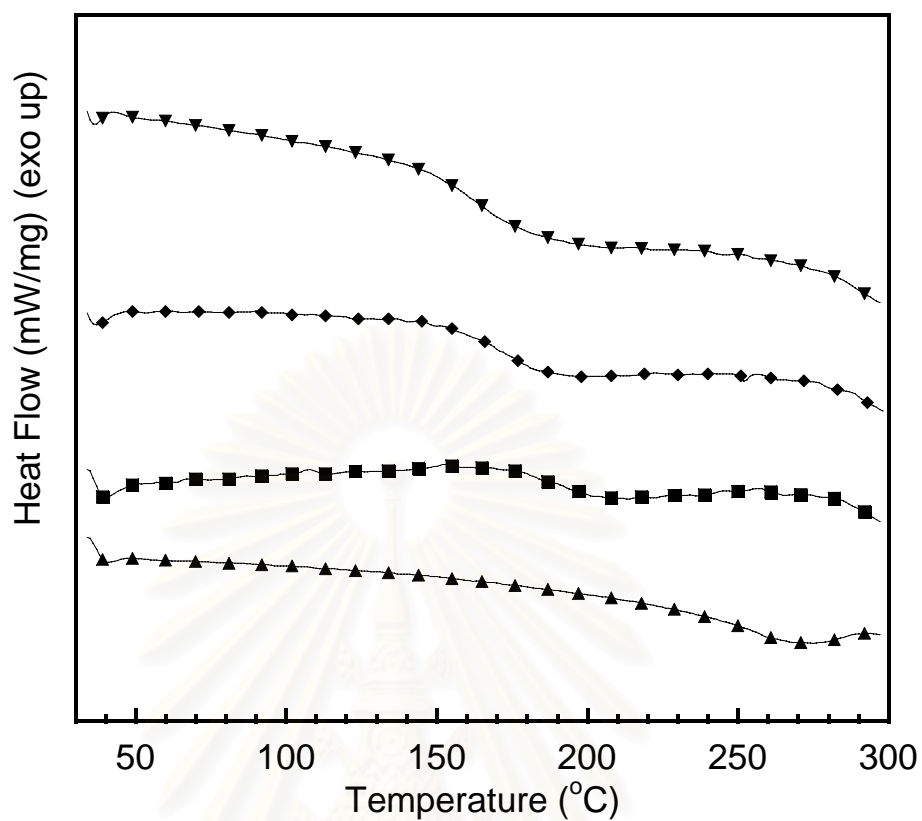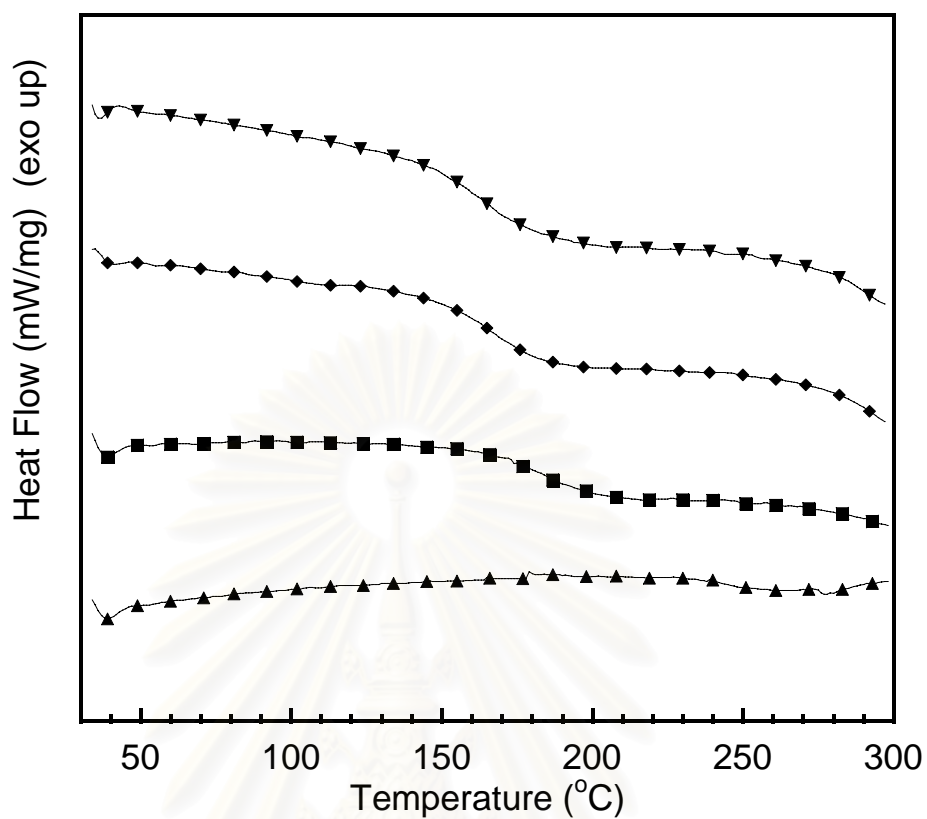
Figure 5.7: DSC thermograms of the fully cured BA:PU2K polymer alloys at various compositions: (▼) 100:0, (◆) 90:10, (■) 80:20, (▲) 70:30

Figure 5.8: DSC thermograms of the fully cured BA:PU3K polymer alloys at various compositions: (▼) 100:0, (◆) 90:10, (■) 80:20, (▲) 70:30

Figure 5.9: DSC thermograms of the fully cured BA:PU5K polymer
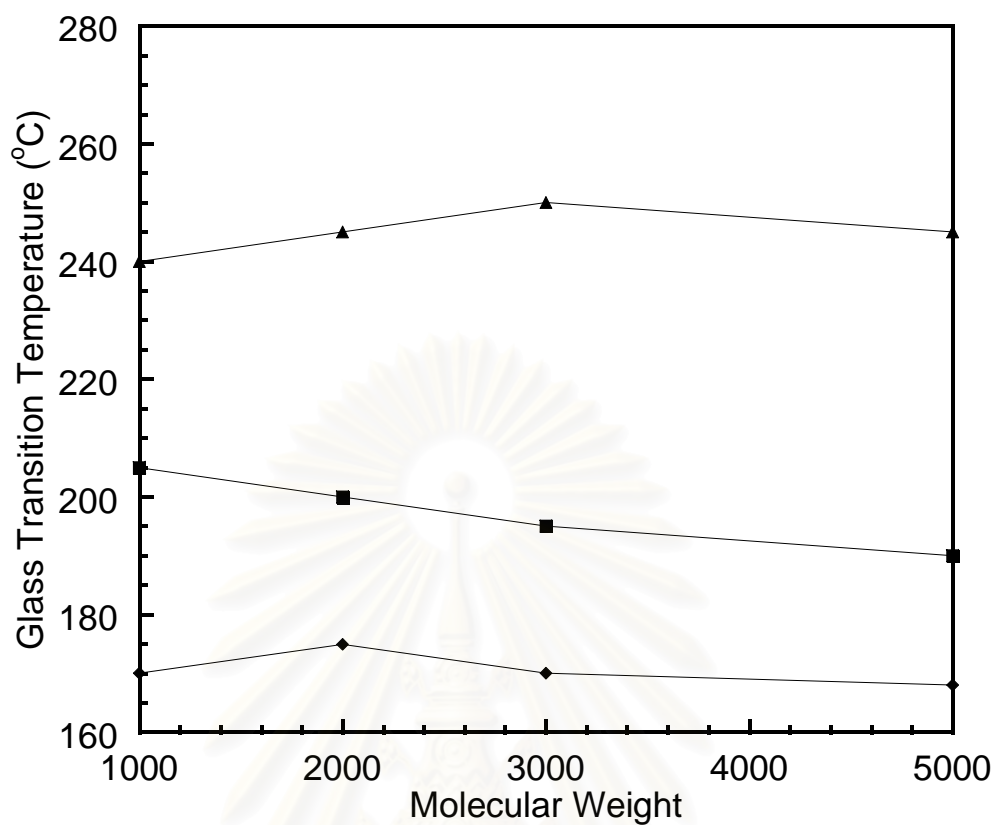alloys at various compositions: (▼) 100:0, (◆) 90:10, (■)
80:20, (▲) 70:30

Figure 5.10: Relationship between MW of polyol and glass transition temperature of BA:PU alloys from differential scanning calorimeter: (◆) 90:10, (■) 80:20, (▲) 70:30

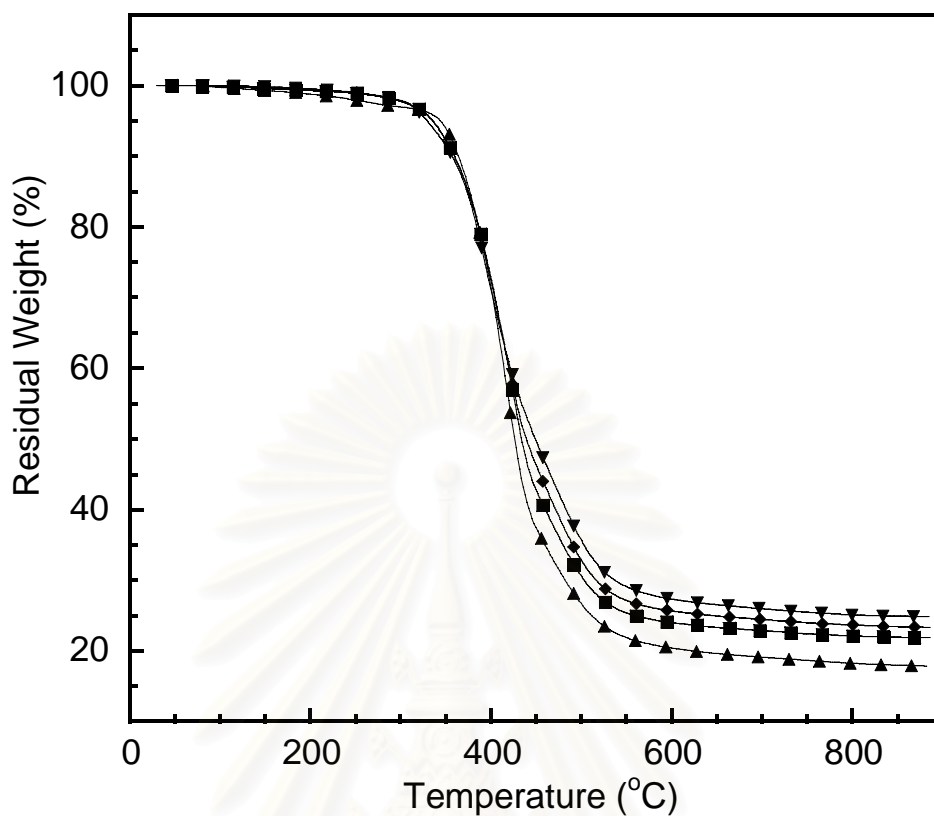**Figure 5.11**: TGA thermograms of the BA:PU2K polymer alloys at various compositions: (▼) 100:0, (◆) 90:10, (■) 80:20, (▲) 70:30
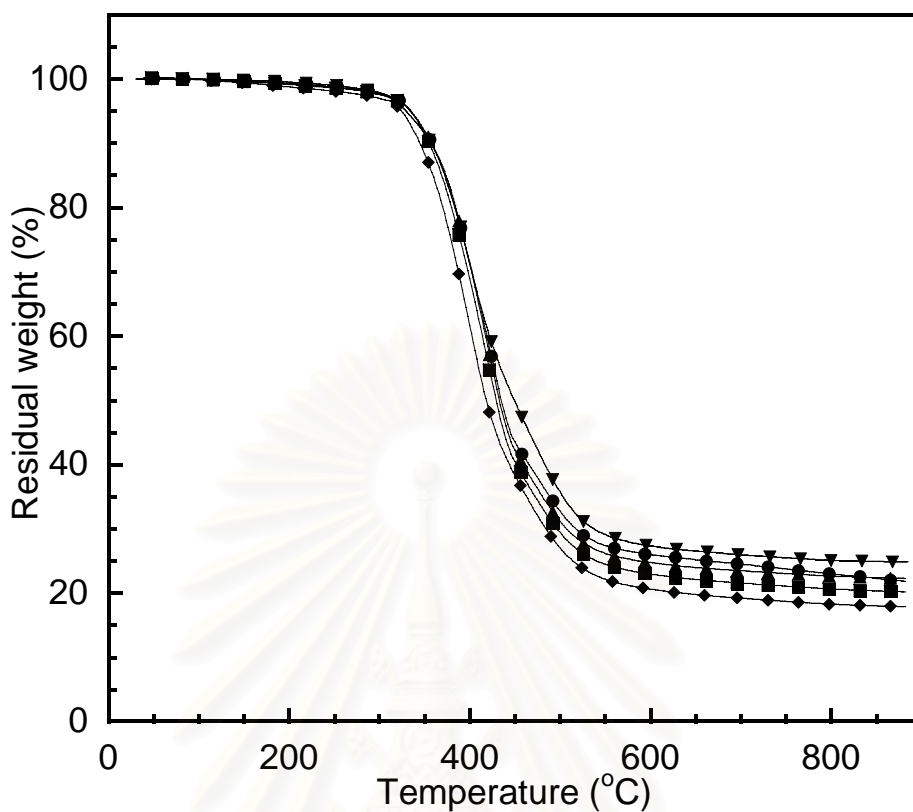
Figure 5.12: TGA thermograms of the BA:PU (80:20) polymer alloys at various polyol molecular weights: (▼) Pure BA, (◆) MW 1000, (■) MW 2000, (▲) MW 3000, (●) MW 5000
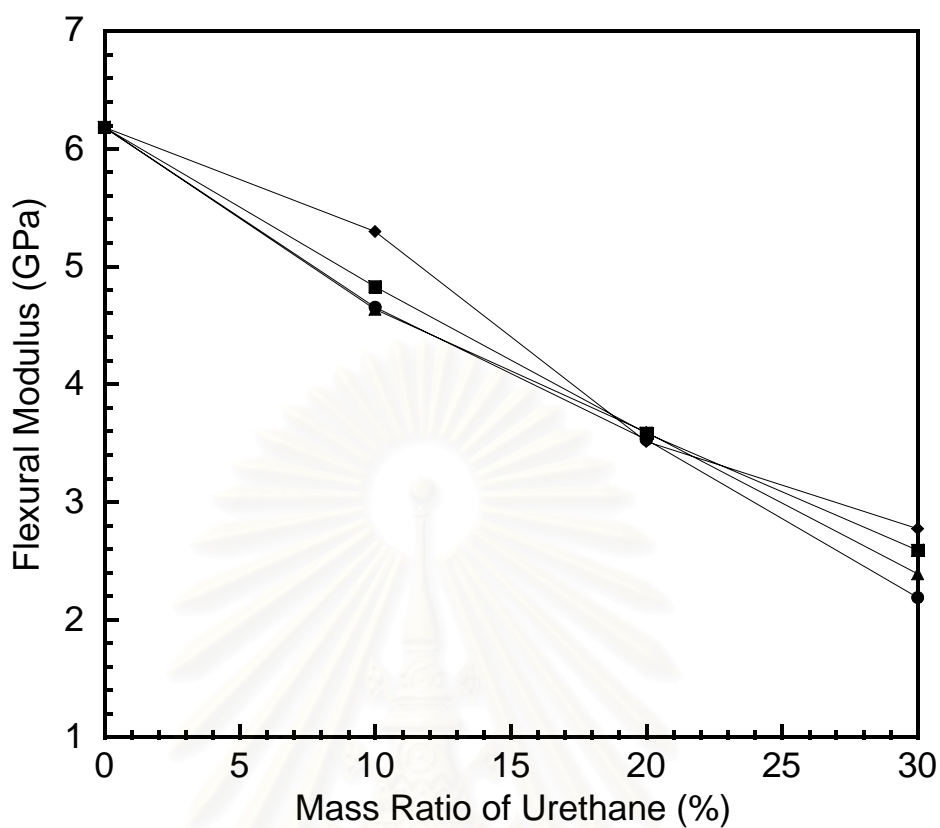
Figure 5.13: Relationship between flexural modulus and urethane fraction of the BA:PU alloys: (◆) MW 1000, (■) MW 2000, (▲) MW 3000, (●) MW 5000
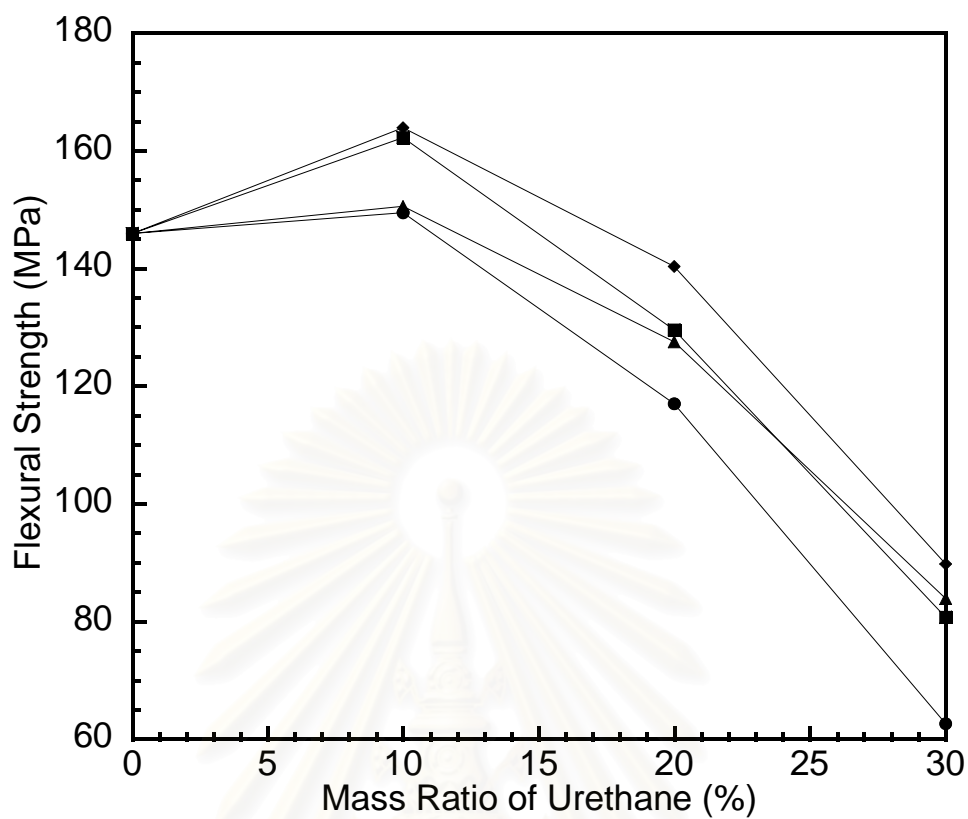
Figure 5.14: Relationship between flexural strength and urethane fraction of the BA:PU alloys: (◆) MW 1000, (■) MW 2000, (▲) MW 3000, (●) MW 5000

Figure 5.15: Stroage moduli of BA:PU1K alloys at various mass ratios:
(▼) 100:0, (◆) 90:10, (■) 80:20, and (▲) 70:30

สถาบันวิทยบริการ

จุฬาลงกรณ์มหาวิทยาลัย

Figure 5.16: Stroage moduli of BA:PU2K alloys at various mass ratios:
(▼) 100:0, (◆) 90:10, (■) 80:20, and (▲) 70:30

Figure 5.17: Stroage moduli of BA:PU3K alloys at various mass ratios:
(▼) 100:0, (◆) 90:10, (■) 80:20, and (▲) 70:30

Figure 5.18: Stroage moduli of BA:PU5K alloys at various mass ratios:
(▼) 100:0, (◆) 90:10, (■) 80:20, and (▲) 70:30
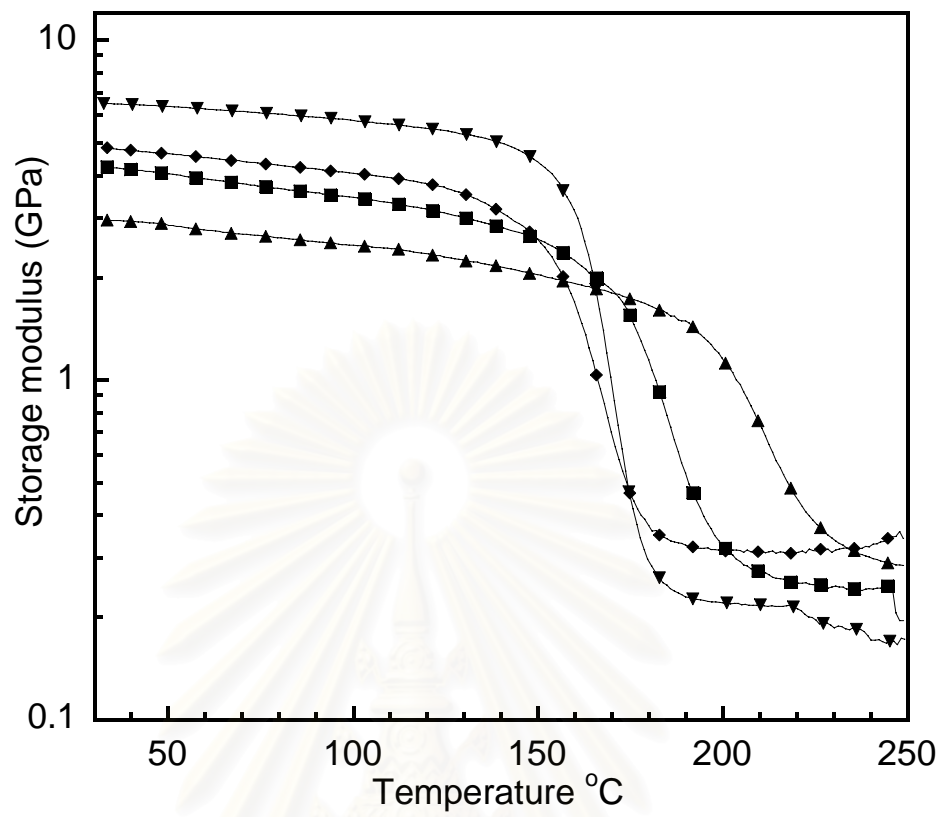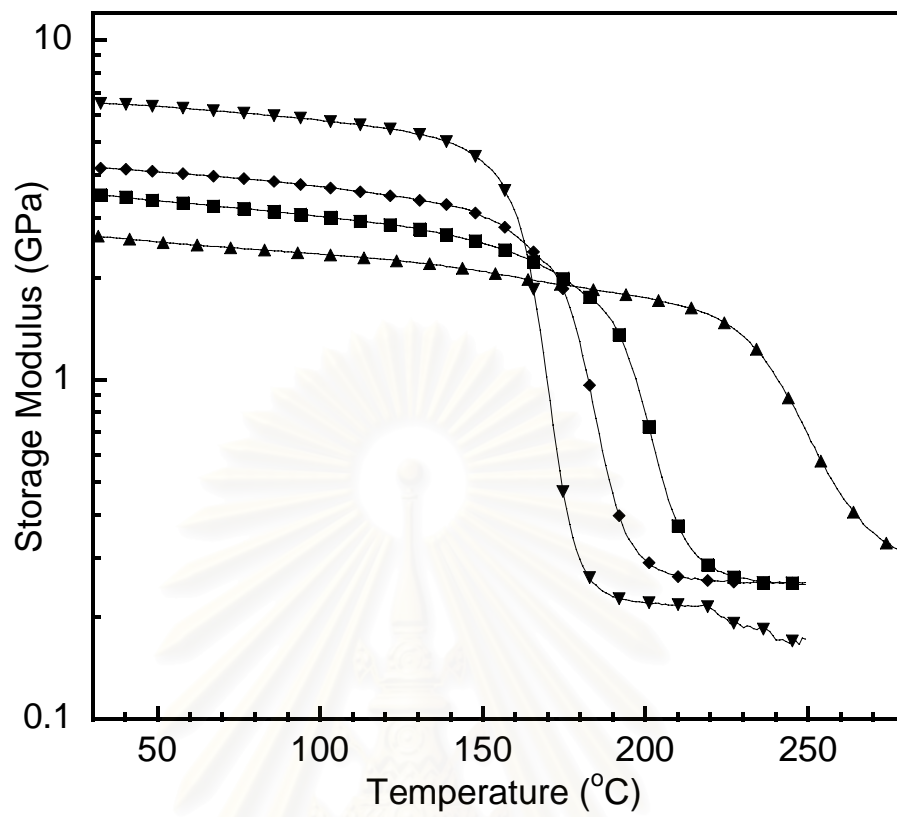
สถาบันวิทยบริการ

จุฬาลงกรณ์มหาวิทยาลัย

Figure 5.19: Loss moduli of BA:PU1K alloys at various mass ratios:
(▼) 100:0, (◆) 90:10, (■) 80:20, and (▲) 70:30
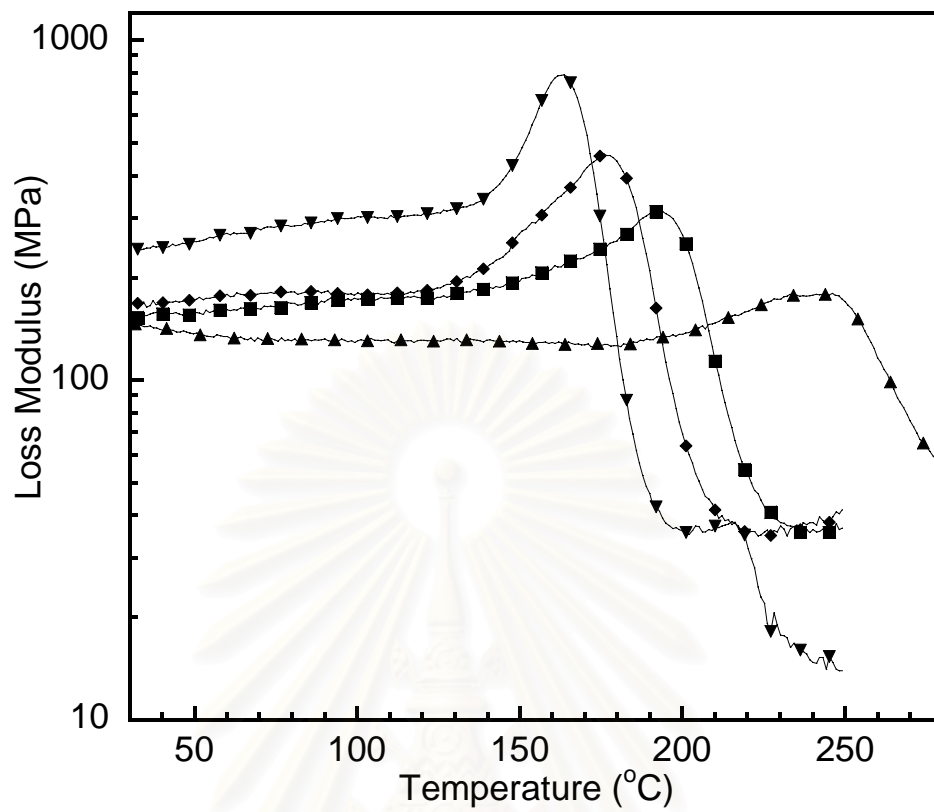
Figure 5.20: Loss moduli of BA:PU2K alloys at various mass ratios: (▼) 100:0, (◆) 90:10, (■) 80:20, and (▲) 70:30
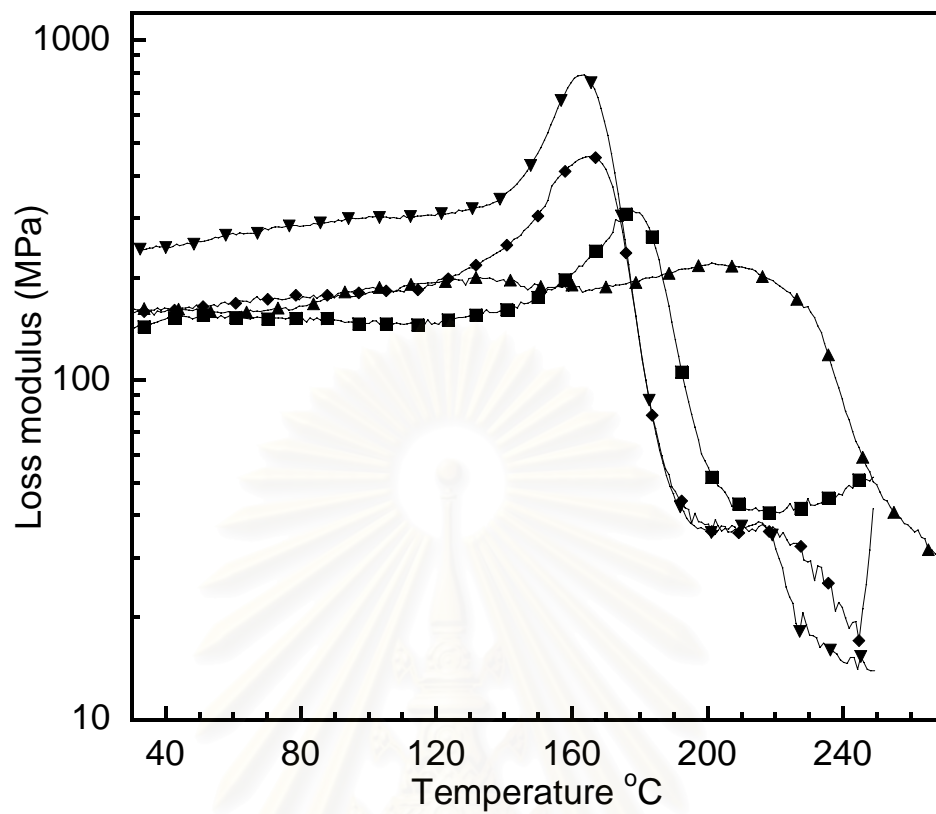
Figure 5.21: Loss moduli of BA:PU3K alloys at various mass ratios: (▼) 100:0, (◆) 90:10, (■) 80:20, and (▲) 70:30
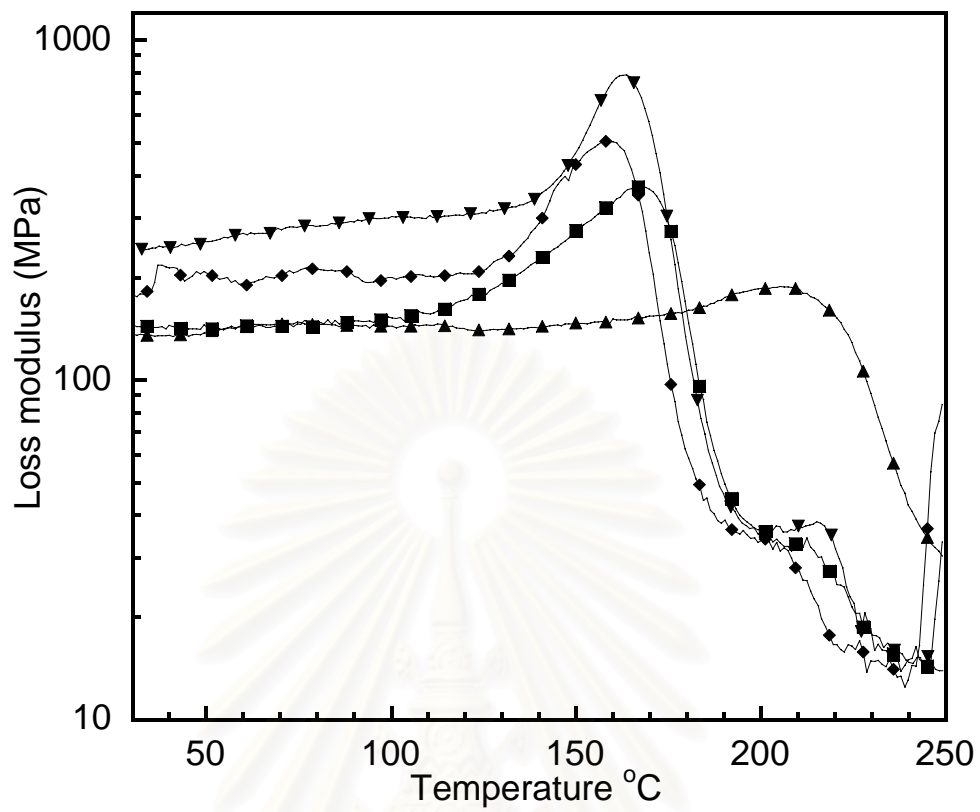
Figure 5.22: Loss moduli of BA:PU5K alloys at various mass ratios:
(▼) 100:0, (◆) 90:10, (■) 80:20, and (▲) 70:30

Figure 5.23: Tanδ of BA:PU1K alloys at various mass ratios: (▼) 100:0,
(◆) 90:10, (■) 80:20, and (▲) 70:30
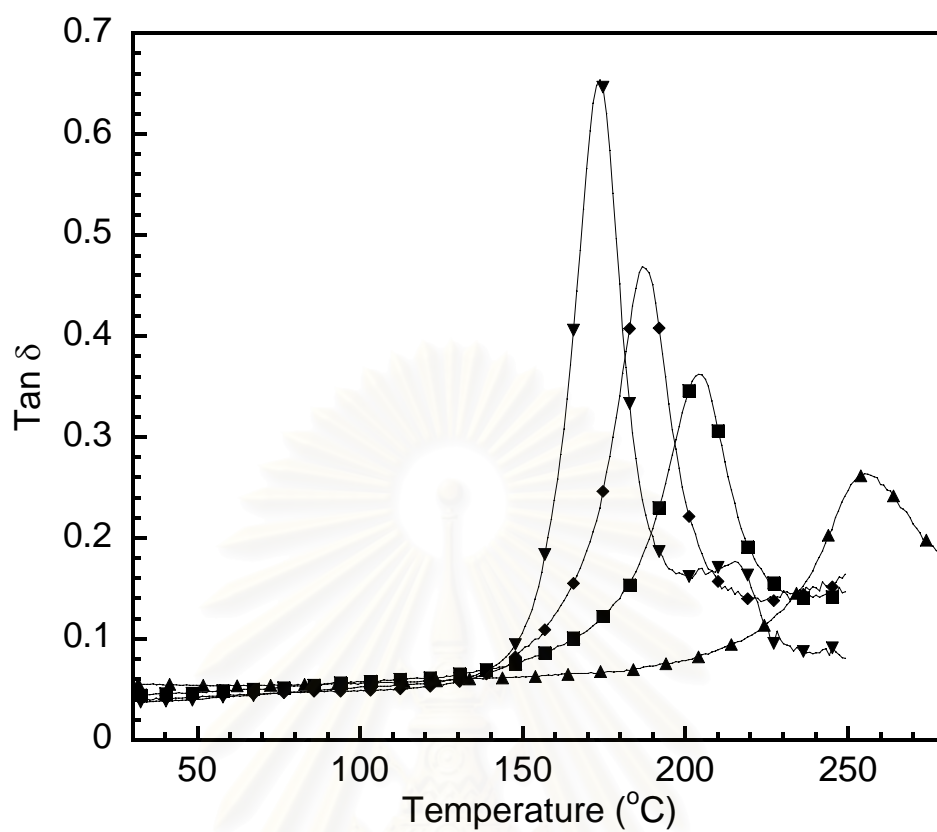
สถาบันวิทยบริการ

จุฬาลงกรณ์มหาวิทยาลัย

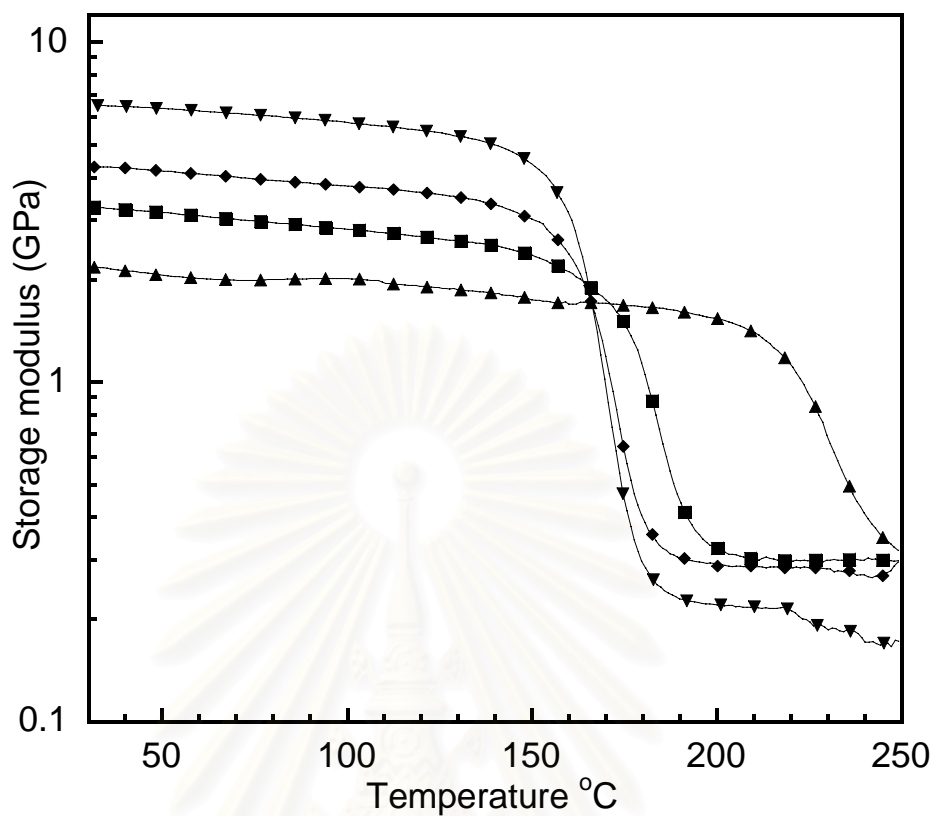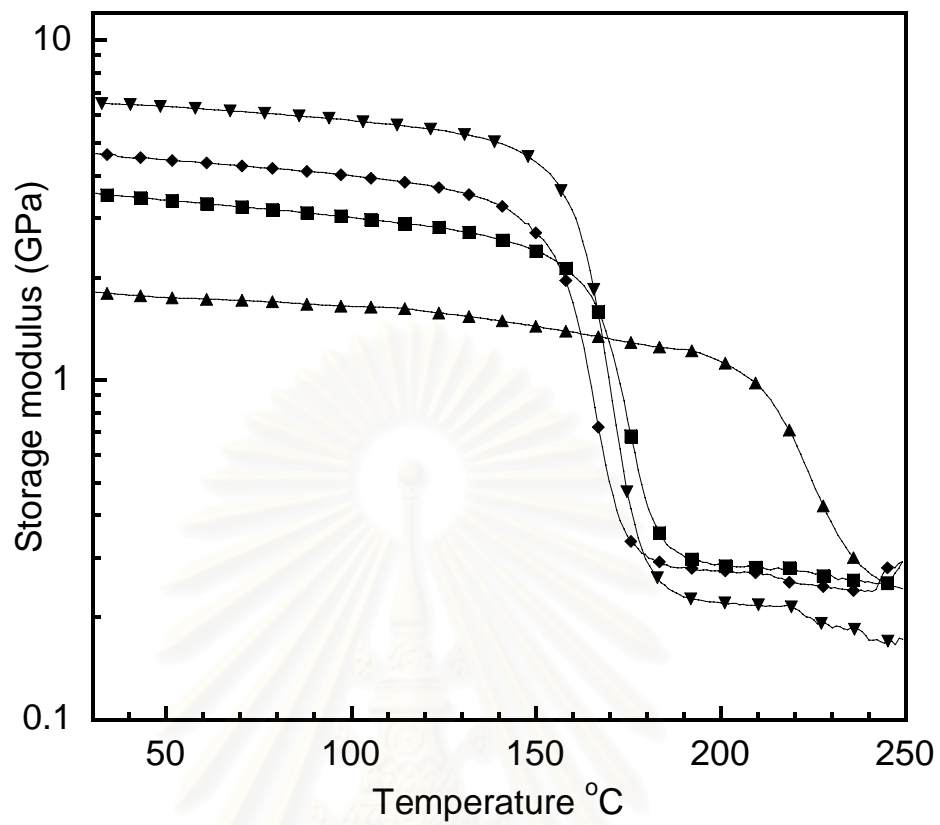**Figure 5.24:** Tan δ of BA:PU2K alloys at various mass ratios: (▼) 100:0, (◆) 90:10, (■) 80:20, and (▲) 70:30
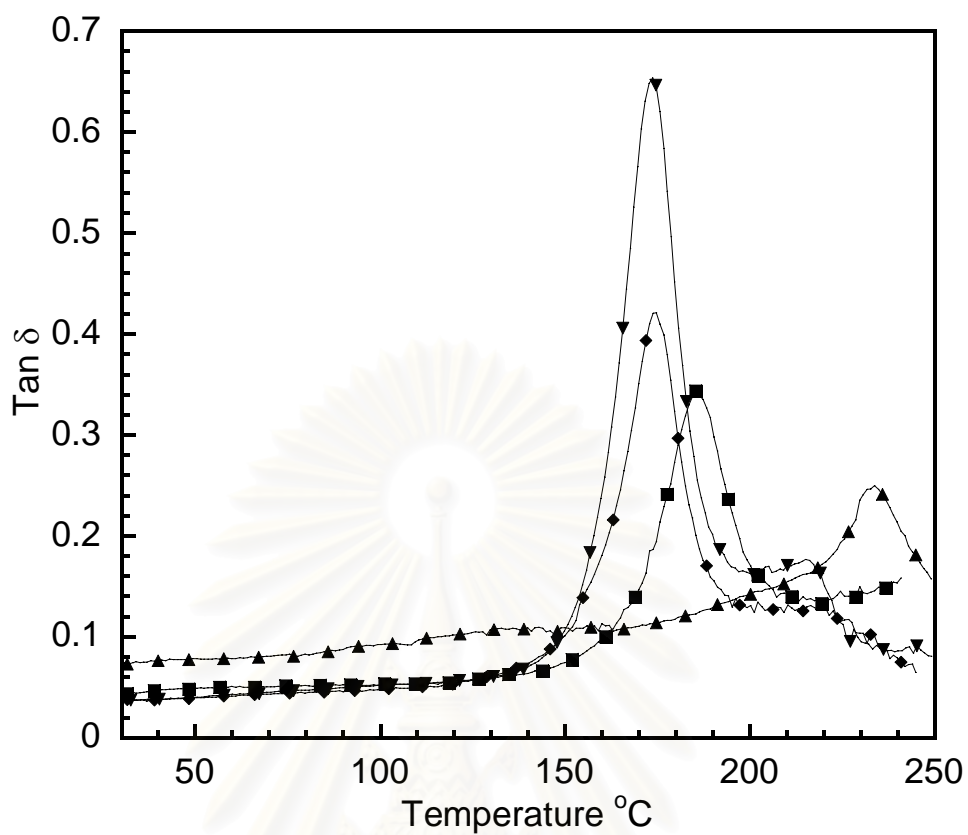
Figure 5.25: Tanδ of BA:PU3K alloys at various mass ratios: (▼) 100:0, (◆) 90:10, (■) 80:20, and (▲) 70:30

สถาบันวิทยบริการ

จุฬาลงกรณ์มหาวิทยาลัย

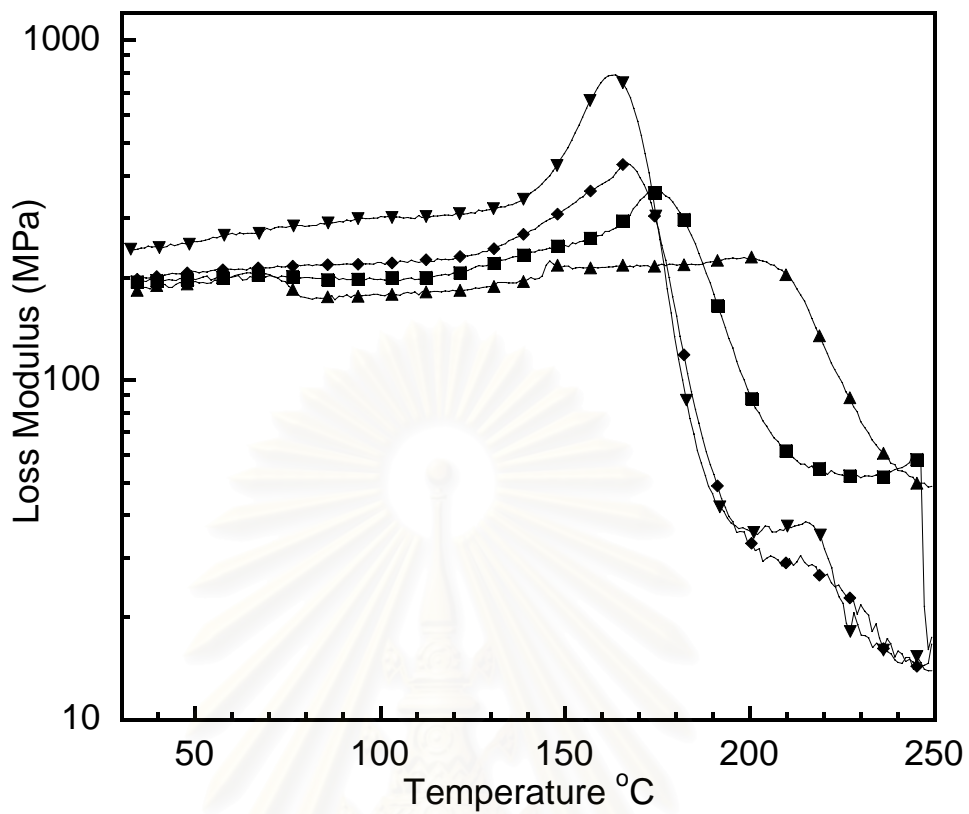**Figure 5.26:** Tanδ of BA:PU5K alloys at various mass ratios: (▼) 100:0, (◆) 90:10, (■) 80:20, and (▲) 70:30

Figure 5.27: Storage moduli of BA:PU (80:20) alloys at various polyol molecular weights: (◆) MW 1000, (■) MW 2000, (▲) MW 3000, and (●) MW 5000

Figure 5.28: Loss moduli of BA:PU2K alloys at various polyol molecular weights: (◆) MW 1000, (■) MW 2000, (▲) MW 3000, and (●) MW 5000

Figure 5.29: Tan δ of BA:PU2K alloys at various polyol molecular weights: (◆) MW 1000, (■) MW 2000, (▲) MW 3000, and (●) MW 5000

สถาบันวิทยบริการ
จุฬาลงกรณ์มหาวิทยาลัย
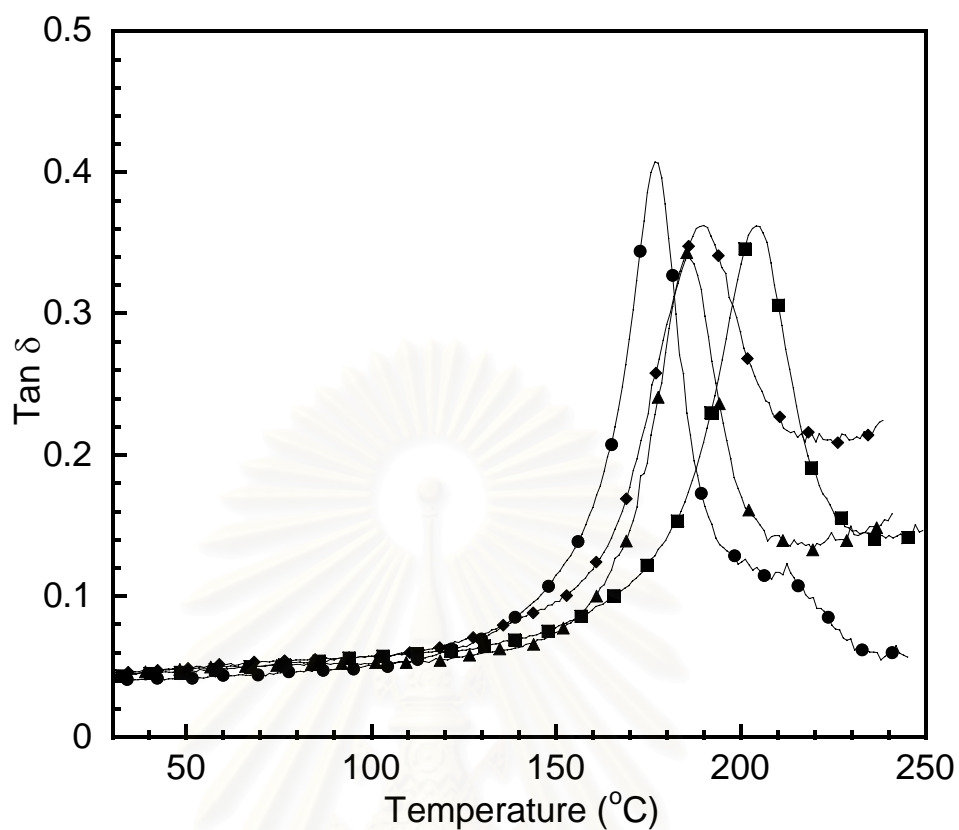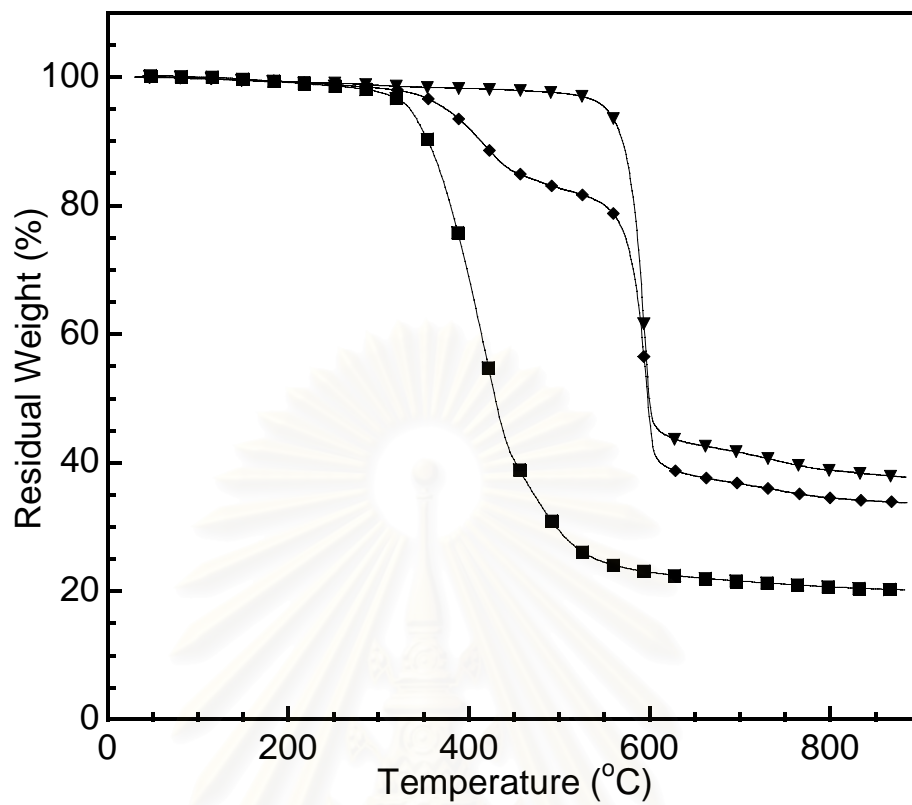
Figure 5.30: TGA thermograms of the polmer metrix content in
Kevlar^{TM}-reinforce composite : (▼) Pure BA, (♦)Kevlar^{TM}-
reinforced composite, (■) Polymer Matrix Alloys of BA:
PU 2K (80:20)
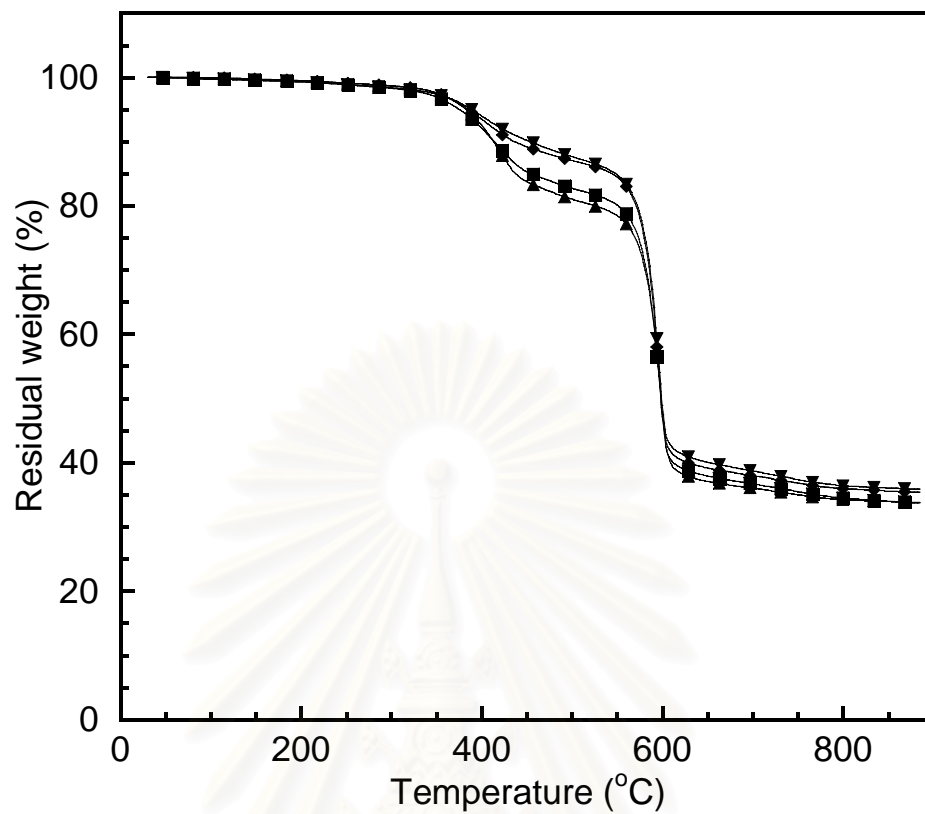
Figure 5.31: Thermal degradation behaviors of the Kevlar[TM]-reinforced
BA:PU2K alloys at various compositions: (▼) Pure BA,
(◆) 90:10, (■) 80:20, (▲) 70:30
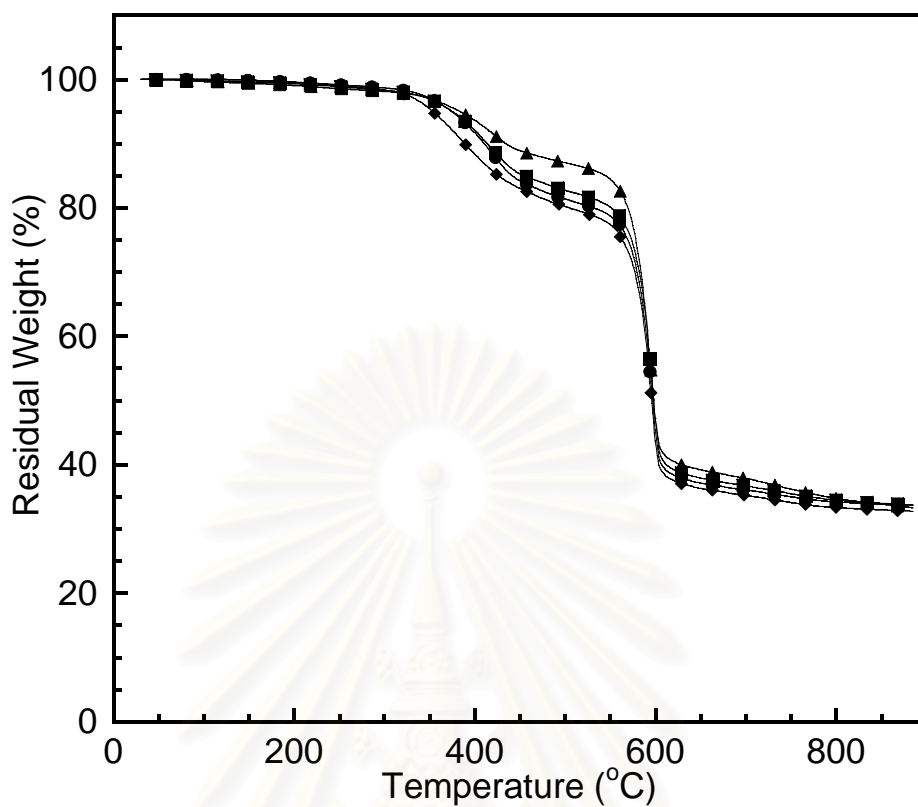
Figure 5.32: Thermal degradation behaviors of the Kevlar[TM]-reinforced BA:PU (80:20) alloys at various polyol molecular weights: (◆)MW 1000, (■) MW 2000, (▲) MW 3000, and (●) MW 5000
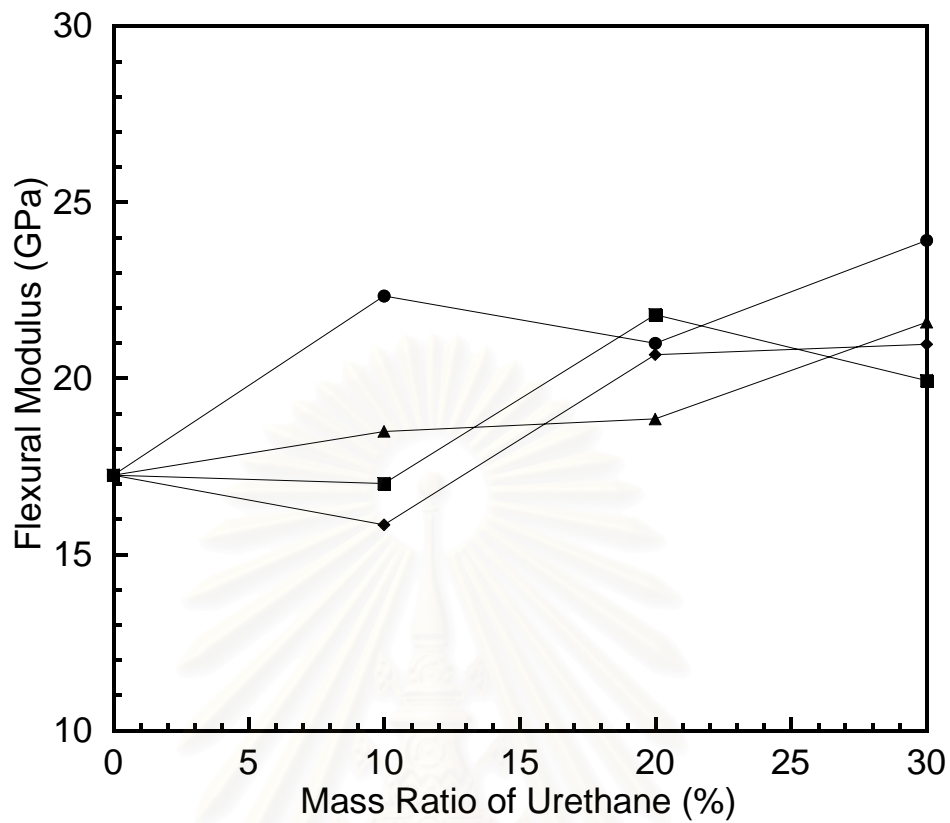
Figure 5.33: Relationship between flexural modulus and urethane fraction of the BA:PU matrix alloys in Kevlar[TM]-reinforced composite : (◆) MW 1000, (■) MW 2000, (▲) MW 3000, (●) MW 5000
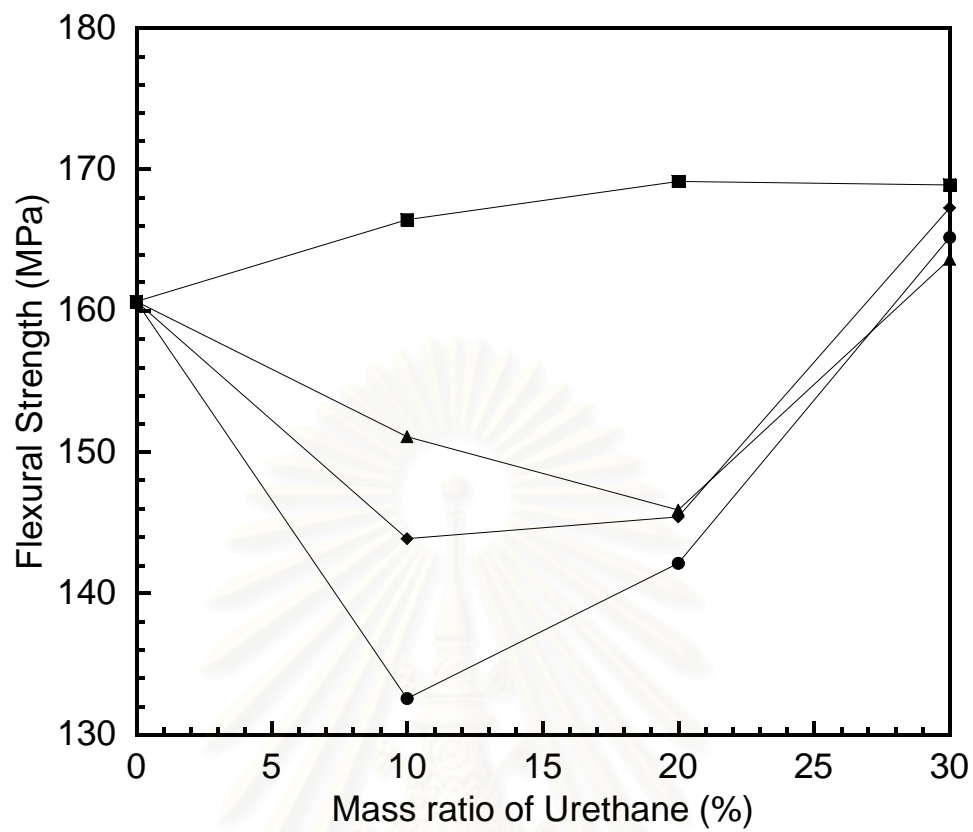
Figure 5.34: Relationship between flexural strength and urethane fraction of the BA:PU matrix alloys in Kevlar^{TM}-reinforced composite : (◆) MW 1000, (■) MW 2000, (▲) MW 3000, (●) MW 5000
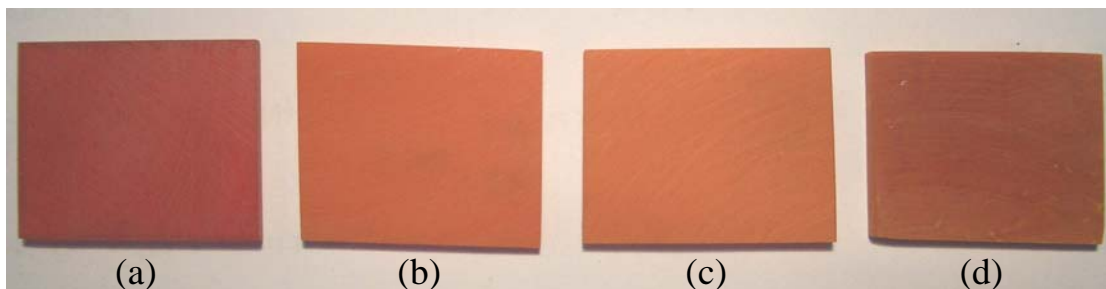
Figure 5.35: The Polymer Alloys Specimens before Immerse in Chloroform: (a) BA:PU2K = 100:0, (b) BA:PU2K = 90:10 , (c) BA:PU2K = 80:20, and (d) BA :PU2K = 70:30
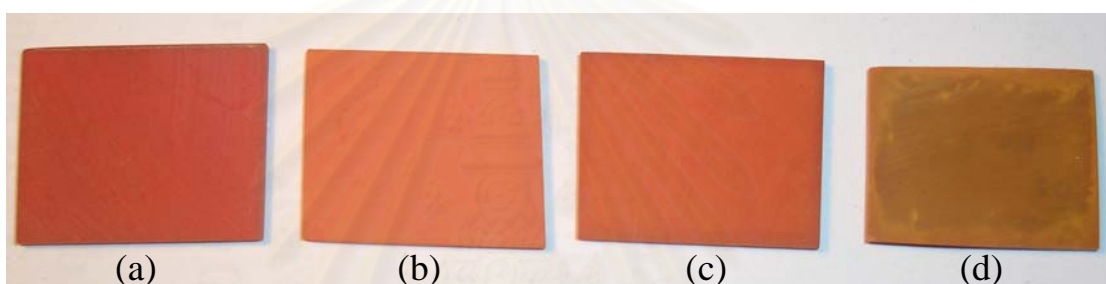
Figure 5.36: The Polymer Alloys Specimens after Immerse in Chloroform: (a) BA:PU2K = 100:0, (b) BA:PU2K = 90:10 , (c) BA:PU2K = 80:20, and (d) BA :PU2K = 70:30
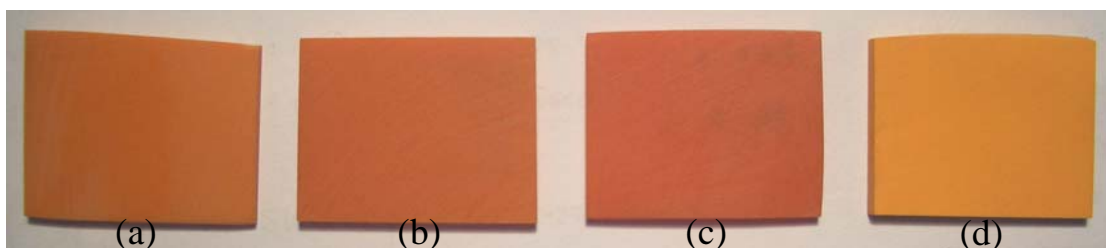
Figure 5.37: The Polymer Alloys Specimens (BA:PU = 80:20) before Immerse in Chloroform: (a) MW 1000, (b) MW 2000, (c) MW 3000, and (d) MW 5000

Figure 5.38: The Polymer Alloys Specimens (BA:PU = 80:20) after Immerse in Chloroform: (a) MW 1000, (b) MW 2000, (c) MW 3000, and (d) MW 5000

Figure 5.39: The Polymer Alloys Specimens Immersed in Chloroform
for 7 days: (a) BA:PU2K = 100:0, (b) BA:PU2K = 90:10,
(c) BA:PU2K = 80:20, and (d) BA :PU2K = 70:30
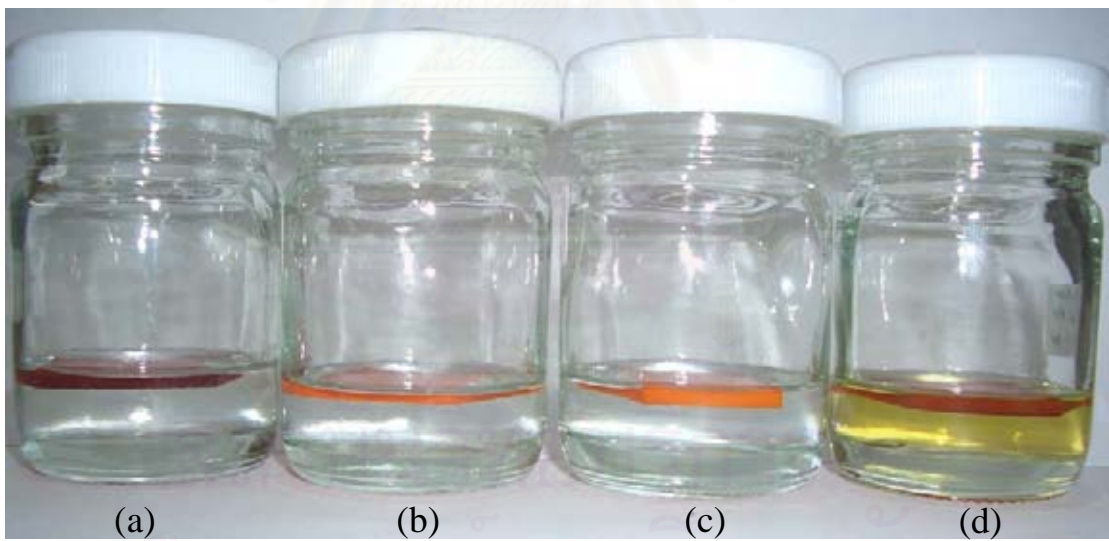
Figure 5.40: The Polymer Alloys Specimens Immersed in Chloroform
for 14 days: (a) BA:PU2K = 100:0, (b) BA:PU2K = 90:10,
(c) BA:PU2K = 80:20, and (d) BA :PU2K = 70:30
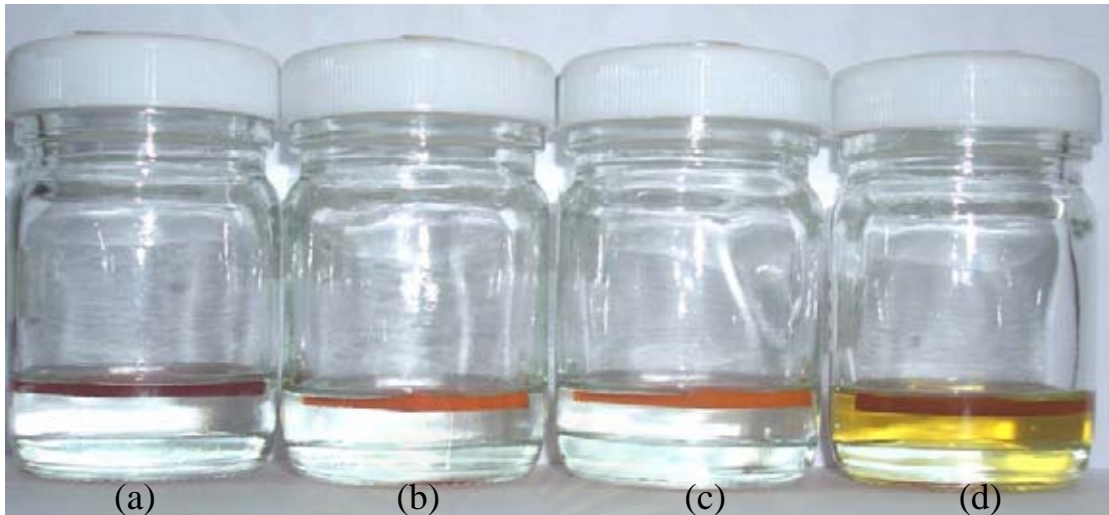
Figure 5.41: The Polymer Alloys Specimens Immersed in Chloroform for 30 days: (a) BA:PU2K = 100:0, (b) BA:PU2K = 90:10, (c) BA:PU2K = 80:20, and (d) BA :PU2K = 70:30
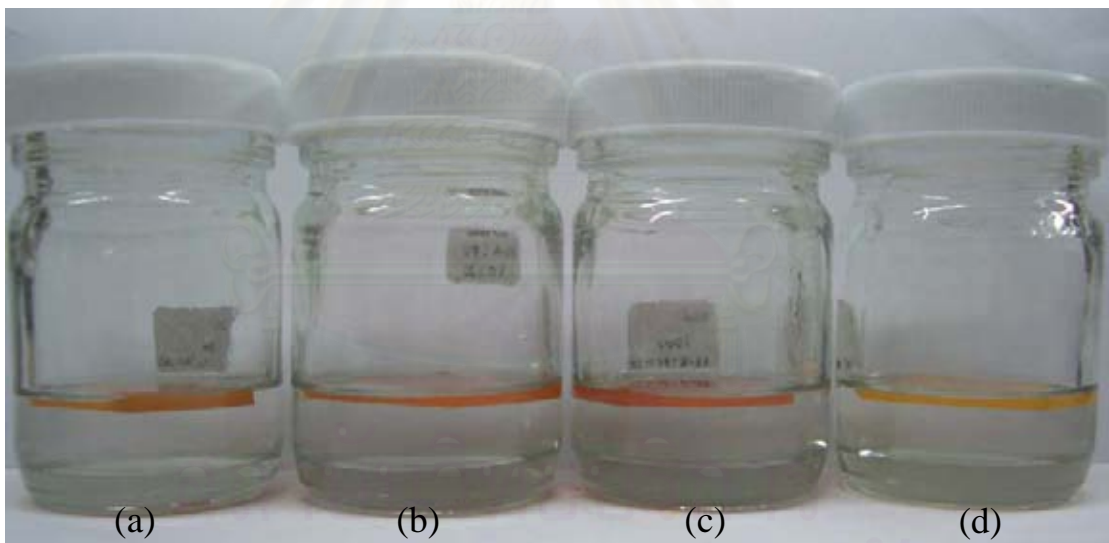
Figure 5.42: The Polymer Alloys Specimens (BA:PU=80:20) Immersed in Chloroform for 7 days : (a) MW 1000, (b) MW 2000, (c) MW 3000, and (d) MW 5000

Figure 5.43: The Polymer Alloys Specimens (BA:PU=80:20) Immersed in Chloroform for 14 days : (a) MW 1000, (b) MW 2000, (c) MW 3000, and (d) MW 5000

Figure 5.44: The Polymer Alloys Specimens (BA:PU=80:20) Immersed in Chloroform for 30 days : (a) MW 1000, (b) MW 2000, (c) MW 3000, and (d) MW 5000

(a) front surface   (a) back surface   (b) front surface   (b) back surface

(c) front surface   (c) back surface   (d) front surface   (d) back surface

(a)   (b)   (c)

side view
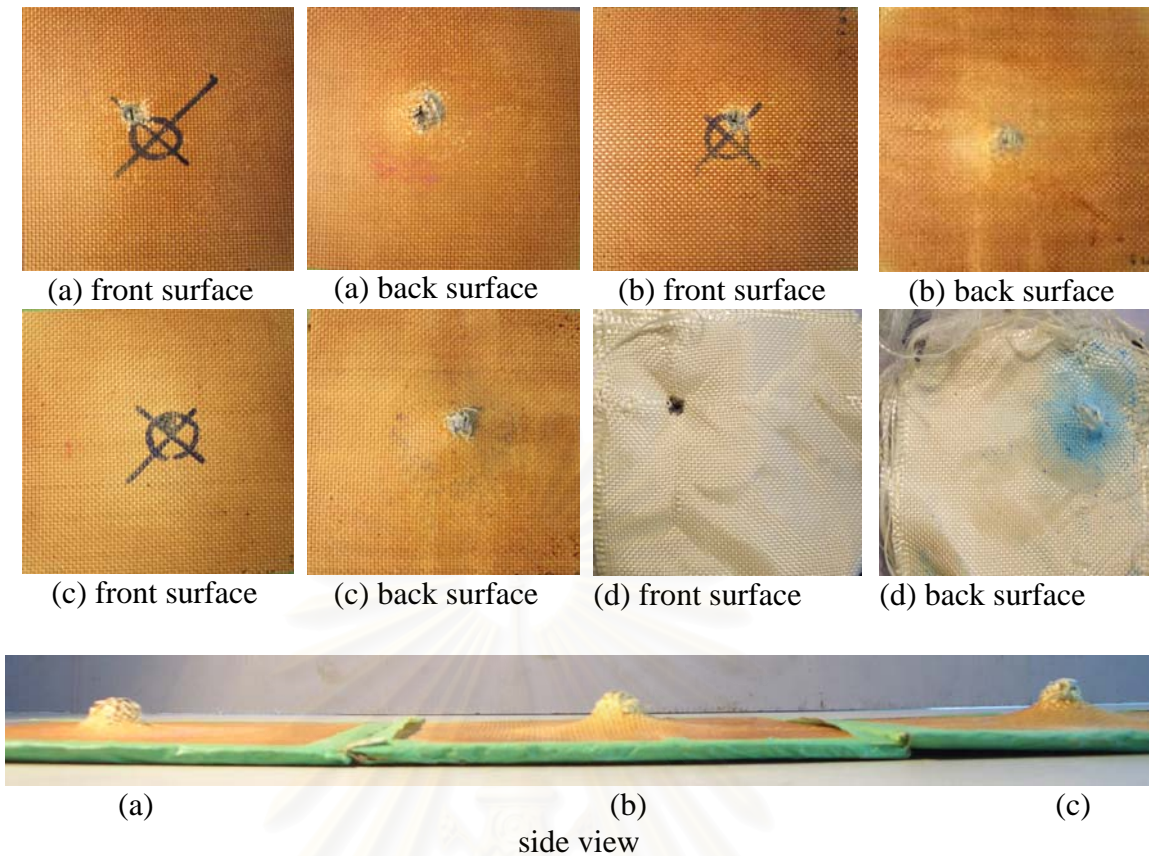
Figure 5.45: Damaged and delaminated area of 5 piles/panel with the samples arrangment of 5/5 after impact with standard lead projectiles with lead outer-coating typically used in 9 mm: (a) Kevlar^{TM}-reinforced hard epoxy, (b) Kevlar^{TM}-reinforced epoxy blend (hard:flexible = 1:1), (c) Kevlar^{TM}-reinforced flexible epoxy and (d) Kevlar^{TM} 10 plies

(a) front surface   (a) 1st back surface   (a) 2nd front surface

(b) front surface   (b) 1st back surface   (b) 2nd front surface

(c) front surface   (c) 1st back surface   (c) 2nd front surface

(d) front surface   (d) 1st back surface   (d) 2nd front surface

(a)   (b)   (c)   (d)

side view
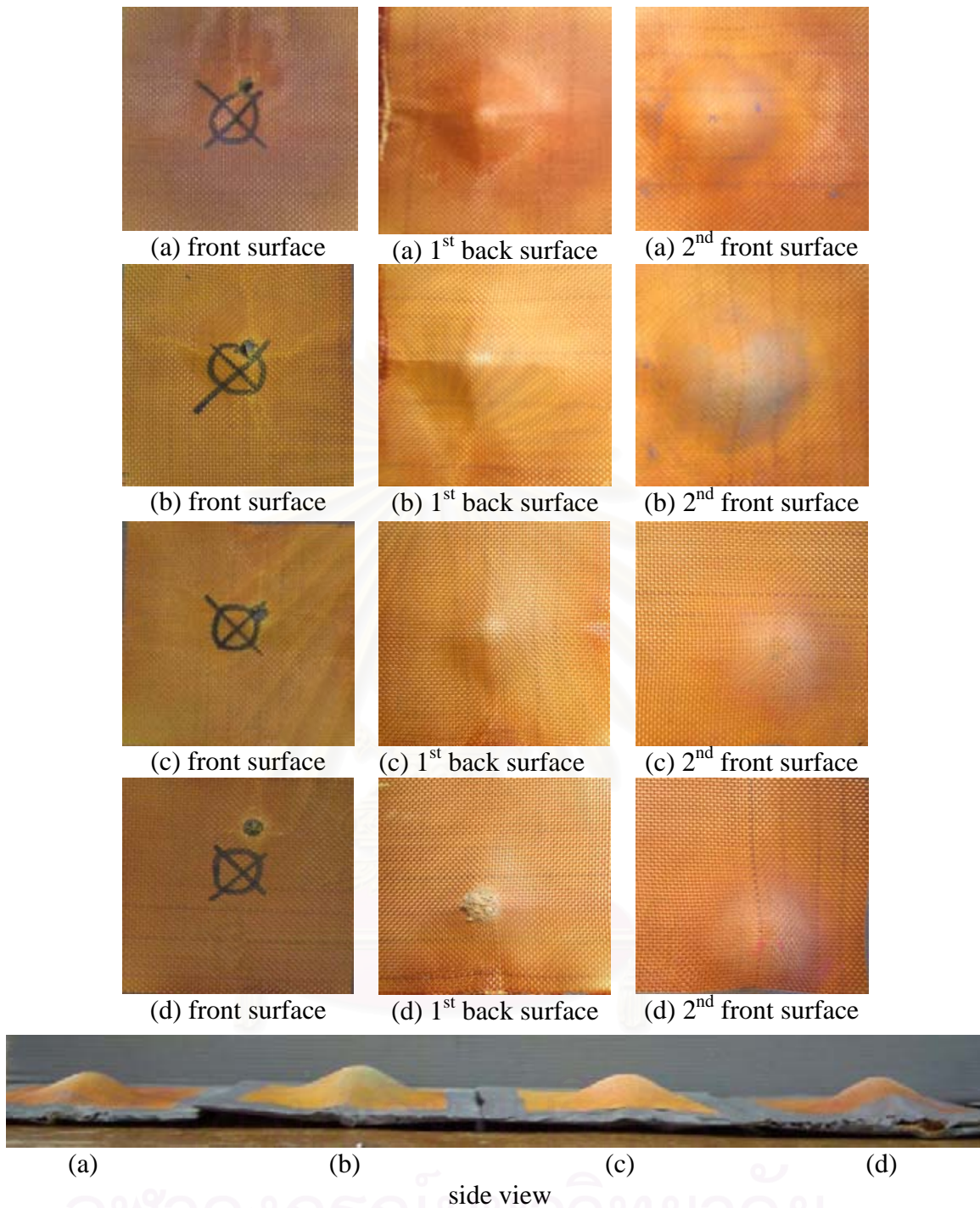
Figure 5.46: Damaged and delaminated area of 5 piles/panel with the samples arrangement of 5/5 after impact with standard lead projectiles with lead outer-coating typically used in 9 mm: (a) Kevlar[TM]-reinforced 100:0 BA:PU2K, (b) Kevlar[TM] reinforced 90:10 BA:PU2K, (c) Kevlar[TM]-reinforced 80:20 BA:PU2K, and (d) Kevlar[TM]-reinforced 70:30 BA:PU2K

(a) front surface   (a) 1st back surface   (a) 2nd front surface

(b) front surface   (b) 1st back surface   (b) 2nd front surface

(c) front surface   (c) 1st back surface   (c) 2nd front surface

(d) front surface   (d) 1st back surface   (d) 2nd front surface

(a)   (b)   (c)   (d)

side view

Figure 5.47: Damaged and delaminated area of 5 piles/panel with the samples arrangement of 5/5 after impact with standard lead projectiles with lead outer-coating typically used in 9 mm: (a) Kevlar[TM]-reinforced 80:20 BA:PU1K, (b) Kevlar[TM] reinforced 80:20 BA:PU2K, (c) Kevlar[TM]-reinforced 80:20 BA:PU3K, and (d) Kevlar[TM]-reinforced 80:20 BA:PU5K
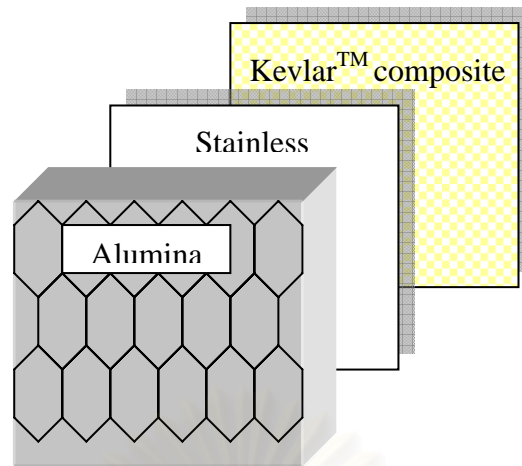
(a)
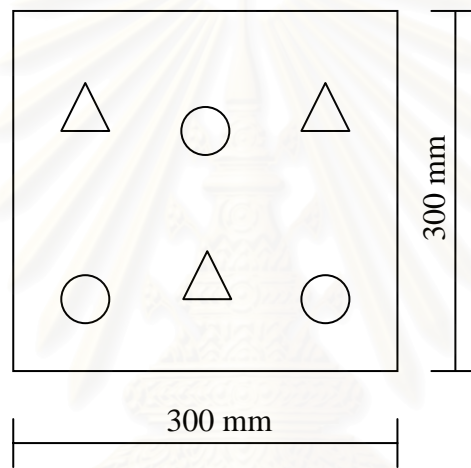
(b)

Figure 5.48: (a) The sample arrangement

(b) The mark of shooting: $\bigcirc$ = 7.62, $\triangle$ = ss109

(a) front surface   (a) back of metal   (a) back of composite

(b) front surface   (b) back of metal   (b) back of composite

(c) front surface   (c) back of metal   (c) back of composite
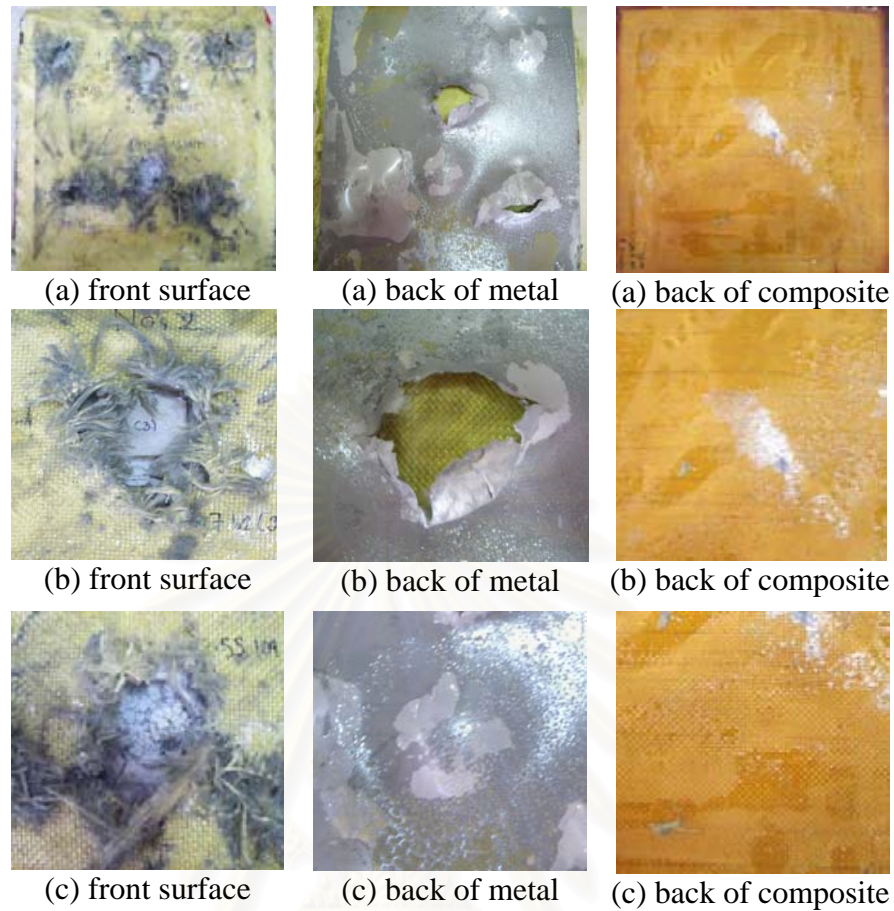
Figure 5.49: Damaged and delaminated area of hard armor composite combined of alumina 10 mm., stainless 1 mm., and Kevlar^{TM}-reinforced composite 11 mm. with the samples arrangement of alumina / stainless / Kevlar^{TM}-reinforced composite after impact with standard 7.62 mm and ss109 ammunition at each of 3 bullet of ammunition per panel: (a) back surface of whole sample, (b) back surface of 7.62 mm ammunition, and (c) back surface of ss109 ammunition

(a)

(b)

(c)

Figure 5.50: Damaged area (side view) of hard armor composite combined of alumina 10 mm., stainless 1 mm., and Kevlar^{TM}-reinforced composite 11 mm. with the samples arrangement of alumina / stainless / Kevlar^{TM}- reinforced composite after impact with standard 7.62 mm and ss109 ammunition at each of 3 bullet of ammunition per panel: (a) whole sample, (b) metal panel, and (c) KevlarTM-reinforce composite

CHAPTER VI

CONCLUSIONS

The the suitable polyol molecular weight using benzoxazine-urethane matrix alloy for Kevlar^{TM}-reinforced composited was investigated. The thermal stability, mechanical properties, and ballistic impact resistance were estimated for the optimal polyol molecular weight as well as resin mixture composition.

The DSC experiment revealed the fully-cured condition of binary mixture to be at 160°C, 170°C, 180°C, and 200°C for 2 hrs at each temperature. Adding the urethane resin in the range of 0-30% by weight, the glass transition temperature of the BA:PU1K, BA:PU2K, BA:PU3K, and BA:PU5K alloys were found to be in the range of 165-240°C, 165-245°C, 165-250°C, and 165-245°C, respectively. For BA:PU alloys system, the degradation temperature at 5% weight loss at various polyol molecular weights were observed to be around 332°C. As a consequence, effects of the molecular weights of the polyol on degradation temperature and char yield of BA:PU alloy were not significant. In addition, flexural strength of the BA:PU alloys exhibited the synergistic behaviour with the ultimate value at BA:PU=90:10 for every polyol molecular weights used polyol.

The ballistic test results of 8-ply Kevlar^{TM}-reinforced BA:PU composites using a 9 mm handgun, with standard lead projectiles having lead outer-coating, revealed that the BA:PU matrix alloy at a molecular weight of 3000 exhibited suitable ballistic impact resistance in comparison with other three molecular weights of the polyol and confirmed the optimum mass ratio of BA:PU to be 80:20 in the polymer alloys. The areal density of 0.23 g/cm^2 was obtained in this composite panel. The hard armor composite of 300×300 mm^2 which was assembled from 10 mm of alumina, 1 mm of stainless, and 11 mm in thickness of Kevlar^{TM}-reinforced composite had the performance in ballistic penetration resistance passed both the NIJ standard level III as well as the impact from ss109 ammunition. In addition, the composite was also evaluated to resist multiple hits from the ammunitions at this high impact level.

REFERENCES

Bajsic, E. G.; Rek, V.; Sendijarevic, A.; Sendijarevic, V.; and Frish, K. C., "The effect of different molecular weight of soft segments in polyurethanes on photooxidative stability," Polym. Degrad. Stab., 52(1996) 223-225.

Bhatnagar, A.; and Tan, C.B.C., "Ballistic fabric laminates," U.S. Patent 20030199215 (2003).

Chiang, W.Y.; and Tsai, C.D., "Synthesis and properties of maleimide-terminated polyurethane AB crosslinked polymers I. Polyurethane/allyl nonyl novolac resin ABCPs," Eur. Polym. J., 35(1999) 1141.

Coppage, Jr.; Edward, A.; and Richard, W., "Anti-ballistic protective composite fabric," U.S. Patent 6127291 (2000).

Das, S.; Yilgor, I.; Yilgor, E.; Inci, B.; Tezgel, O.; Beyer, F. L.; and Wilkes G. L., "Structure-proprety relationships and melt rheology of segmented, non-chain extended polyureas: Effect of soft segment molecular weight," Polymer, 48(2007) 290-301.

Eceiza, A.; Caba, K.; Kortaberria, G.; Gabilondo, N.; Marieta, C.; Corcuera, M. A.; and Mondragon, I., "Influence of molecular weight and chemical structure of soft segment in reaction kinetics of polycarbonate diols with 4, 4' – diphenylmethane diisocyanate," Eur. Polym. J., 41(2005) 3051-3059.

Hepburn, C., "Polyurethane elastomers," 2nd edition, London, Elsevier Science Publishing, 1992.

Heijkants, R. G. J. C.; Calck, R. V.; Tienen, T. G.; Groot, J. H.; Buma, P.; Pennings, A. J.; Veth, R. P. H.; Schouten, A. J., "Uncatalyzed synthesis, thermal and mechanical properties of polyurethanes based on poly(ε-caprolactone) and 1,4-butane diisocyanate with uniform hard segment," Biomaterials, 26(2005) 4219-4226.

Irusta, L.; and Fernandez-Berridi, M. J., "Aromatic poly(ester-urethanes): effect of the polyol molecular weight on the photochemical behaviour," Polymer, 41(2001) 3297-3302.

Ishida, H., "Process for preparation of benzoxazine compounds in solventless systems," U.S. Patent 5,543,516 (1996).

Ishida, H.; and Allen, D.J., "Mechanical characterization of copolymers based on benzoxazine and epoxy," <u>Polymer</u>, 37(1996) 4487-4489.

Ishida, H.; and Low, H. Y., "Improved thermal stability of polybenzoxazines by transition metals," <u>Polym. Degrad. Stab.</u>, 91(2006) 811-815.

James Korley, L. T.; Pate, B. D.; Thomas E. L.; and Hammond, P. T., "Effect of the degree of soft and hard segment ordering on the morphology and mechanical bahaviour of semicrystalline segmented polyurethanes," <u>Polymer</u>, 47(2006) 3074-3078.

Jang, J. Y.; Jhon, Y. K.; Cheong, I. W.; and Kim J. H., "Effect of process variables on molecular weight and mechanical properties of water-based polyurethane dispersion," <u>Colloids Surf., A</u>, 196(2002) 139-140.

Jimenez, G.; Asai, S.; Shishido, A.; and Sumita, M., "Effect of the soft segment on the fatigue behavior of segmented polyurethanes," <u>Eur. Polym. J</u>., 36(2000) 2043-2049.

Jubsilp, J.; Damrongsakkul, S.; Takeichi, T.; and Rimdusit, S., "Curing kinetics of arylamine-based polyfunctional benzoxazine resins by dynamic differential scanning calorimetry," <u>Thermochim. Acta</u>, 447(2006) 133-135.

Krol, P.; and Pilch-Pitera, B., "A study on the synthesis of urethane oligomer," <u>Eur. Polym. J</u>., 39(2003) 1231-1232.

Lewin, M.; Preston, J.; and Sello, S.B., "Handbook of fiber science and technology," New York, Marcel Dekker, 1989.

Li, H. L.; Lin, L. C.; Prevorsek. D.C.; and Chin, H.B., "Ballistic resistant composition article having improved matrix system," <u>U.S. Patent 5,330,820</u> (1994).

Mark, J. E., "Physical properties of polymer handbook," Newyork, AIP Press, 1996.

Mukhopadhyay, S. K.; and Joyce, M.A., "High-performance fibres," Manchester, Textile Institute, 1993.

Oprea, S.; Vlad, S.; and Stanciu, A., "Poly(urethane-methacrylate)s. Synthesis and characterization," <u>Polymer</u>, 42(2001) 7257-7266.

Park, A. D., "Lightweight soft body-armor product," <u>U.S. Patent 6,651,543</u> (2003).

Park, R.; and Jang J., "Effect of laminate thickness on impact behaviour of aramid fiber/vinylester composites," <u>Polymer Testing</u>, 22(2003) 939-946.

Pathomsap, S., <u>Development of Ballistic Armor from Kevlar^{TM} Fiber and Polybenzoxazine Alloys</u> Master's Degree. Department of Chemical Engineering, Faculty of Engineering, Chulalongkorn University, 2005.

Pattanayak, A.; and Jana S. C., "Thermoplastic polyurethane nanocomposites of reactive silicate clays: effects of soft segments on properties," Polymer, 46(2005) 5184- 5185.

Rimdusit, S.; and Ishida, H., "Development of new class of electronic packaging materials based on ternary systems of benzoxazine, epoxy, and phenolic resins," Polymer, 41(2000) 7941-7943.

Rimdusit, S.; Pirstpindvong, S.; Tanthapanichkoon, W.; and Damrongsakkul, S., "Toughening of Polybenzoxazine by Alloying With Urethane Prepolymer and Flexible Epoxy: a comparative study," Polym. Eng. Sci., 45(2005) 288-297.

Sujirote, K.; Dateraksa, K.; and Chollacoop, N, "Practical Requirements for Alumina Armor System," Am. Ceram. Soc. Bull., 86(2006) 22-25.

Takeichi, T.; Guo, Y.; and Agag, T., "Synthesis and Characterization of Poly (urethane-benzoxazine) Films as Novel Type of Polyurethane/Phenolic Resin Composites," J. Polym. Sci., Part A: Polym. Chem., 38(2000) 4165-4175.

Ubaghs, L.; Keul, H.; and Hocker, H., "Novel intramolecular blocked isocyanates as stable one-component system for poly(urea urethane)s," Polymer, 46(2005) 1460-1464.

Wang, L. F.; and Wei, Y. H., "Effect of soft segment length on properties of fluorinated polyurethanes," Colloids Surf.,B, 41(2005) 252-254.

Yang, H. H., "Kevlar aramid fiber," West Sussex, John wiley&Sons Ltd., 1993.

Zuo, M.; Xiang, Q.; and Takeichi, T., "Preparation and properties of novel poly(urethane-imide)s," Polymer, 39(1998) 6884-6885.

Zuo, M.; and Takeichi, T., "Novel method for the preparation of poly(urethane-imide)s and their properties," J. Polym. Sci., Part A: Polym. Chem., 35(1997) 3745-3753.

Zuo, M.; and Takeichi, T., "Preparation and characterization of poly(urethane-imide) films prepared from reactive polyimide and polyurethane prepolymer," Polymer, 40(1999) 5155-5158.

http://www.justnet.org/txtfiles/BodyArmorStd/NIJSTD010103.html

http://www.nps.gov

http://www.toyobo.co.jp

APPENDICES

APPENDIX A

Physical Property of Benzoxazine:Urethane Polymer Alloys

Appendix A-1: Density of BA:PU alloys

Composition (BA:PU)	Density (g/cm^3)				
	Theory	MW 1000	MW 2000	MW 3000	MW 5000
100:0	1.188	1.188	1.188	1.188	1.188
90:10	1.172	1.171	1.161	1.162	1.162
80:20	1.156	1.143	1.134	1.135	1.129
70:30	1.141	1.131	1.103	1.109	1.108

Thermal Characterization of Benzoxazine:Urethane Polymer Alloys

Appendix A-2: Glass transition temperature of BA:PU alloys

BA:PU Systems Compositions	Glass Transition Temperature (^{o}C) from DSC			
	MW 1000	MW 2000	MW 3000	MW 5000
100:0	165	165	165	165
90:10	170	175	170	168
80:20	205	200	195	190
70:30	240	245	250	245

Appendix A-3.1: Degradation temperature of BA:PU2K alloys at various composition

Compositions	Degradation Temperature (^{o}C)	
	5 % weight loss	10 % weight loss
100:0	330	357
90:10	336	360
80:20	336	360
70:30	344	365

Appendix A-3.2: Degradation temperature of BA:PU (80:20) alloys at various polyol molecular weight

Polyol Molecular Weight	Degradation Temperature (^{o}C)	
	5 % weight loss	10 % weight loss
1000	324	344
2000	334	356
3000	334	358
5000	334	358

Appendix A-4.1: Char yield of BA:PU2K alloys at various composition

Compositions	Char Yield (%)
100:0	25.1
90:10	23.6
80:20	22.1
70:30	18.2

Appendix A-4.2: Char yield of BA:PU(80:20) alloys at various polyol molecular weight

Polyol Molecular Weight	Char Yield (%)
1000	18.3
2000	20.6
3000	22.6
5000	22.9

APPENDIX B

Physical Property of Kevlar[TM] Fiber-reinforced
Benzoxazine:Urethane Alloys

Appendix B-1: Density of Kevlar[TM] Fiber-reinforced BA:PU Alloys

Composition (BA:PU)	Density (g/cm^3)				
	Theory	MW 1000	MW 2000	MW 3000	MW 5000
100:0	1.374	1.245	1.245	1.245	1.245
90:10	1.370	1.257	1.268	1.249	1.229
80:20	1.365	1.239	1.240	1.236	1.242
70:30	1.361	1.262	1.257	1.261	1.246

Thermal Characterization of Kevlar^{TM} Fiber reinforced
Benzoxazine:Urethane Alloys

Appendix B-2.1: Degradation temperature of Kevlar^{TM} fiber-reinforced BA:PU2K alloys at various composition

Compositions	Degradation Temperature (^{o}C)	
	5% weight loss	10% weight loss
100:0	389	453
90:10	385	436
80:20	375	414
70:30	383	413

Appendix B-2.2: Degradation temperature of Kevlar^{TM} fiber-reinforced BA:PU(80:20) alloys at various polyol molecular weight

Polyol Molecular Weight	Degradation Temperature (^{o}C)	
	5% weight loss	10% weight loss
1000	354	389
2000	375	414
3000	384	434
5000	375	411

Appendix B-3.1: Char yield of Kevlar^{TM} fiber-reinforced BA:PU2K alloys at various composition

Compositions	Char Yield (%)
100:0	36.4
90:10	35.9
80:20	34.5
70:30	34.2

Appendix B-3.2: Char yield of Kevlar^{TM} fiber-reinforced BA:PU(80:20) alloys at various composition

Polyol Molecular Weight	Char Yield (%)
1000	33.3
2000	34.5
3000	34.7
5000	34.2

APPENDIX C

Mechanical Characterization of Benzoxazine:Urethane Alloys

Appendix C-1.1: Flexural modulus of BA:PU alloys

Compositions	Flexural Modulus (GPa)			
	MW 1000	MW 2000	MW 3000	MW 5000
100:0	6.2 ± 0.1	6.2 ± 0.1	6.2 ± 0.1	6.2 ± 0.1
90:10	5.3 ± 0.1	4.8 ± 0.3	4.6 ± 0.7	4.7 ± 0.4
80:20	3.5 ± 0.3	3.6 ± 0.3	3.6 ± 0.2	3.5 ± 0.0
70:30	2.8 ± 0.2	2.6 ± 0.1	2.4 ± 0.1	2.2 ± 0.1

Appendix C-1.2: Flexural strength of BA:PU alloys

Compositions	Flexural Strength (MPa)			
	MW 1000	MW 2000	MW 3000	MW 5000
100:0	145.9 ± 19	145.9 ± 19	145.9 ± 19	145.9 ± 19
90:10	163.9 ± 5	162.2 ± 11	150.5 ± 19	149.4 ± 19
80:20	140.3 ± 5	129.6 ± 15	127.5 ± 20	117.0 ± 8
70:30	89.7 ± 20	80.0 ± 11	83.9 ± 10	62.7 ± 7

Appendix C-2.1: Flexural modulus of Kevlar[TM] fiber-reinforced BA:PU Alloys

Compositions	Flexural Modulus (GPa)			
	MW 1000	MW 2000	MW 3000	MW 5000
100:0	17.3 ± 1.0	17.3 ± 1.0	17.3 ± 1.0	17.3 ± 1.0
90:10	15.8 ± 1.0	17.0 ± 0.4	18.5 ± 1.5	22.3 ± 3.6
80:20	20.7 ± 1.0	21.8 ± 0.8	18.8 ± 1.8	21.0 ± 2.5
70:30	21.0 ± 3.0	19.9 ± 1.6	21.6 ± 0.2	23.9 ± 1.0

Appendix C-2.2: Flexural strength of Kevlar[TM] fiber-reinforced BA:PU Alloys

Compositions	Flexural Strength (MPa)			
	MW 1000	MW 2000	MW 3000	MW 5000
100:0	160.7 ± 5	160.7 ± 5	160.7 ± 5	160.7 ± 5
90:10	143.8 ± 8	166.4 ± 14	151.1 ± 6	132.5 ± 14
80:20	145.4 ± 5	169.1 ± 3	145.9 ± 6	142.1 ± 10
70:30	167.3 ± 17	168.9 ± 13	163.6 ± 4	165.1 ± 7

Appendix C-3: Storage modulus of BA:PU alloys.

Compositions	Storage Modulus (GPa)			
	MW 1000	MW 2000	MW 3000	MW 5000
100:0	6.49	6.49	6.49	6.49
90:10	4.84	4.18	4.29	4.57
80:20	4.23	3.50	3.25	3.54
70:30	2.97	2.65	2.17	1.82

APPENDIX D

Comparison of properties of two types of BA:PU alloys used in Kevlar[TM]-reinforced composite

Property	Pathomsap, 2005	This Work (MW 3000)
Density (g/cm^3)	1.29	1.24
Flexural Modulus (GPa)	16.1 ± 2.7	18.8 ± 1.8
Flexural Strength (MPa)	109.2 ± 22	145.9 ± 6
Degradation Temperature (^{o}C) @ 5% weight loss	351	384
Char Yield (%)	40.5	34.2
Cost (Baht) (size 30×30 cm^2)	6,180	5,920

APPENDIX E

LIST OF PUBLICATION

1. Pakawan Kamonchaivanich, Tharathon Mongkhonsi, and Sarawut Rimdusit, "Effect of Diol Molecular Weight on Properties of Benzoxazine-Urethane Polymer Alloys", Proceeding of the 13th Regional Symposium on Chemical Engineering 2006, Singapore, Dec. 3 – Dec. 5, 2006, Ref. No. B2OR10.

Effect of Diol Molecular Weight on Properties of Benzoxazine-Urethane Polymer Alloys

Pakawan Kamonchaivanich, Tharathon Mongkhonsi, Sarawut Rimdusit[*]

Department of Chemical Engineering, Faculty of Engineering,
Chulalongkorn University, Bangkok 10330, Thailand
*Corresponding Author E-mail: sarawut.r@chula.ac.th

ABSTRACT

Recently, a new thermoset resin namely benzoxazine resin is developed. The polymer possesses various outstanding properties such as high thermal stability, easy processibility, low water absorption, near-zero shrinkage after curing with excellent mechanical properties. However, due to its rather high rigidity benzoxazine resin may not be suitable for some applications especially when toughness is required. In this study, polybenzoxazine toughness was improved using a flexible urethane resin based on TDI-polypropylene glycol at varied molecular weights of the polypropylene glycol i.e. 1000, 2000, 3000 and 5000. The experimental results showed that the glass transition temperature (T_g) of the alloys was enhanced with increasing the urethane content at a fixed molecular weight of the diol. In addition, the various diol molecular weights showed significant influence on the rubbery plateau modulus and glass transition temperature of the obtained alloys. The use of urethane resin based on diol with molecular weight of 2000 (diol 2000) provided the ultimate T_g, flexural modulus, and flexural strength of the alloys comparing at the same urethane content. The urethane resin based on diol 2000 is likely to provide urethane resin with a suitable chain length for alloying with the benzoxazine resin; therefore, resulted in the observed ultimate polymer alloy properties.

INTRODUCTION

Benzoxazine resin has been recently developed to show various intriguing properties such as high thermal stability, easy processibility, low water absorption, near zero shrinkage after processing with excellent mechanical properties. A method for preparing a desired benzoxazine compound comprises of a reaction of a phenolic compound, a primary amine, and an aldehyde but not solvent other than for the solvency which the reactants may have for each other (Ishida, H. 1996). Because the resin does not release by-products during polymerization, making the polybenzoxazine highly useful for various composite applications. One outstanding property of the benzoxazine resin is an ability to alloy with various types of resins. Alloying of benzoxazine resin with isophorone diisocyanate-based urethane prepolymers or with flexible epoxy could significantly improve the toughness of the polybenzoxazine (Rimdusit, S. et al 2005). The chain distance between junction points would substantially affect the movement of the network, the degree of crosslinked density, and the resulting heterogeneous network behavior. The purpose of this work is to investigate the characteristics of benzoxazine resin alloying with toluene diisocyanate-based urethane prepolymer at varied molecular weights of the polypropylene glycol in the urethane synthesis.

EXPERIMENTAL

Resin and Specimen Preparation

Bisphenol A, aniline, and paraformaldehyde at a 1:2:4 molar ratio was used for synthesizing the benzoxazine monomer using patented solventless synthesis technique (Ishida, H. 1996). These three reactants were continuously mixed at about $110^{o}C$ for approximately 2 hours. The urethane prepolymer was prepared from toluene diisocyanate and polypropylene glycol at a 2:1 molar ratio at varied molecular weights of the polypropylene glycol i.e. 1000, 2000, 3000 and 5000. The two reactants were directly mixed in a four-necked round bottomed flask and the mixture was continuously stirred under a nitrogen stream at $60^{o}C$ for 2 hours.

The benzoxazine monomer was blended with various molecular weights of the urethane prepolymer at a desirable mass fraction. The blends were heated to about $150^{o}C$ in aluminum pan and were mixed mechanically for about 15 minutes to obtain a homogeneous mixture. The molten mixture was poured into an aluminum mold and step-cured in an air-circulated oven at 160, 170, 180, 190, $200^{o}C$ for 2 hours each. Then, the specimens were ready for further characterization.

RESULTS AND DISCUSSION

Table 1: Molecular weights of the polyols determined via monomer/initiator ratio and GPC

Polymer code	M_n (M/I ratio) (g/mol)	M_n (GPC) (g/mol)	PDI
Diol 1010	1000	1028	1.07
Diol 1020	2000	2022	1.06
Diol 3003	3000	2887	1.06
Diol 3009	5000	4396	1.27

(M/I ratio: monomer/initiator ratio obtained from TPI Polyol CO., LTD.)

As shown in Table 1, the Diol molecular weights for urethane resin preparation measured by GPC is relatively in good agreement with the values derived from the monomer/initiator ratio obtained from TPI Polyol CO., LTD. The polydispersity index (PDI) of the diols is relatively narrow and quite constant.
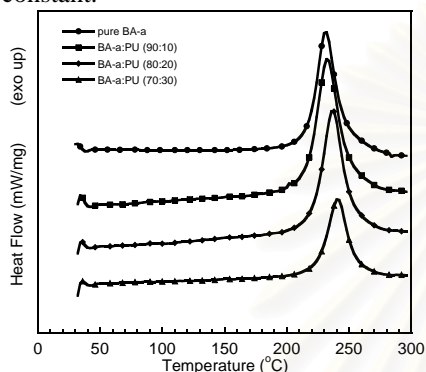

Figure 1: DSC thermograms of BA-a: PU at various composition with diol MW = 2000.
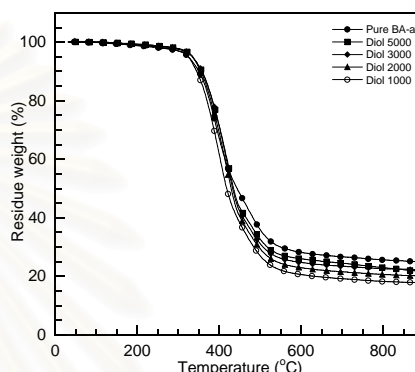

Figure 2: TGA thermograms of BA-a: PU at various MW's.

DSC thermogram exhibits a decrease of the area under the curing peak when the amount of urethane resin increased. This related to the decease in the number of moles of the reacted functional groups of each component in the polymer alloys. In addition, the exothermic peak was shift to a higher temperature when the urethane mass ratio was increased s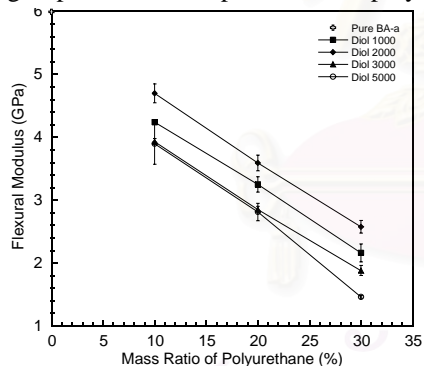uggesting curing retardation occurred in the mixture. Figure 2 shows the TGA thermograms of the BA-a: PU alloys (at a fixed mass ratio of 80:20) at various MW of diols under nitrogen atmosphere. The diol molecular weight reveals negligible effect on 5% weight loss of the alloys. Moreover, char yield of these alloys was found to increase with the MW of the diols. In addition, the flexural modulus of the alloys decreased with increasing the mass ratio of the polyurethane in the polymer alloys. The urethane resin based on diol 2000 also exhibits the highest flexural modulus and is likely to provide the resin with an optimum chain length for alloying with the benzoxazine resin; therefore, resulted in the observed ultimate polymer alloy properties.

Figure 3: Flexural modulus of the alloys at various composition of each MW of diol.

CONCLUSIONS

The presence of urethane resin in benzoxazine resin can slightly retard the curing reaction of the mixture. This investigation shows that the effect of urethane resin based on diol with molecular weight of 2000 provides the ultimate flexural modulus of the obtained fully cured alloys comparing at the same urethane content. Finally, the decomposition temperature increases with increasing the molecular weights of the diols.

REFERENCES

Ishida, H. (1996). *Process of benzoxazine compounds in solventless systems.* U.S. Patent 5,543,516.

Rimdusit, S.; Pirstpindvong, S.; Tanthapanichakoon, W., and Damrongsakkul, S. (2005). *Toughening of polybenzoxazine by alloying with urethane prepolymer and flexible epoxy: a comparative study.* Polym. Eng. Sci. **(45)**, 288-296.

VITA

Miss Pakawan Kamonchaivanich was born in Bangkok, Thailand on March 31, 1983. She completed senior high school at Saint John's College, Thailand in 2001 and received Bachelor degree from the Department of Chemical Technology, Faculty of Science, Chulalongkorn University, Thailand in 2005. She continued her study for Master degree at Department of Chemical Engineering, Faculty of Engineering, Chulalongkorn University Bangkok, Thailand.